POSITRON ANNIHILATION IN MOLECULAR LIQUID-SOLID SYSTEMS

A Thesis

Submitted to

the Faculty of Graduate Studies

University of Manitoba

In Partial Fulfillment

of the Requirements for the Degree

Doctor of Philosophy

---

by

Alexander M. Cooper

Winnipeg, Canada

June 1969

TABLE OF CONTENTS

LIST OF FIGURES

LIST OF PLATES

LIST OF TABLES

ACKNOWLEDGEMENTS

I would like to express my sincere thanks to my supervisor Dr. B. G. Hogg for the guidance and constant encouragement given by him throughout the course of this work.

I would also like to thank Dr. S. K. Mark for his valuable advice concerning the construction of the electronic equipment.

Finally I would like to thank Dr. S. Y. Chuang, Dr. W. Holt, G. DeBlonde and A. Gould for their assistance during the experimental work and for many helpful discussions.

This work was supported by the National Research Council of Canada and the American Chemical Society.

ABSTRACT

A fast-slow time sorting system, with day to day resolution of 300 picoseconds, has been constructed to measure positron lifetimes and intensities in Ammonia, Cyclohexane, Methane and Butane. For each substance lifetimes and intensities have been studied over a range of temperatures including in each case a liquid-solid phase change and in the case of Cyclohexane a solid-solid phase change as well.

The data were analyzed using a multi-exponential computer program and the parameters τ_2, τ_1, I_2 and I_1 extracted for each substance at the various temperatures.

The experimental τ_2's obtained for Ammonia and Methane over the entire temperature range studied (including the phase transitions) agree very well with the theoretical values calculated from the Free Volume Model.

The experimental I_2's obtained show the mechanism of positronium formation proposed by Brandt and Spirn to be incorrect and an alternate mechanism is postulated which explains the experimental I_2's.

A study of the solid-solid phase transition in Cyclohexane yielded a large discontinuity in τ_2 at the transition temperature and points up the value of the positron probe in exploring phase transitions of this type.

CHAPTER I

INTRODUCTION

1.1 The Discovery of Positrons

The positron as a particle was first predicted by Dirac in 1930. His prediction arose from the relativistic wave equation for electron energy:

$$E = \pm\sqrt{m_o^2c^4 + p^2c^2}$$

where E is the total energy of the electron, m_o its rest mass, p its momentum and c the speed of light. Since this equation had both negative and positive energy solutions with the negative solution corresponding to the case of an electron with a charge of +e, Dirac postulated the existence of positrons or "holes." The particles thus predicted were first detected in 1932 by Anderson in cloud chamber photographs of Cosmic Ray showers. Anderson discovered the particles which he named "positrons" when he applied a magnetic field across his cloud chamber and found particles with electronic mass but positive electronic charge.

With the advent of artificial radioactivity positron sources have become readily obtainable from a number of radioactive isotopes.

1.2 Characteristics of Positron Annihilation

The positron is an elementary particle which along with electrons, muons and neutrinos belongs to the class known as Leptons. Since the positron is the antiparticle of the electron the two particles can thus annihilate as a pair to form gamma rays.

The spin of the positron like that of the electron is equal to $\frac{1}{2}$ and as with other particles of $\frac{1}{2}$ integer spin positrons obey Fermi-Dirac statistics.

When positrons and electrons collide annihilation can take place with the emission of one, two or three photons. However in the case of annihilation with the emission of only one photon a third body must be present to absorb the recoil momentum and thus conserve the momentum of the system.

To understand two and three photon annihilation we consider a positron-electron pair in an S state. This is sufficient since in higher orbital angular momentum states the positron and electron wave functions do not overlap sufficiently for appreciable annihilation to occur. The positron-electron pair can exist in one of two substates, the singlet state $^1S_0$ with spin zero and the triplet state $^3S_1$ with spin one. Now according to Yang (1950) the appearance of two photons upon annihilation is only possible for annihilation from the singlet state. It is known that the relative intrinsic parity for a particle-antiparticle pair is negative and thus for the

positron-electron pair $P_i = (-1)$. Then the charge conjugation for the system is

$$P_c = P_i P_S = (-1)(-1)^{S+1} = (-1)^S$$

where P_S is the spin parity of the system. Therefore the charge conjugation is positive for the singlet state (S=o) and negative for the triplet state (S=1). Now since the charge conjugation of a photon is negative, for a system of n photons $P_c = (-1)^n$. Thus if charge conjugation is invariant in electromagnetic interactions, annihilation from the singlet state (^1S_o) must be accompanied by two photons while annihilation from the triplet state ($^3S_1$) must be accompanied by an odd number of quanta (in this case 3 quanta).

This feature of positron-electron annihilation has led to a search for charge non-conservation through the study of three photon decay of the singlet state (^1S_o)(A. P. Mills and S. Berko 1967).

A final feature of the annihilation process is the probability of occurence of each of the possible decay modes. Ore and Powell (1949) have shown that the ratio of the three photon to two photon cross section is 1/372 and Goldanskii (1968) has shown that the one photon rate will be more than two orders of magnitude less than the three photon rate.

1.3 Discovery and Properties of Positronium

The possible existence of a bound positron-electron

system was first postulated by Mohorovicic in 1934. In 1945 Ruark named this bound system positronium and then in 1951 Deutsch carried out experiments confirming its existence.

The positronium atom is analogous to the hydrogen atom except that its reduced mass is one-half of the electron mass. Thus from simple Bohr theory one finds the Bohr radius for positronium is equal to

$r_p = \frac{2\hbar^2 n^2}{me^2 Z^2} = 2a_o = 1.06$ Angstroms while in the same way the ground state energy becomes $E = \frac{e^2}{2r_p} = \frac{e^2}{4a_o} = 6.77$ eV.

There are two ground state configurations for positronium; the triplet state (ortho-positronium) and the singlet state (para-positronium) with the spins being respectively parallel and anti-parallel. Since the triplet state has three magnetic substates (m = 1, 0, -1) while the singlet state has only one (m=0) the statistical weight of the triplet state is three times that of the singlet state. Thus triplet positronium will be formed three-quarters of the time and singlet positronium will be formed one-quarter of the time. Following the argument of the last section triplet positronium will undergo decay by three quanta annihilation while singlet positronium decays by two quanta annihilation. The lifetimes of triplet and singlet positronium annihilating in vacuum have been calculated as 1.4×10^{-7} seconds and 1.25×10^{-10} seconds (Ore and Powell 1949).

In the formation of positronium, high energy positrons are degraded in energy by various processes such as ionizing and excitation collisions until they reach an energy at which positronium formation becomes favorable. This energy lies within the so-called "Ore Gap" first proposed by A. Ore in 1949. The "Ore Gap" which is controlled by the parameters of the media under investigation and the way in which Ore's theory predicts formation probabilities will be discussed in Chapter V.

1.4 Experimental Methods of Studying Positron Annihilation

There are three experimental methods by which information on positron decay may be gained. The first of these is through the measurement of the triplet annihilation rate by the use of a triple coincident circuit. Since theory predicts that the ratio of three γ to two γ annihilation for free positrons will be 1/372 whenever a rate larger than this is found we have proof of positronium formation. Unfortunately this method cannot distinguish between the case where positronium is not formed and the case where the triplet positronium is quenched by various mechanisms such that it decays by two photon annihilation. Therefore at the present time this method is used only infrequently.

The second method of studying positron annihilation is through the measurement of the mean lifetimes of the annihilating positrons. In this type of experiment a nuclear γ ray is used as a start signal and the subsequent annihilation

radiation is used as a stop signal for a coincidence circuit. It was through experiments of this type that Deutsch in 1951 first showed the existence of positronium in gases. Two types of information are found in experiments of this kind, first the decay rates for the various processes by which positrons can annihilate and second the percentage of positrons decaying by each of the different modes. Since in previous work on condensed media the long lifetime observed has been attributed to triplet positronium this method then allows one to measure directly the amount of positronium formed in a system. Thus by use of the lifetime method one is able to study the effect changes in a given system have on both decay rates and the relative abundance of positrons decaying by the different decay modes.

The third method of measurement is by the technique of angular correlation of the two photon annihilation radiation. When a positron-electron pair at rest annihilates with the emission of two photons an energy of $2\ mc^2$ is released. Since momentum must be conserved these two photons each having a momentum mc must be emitted at 180 degrees to one another in the centre of mass system. Now if the annihilating pair has some momentum at the time of annihilation, then the photon pair will be emitted at an angle differing from 180 degrees by an amount of the order v/c, where v is the velocity of the centre of mass of the annihilating pair. Thus by measuring the

departure of the emitted photons from 180 degrees it is then possible to find the momentum distribution of the annihilating pairs. In recent years the analysis of the raw angular correlation data into momentum distributions has been done mainly by electronic computer (S. Y. Chuang 1968).

Figure 1-1 illustrates a typical parallel slit angular correlation apparatus.

1.5 Factors Influencing the Annihilation of Positronium

Since the initial discovery of positronium considerable work has been carried out in studying the various factors which effect the lifetime of positronium. Thus positronium lifetimes have been studied as a function of;

Temperature: R. E. Bell and R. L. Graham 1953, H. S. Landes, S. Berko and A. J. Zuchelli 1956, W. Brandt, S. Berko, and W. W. Walker 1960, W. Brandt and I. Spirn 1966

Pressure: R. K. Wilson, P. O. Johnson and R. Stump 1963

Crystallinity: S. J. Tao and J. H. Green 1965

Irradiation: G. Fabri and E. Germagnoli 1962, D. Fabri, G. Poletti, G. Randone 1966

Magnetic Fields: L. A. Page and M. Heinberg 1956, G. Iaci et al. 1962, G. Fabri et al. 1964

Chemical Quenching: T. A. Pond 1952, S. Berko, A. J. Zuchelli 1956, D. A. L. Paul 1958, J. Lee and G. J. Celitans 1965, D. P. Kerr, A. M. Cooper and B. G. Hogg 1965.

From these studies certain insights into the various

Figure 1-1

Angular Correlation Apparatus

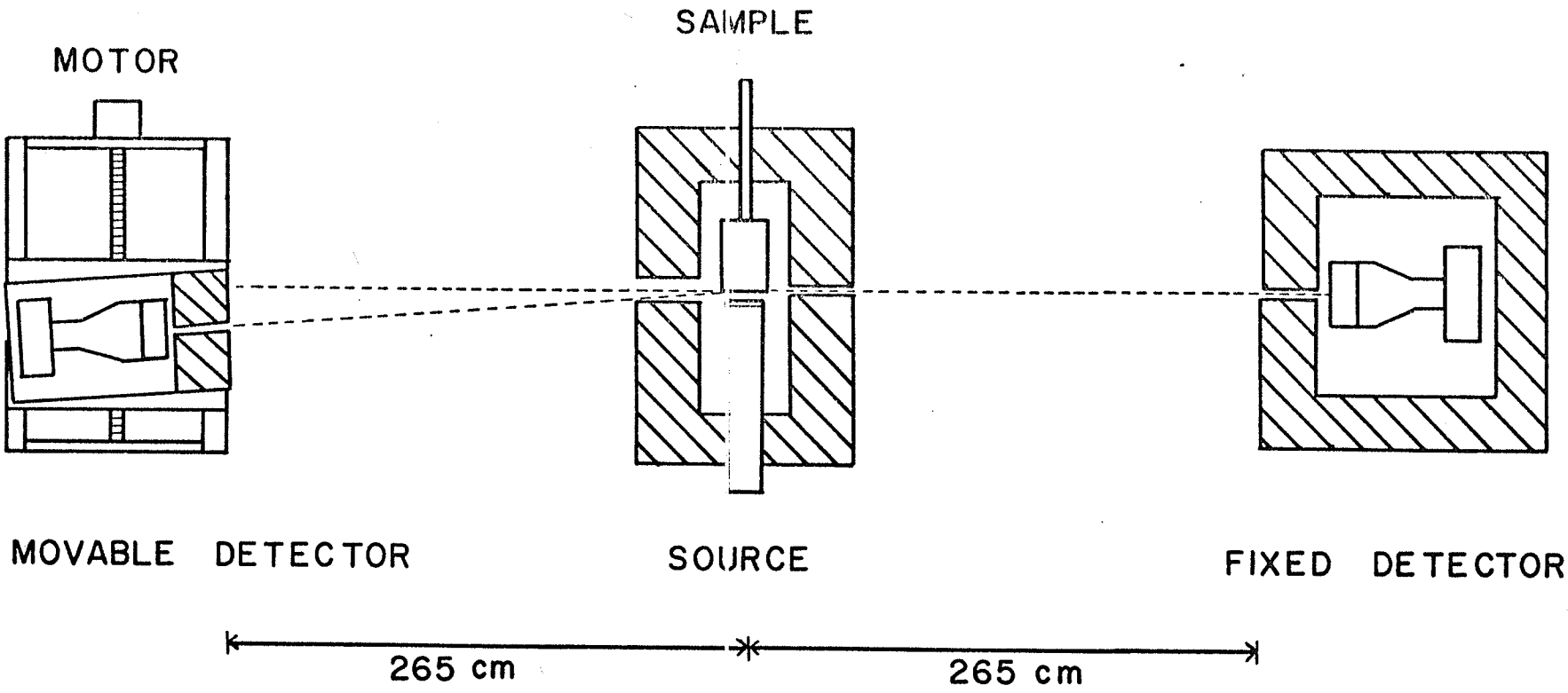
SAMPLE
MOTOR
MOVABLE DETECTOR
SOURCE
FIXED DETECTOR
265 cm
265 cm

mechanisms by which triplet positronium can have its lifetime shortened or quenched have been noted.

Foremost among the quenching processes would seem to be the "pick-off" process since in all condensed media this process is the basic one governing the triplet positronium lifetime. In the "pick-off" process due to the continual scattering of the positronium by the surrounding molecules, the positron in triplet positronium may annihilate with an electron from a molecule whose spin relative to the positron is anti-parallel. This process accounts for the long lived lifetime of positronium of about 10^{-9} seconds in condensed medias rather than the lifetime of 1.4×10^{-7} seconds predicted for triplet positronium in free space.

The second quenching process we consider is that caused by an external magnetic field. In the ground state triplet positronium ($^3S_1$) is about 8.4×10^{-4} eV above the ground state of singlet positronium (^1S_o). When a constant magnetic field is applied the levels in triplet positronium are split and in the case of the m = o levels in the singlet and triplet cases the energy separation between them becomes greater. This increases slightly the transition probability between them resulting in an increased probability of triplet to singlet conversion or quenching.

A third process considered possible in the quenching

of triplet positronium is that of paramagnetic quenching. In this case the quenching occurs not only from the action of an external field but also from the fields of paramagnetic admixtures in the sample. Ore (1949) has shown however that even for a gas as paramagnetic as oxygen the spin flip through magnetic interaction would take of the order of 10^{-5} seconds, which is two orders of magnitude less than the case for spontaneous three photon decay. Therefore it would seem unlikely that this process is of any consequence in the quenching of triplet positronium.

The final type of quenching may be considered under the heading of chemical quenching. Under this heading would be included the chemical reactions of addition, substitution, oxidation and the possibility of the formation of positronium compounds.

In this work studies are conducted to ascertain the effect on positron lifetimes and intensities due to variation in temperature and change of phase for various substances. From information of this type some of the theories and models currently proposed to explain positron decay processes can be tested. Also from studies of this type information is gained as to the usefulness of positrons as probes in studying various materials.

CHAPTER II

INSTRUMENTATION

2.1 Introduction

The measurement of time intervals between various nuclear or atomic events has been a study important to physics for many years. Originally studies of this type were conducted using simple coincidence elements which gave an output when two input pulses arrived at the coincidence element within a given resolving time. Many circuits were designed to achieve this end and almost all worked satisfactorily. The next development in this field was the addition of pulse amplitude selection to each of the two input sides to allow identification of the events under study. This was originally done by placing pulse height analyzers prior to the coincidence element in the circuit. This method however had the defect that the slow response of the pulse height analyzers severely limited the resolution obtainable by the coincidence circuit. This problem was overcome through the use of the fast-slow principle first described by Bell and Petch in 1949. In their method the fast coincidence was obtained for pulses unselected as to amplitude while the pulse height analysis was performed on pulses unselected as to time. Then through the use of a slow coincidence circuit pulses which satisfied both criteria were identified.

The fast coincidence circuit discussed thusfar only

gives information as to whether two events fall within a given time range, rather than giving the time distribution of the events. To achieve time distributions, experiments were originally performed by the placing of known delays between the two sides and counting for a given period of time at each different delay. This method was rather tedious but did achieve the desired effect of producing a time distribution of the events under consideration. Finally Time to Amplitude Converter (T.A.C.) circuits were introduced for use in the nsec region (Fraser and Milton 1953) which allowed time differences to be converted to voltage pulses which could then be displayed on multichannel analyzers. With the advent of this type of circuit we are at the level of present day time sorting systems. Although various other modifications have become standard and resolution obtainable has steadily improved the fast-slow system employing a T.A.C. has become standard for time measurements in the nsec region.

2.2 General Description of the System

A block diagram of the time sorting system used in this work is shown in Fig. 2-1. The system is conceptually the same as the fast-slow system described by Bell et al. (1952). Most of the actual circuitry was designed and built at the University of Manitoba. The system consists of three separate parts; the Fast side, the Slow side and the calibration section. Each of these various parts of the circuit will be described

Figure 2-1

Block Diagram of the Time Sorting System

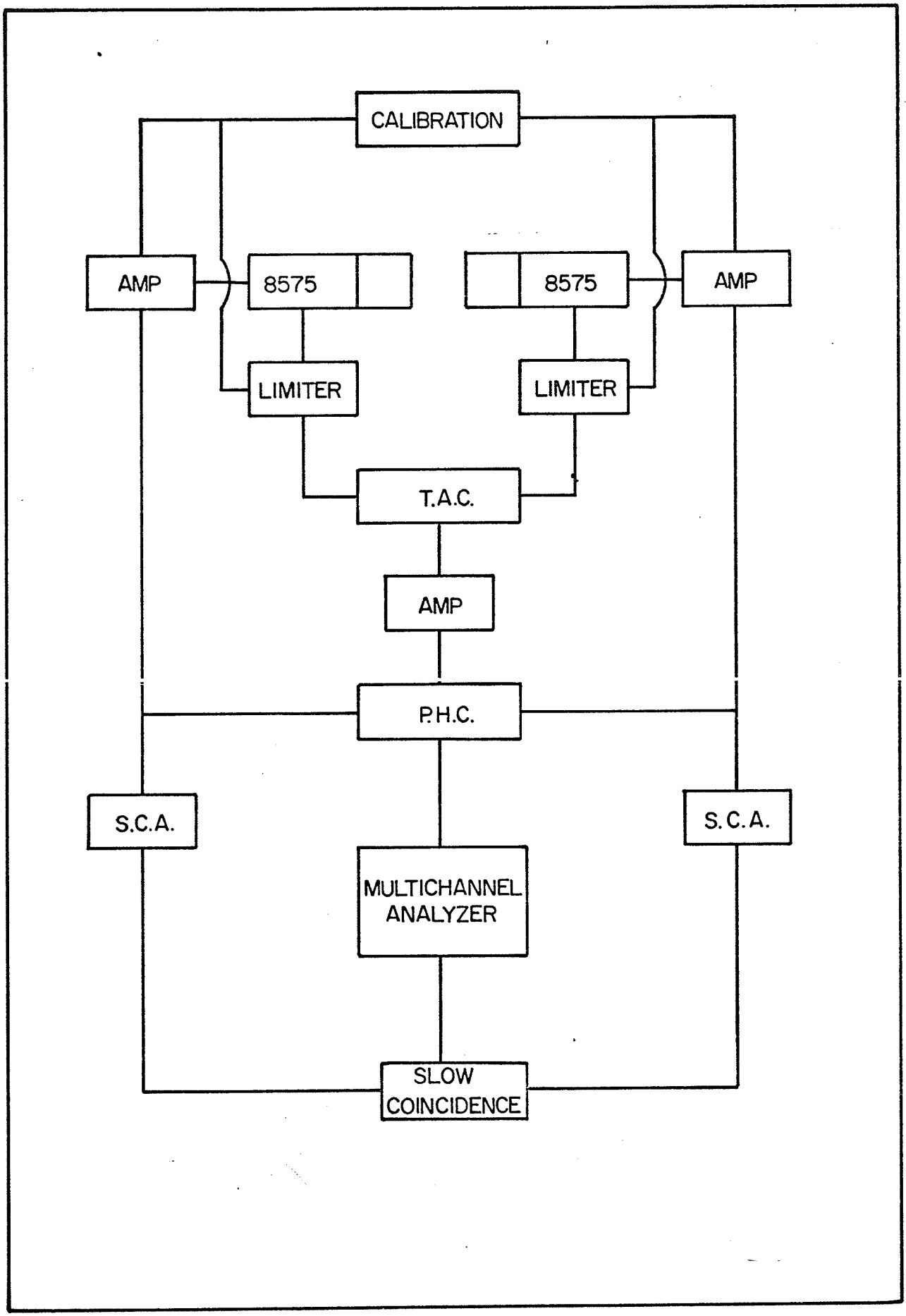
CALIBRATION
AMP
8575
8575
AMP
LIMITER
LIMITER
T.A.C.
AMP
P.H.C.
S.C.A.
S.C.A.
MULTICHANNEL ANALYZER
SLOW COINCIDENCE

The Time Sorting System

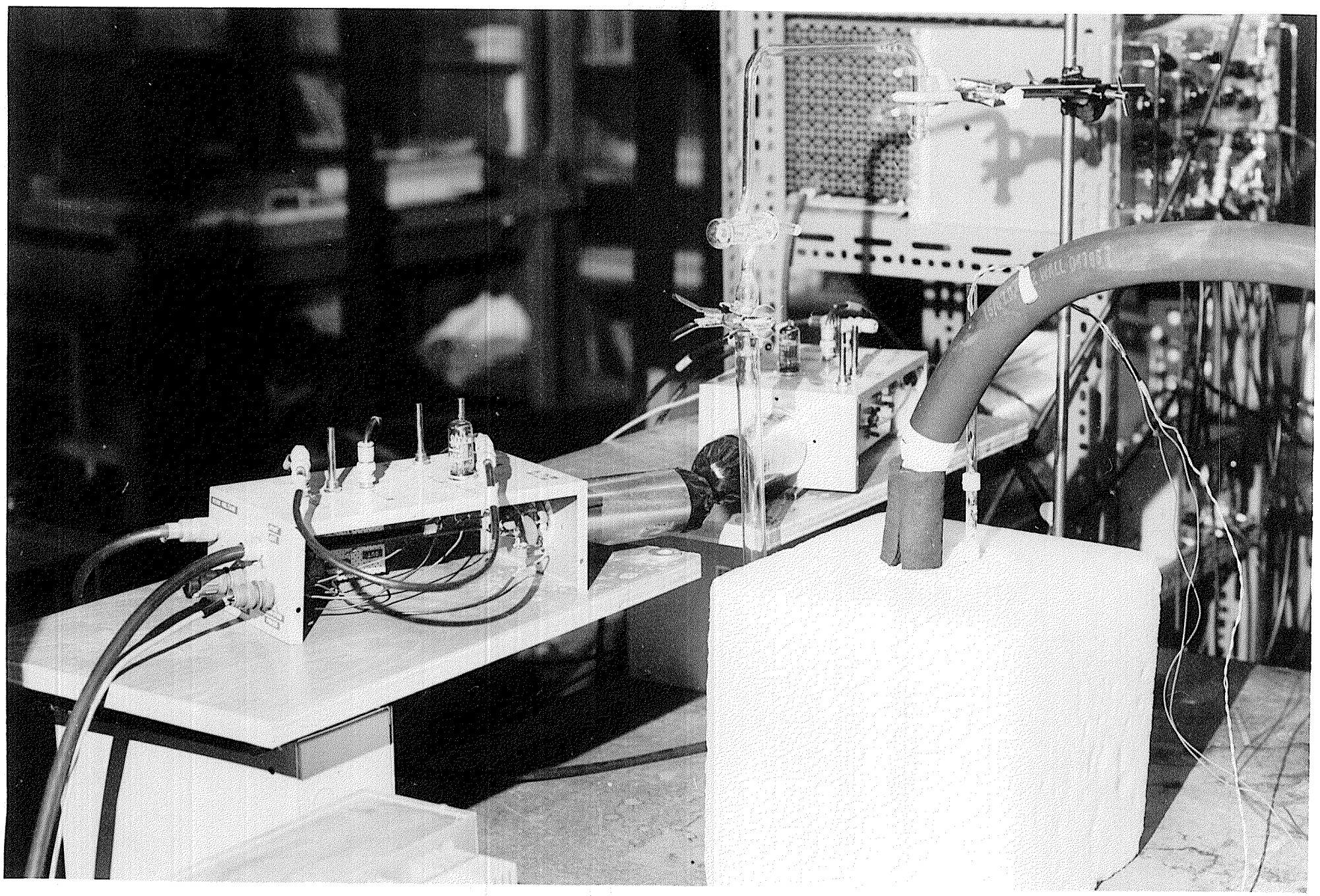

in more detail in later sections and so here we will present only an overall view of how the apparatus functions.

In positron lifetime studies the problem is to determine the relative delay between the appearance of the positron from the Na^{22} nucleus and the subsequent appearance of one of the γ rays which appears upon the annihilation of the positron. This is done by detecting in one phototube the 1.28 MeV γ ray which is given off coincident with the positron's formation, (coincident in the sense that the time difference in emission is much smaller than the resolving time of the apparatus), and by detecting in the other phototube one of the .511 MeV annihilation γ rays. The two phototube signals thus formed are then fed to their respective limiters where they are converted to fast rising flat topped pulses. These pulses are then routed to the T.A.C. where they are both clipped to about 40 nsec in length. They are then overlapped in such a way that the output from the T.A.C. circuit is proportional to the amount of overlap, or what is more important, proportional to the time difference between the two events. The output from the T.A.C. is then fed through a linear amplifier to the Pulse Height Compensator (P.H.C.). The P.H.C. unit is an analogue circuit which serves to correct the T.A.C. signal for errors introduced due to dealing with pulse heights of various size from the phototubes. The output from the P.H.C. is then routed to the multichannel analyzer and if the Slow side which we will

discuss next has opened the gate, the signal will be recorded.

The Slow portion of the fast-slow system consists of emitter followers which take a linear signal from the 10th dynode of each of the phototubes and feed it through amplifiers to each of the single channel analyzers and to the P.H.C. In the P.H.C. the linear amplifier signals are added to the T.A.C. output to give the corrected signal. The single channel analyzers allow one to choose the appropriate part of the spectrum and if the signal meets this requirement then an output from the single channel analyzer is fed to the slow coincidence unit. If signals from each of the single channel analyzers arrive within the slow coincidence unit's resolving time a gating signal is produced which activates the multi-channel analyzer and lets it accept a count.

Finally the third part of the system consists of the calibration circuitry which allows one to determine the relative sensitivity of the whole system. In this apparatus calibration is achieved by the use of an air-cored helical delay line, fed by a mercury pulser, which allows one to place accurately known delays of different values between the two limiters. This allows an integral linearity curve to be produced on the multichannel analyzer and from this curve the sensitivity per channel of the apparatus can be deduced.

In the subsequent sections of this chapter the various elements of the system will be described more fully and the

details of their operation outlined.

2.3 Phototubes and Scintillators

During the course of the building of the time-sorting system a number of photomultipliers were used. These included the Phillips 56AVP, the R.C.A. 6342A and the R.C.A. 8575. Since the system involving the 56AVPs has been described previously (Cooper 1965) and since the 6342A was used mainly in the testing of various aspects of the circuit, only the 8575 which was the photomultiplier finally used will be described.

The R.C.A. 8575 is a 12 stage, head on, flat faced photomultiplier containing an extremely high photon conversion efficiency (Potassium Cesium Antimonide) photocathode. The high cathode quantum efficiency (28% at 3850 angstroms) and the very good timing characteristics of the phototube (anode pulse rise time 2.1 nsec, electron transit time 31 nsec) coupled with the low dark current and high amplification all combine to make this tube ideal for fast time work.

The dynode chain used with the 8575 is shown in Fig. 2-2 and more or less conforms with R.C.A. literature as to the tapering of the interdynode resistances.

With the dynode resistances used the voltage divider carried a static current of 2 mA at 2000 volts. Also to insure that during the pulse duration the dynode voltages could not deviate by more than a few percent from the normal interstage

Figure 2-2

R.C.A. 8575 Photomultiplier and Dynode Chain

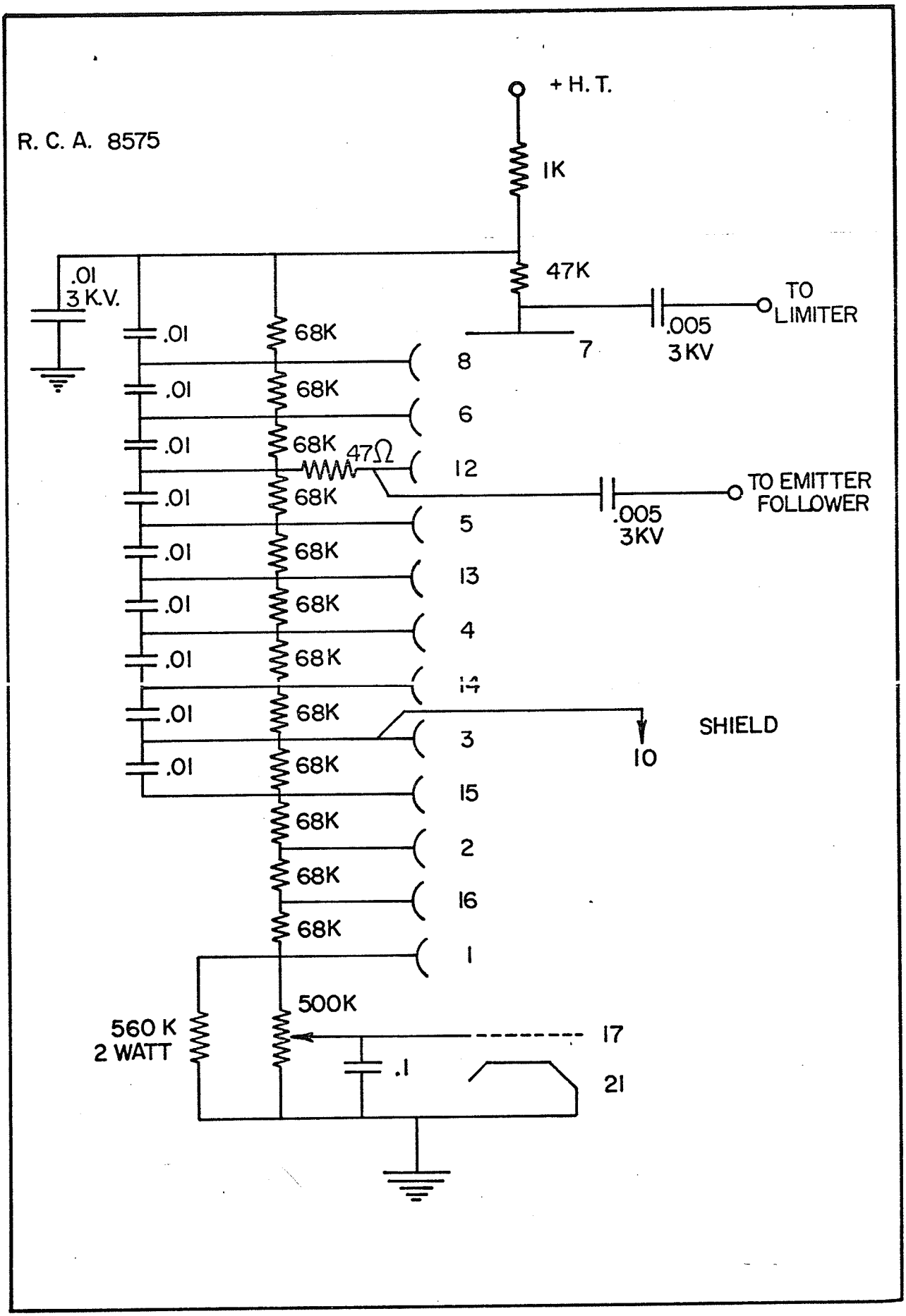
R. C. A. 8575
+ H. T.
1K
47K
.01
3 K.V.
.01
68K
8
6
12
5
13
4
14
3
15
2
16
1
7
.005
3KV
TO
LIMITER
47Ω
TO EMITTER
FOLLOWER
SHIELD
10
500K
560 K
2 WATT
17
.1
21

voltage, non-inductive capacitances were employed across the last eight stages to serve as charge reservoirs throughout the duration of the pulse.

The focusing electrode between the cathode and dynode #1 was connected to the arm of a 500 kilohm potentiometer and was adjusted to give optimum tube response. This was found to be at a point with somewhat less than the greatest gain available.

Both tubes were, as recommended, shielded by use of mu-metal shielding wrapped around the phototubes and held at the cathode potential of the tubes.

An interesting aspect of working with the 8575 photo-tubes is that in their delivered form they have transparent glass bottoms and are supplied with semi-transparent teflon bases. To insure the light tightness required under these conditions the original limiters were constructed in light tight boxes with aluminum sleeves fitted around the phototubes. This arrangement proved satisfactory as to the exclusion of light but was found to be inconvenient in the actual testing and operation of the circuit. A second method was then tested in which non-transparent, non conducting, black paint was applied to the bottom of the phototubes and open limiter boxes were used. This procedure proved totally satisfactory and since it was much more convenient, was employed throughout the rest of this work.

Power for the system was provided by a Sola transformer which had a line regulation of $\pm 1\%$ for a total primary variation

of 30%. High voltage for the phototubes was provided by a Fluke power supply with line regulation of .001% for a 10% line change from nominal.

The scintillators used throughout this work consisted of highly polished plastic crystals of NE 102A which were coated with white reflecting paint. Crystals of various sizes were tested in order to obtain the optimum compromise between efficiency and resolution and those decided upon were 1" diameter by 1" long.

Since the optical coupling between the scintillator crystal and the face of the photomultiplier has been shown to be very important (Kerr and Hogg 1962), with poor coupling resulting in spurious tails on the time curves, considerable care was taken to achieve good optical coupling. This was done mainly by the use of Dow Corning compound C-20057 which had good optical qualities and also had the desirable property that it did not develop air bubbles between the surfaces to be joined.

2.4 Limiter Circuit

Since the T.A.C. circuit used in the time sorting system was of the pulse overlap type, this necessitated a limiter circuit producing fast rising flat topped pulses of reasonably long duration.

The limiter circuits used in this work were based on the sharp cutting off of hard driven E810F pentodes. The circuit, which is shown in Fig. 2-3, was run with a plate voltage of 150 volts and a negative grid bias of approximately 2.3 volts which resulted in a plate current of about 18 mA. The grid bias was set by locking the grid at .5 volt through

Figure 2-3

Limiter Circuit

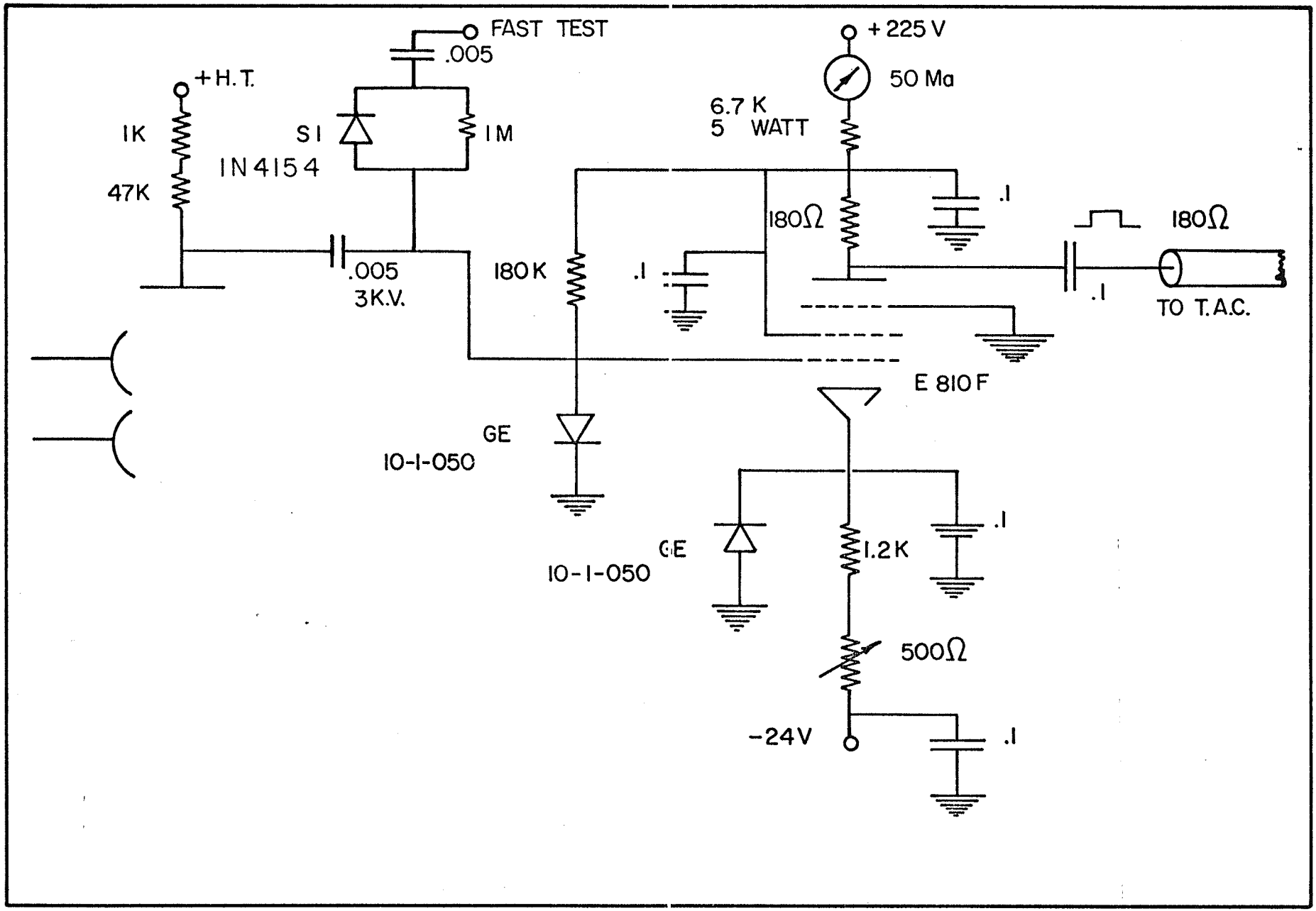
FAST TEST
.005
+H.T.
1K
47K
S1
IN4154
1M
.005
3K.V.
+225 V
50 Ma
6.7 K
5 WATT
180Ω
.1
180Ω
180K
.1
.1
TO T.A.C.
E 810 F
GE
10-1-050
GE
10-1-050
1.2K
.1
500Ω
-24V
.1

the use of a fast diode and then adjusting the cathode to the required potential through the use of the 500 ohm potentiometer. This ability to adjust the grid bias was important since for the most efficient operation of the T.A.C. it was desirable to have both limited pulses of the same height. Since the pulse height is controlled by the plate current in the E810F tube small variations in various tubes could be compensated for by adjustment of the cathode potential. Because variations in the pulse heights at the anode caused by changes in the plate current cause drifts in the time spectrum they must be minimized as far as possible. The 50 mA meter in the plate circuit allows the plate current to be monitored and therefore checked as a source of trouble if drifts in the apparatus occur. In actual practice very little trouble was encountered with this aspect of the circuitry although it was found adviseable to change the E810F tubes approximately every six months.

The fast rising negative pulses from the photomultiplier which arrived at the grid of the E810F caused the tube to be cut-off thus causing pulses with rise times of about 1 nsec to be formed across the 180 ohm plate resistor. The duration of the output pulse is approximately .5 microsecond which is long enough to ensure that when it is clipped to its desired size the portion used is completely flat.

The pulses formed at the plate of the E810F were

approximately 1.5 volts in size and from the plate were fed into RG 114/u cable which has an impedance of approximately 180 ohms and thus matches the plate resistor. To avoid the mismatching which connectors would cause, the RG 114/u cable was soldered directly into the circuit.

It has been found in various studies of leading edge timing (Gedcke and McDonald 1967; Schwarzchild 1963) that the optimum time resolution for a system is obtained when the limiters are triggered by 10 to 15% of the height of the total pulse. In our case this was achieved by variation of the high voltage supply so that the pulses delivered by the photomultipliers were of the correct height. Since the E810F tubes were completely cut-off at 3 volts and since we ran them at a negative bias of 2.2 volts the first .8 volts of the pulse served to cut them off. The high voltage was accordingly varied to provide pulses of approximately 5 volts in height for pulses of the energy with which we were dealing.

The calibration apparatus was coupled to the grids of the limiters via a fast silicon diode instead of the more conventional small capacitor. This had the effect of reducing by a factor of 10 the pulse height required from the test circuit to activate the limiters properly. This allowed use of a standard 10 volt mercury pulser in the calibration circuit.

In Fig. 2-3 the 1 megohm resistance across the diode

serves to restore the D.C. level after each pulse.

2.5 Time to Amplitude Converter

The T.A.C. circuit used in the time-sorting system is of the pulse overlap type and in principle is similar to that outlined by Bell (1966).

Fig. 2-4 is a schematic diagram of how the pulses appear at the input of the conversion element. The 0.5 microsecond fast-rising flat topped pulses from each of the limiters travel down their respective cables and are clipped to a length of 40 nsec by the clipping cable. The clipping cable has a characteristic impedance of 93 ohms so that the return pulse down the clipping cable is matched by the two 180 ohm limiter cables.

Sections A and B of Fig. 2-4 show how the prompt pulses appear as they arrive at the junction point after they have been clipped. They are both of equal amplitude and length and are offset from one another by 10 nsec due to the different lengths of the limiter cables. Section C shows how the input pulse to the conversion element appears due to the overlap of the two pulses. The overlap portion is twice the size of the single pulses and is 30 nsec in length. The equipment is arranged so that the pulses arriving from limiter #1 are the prompt pulses, as selected by the side channels, and those from limiter #2 are from the delayed radiation. Thus coincident pulses give maximum overlap and therefore maximum

Figure 2-4

T.A.C. Input Pulses

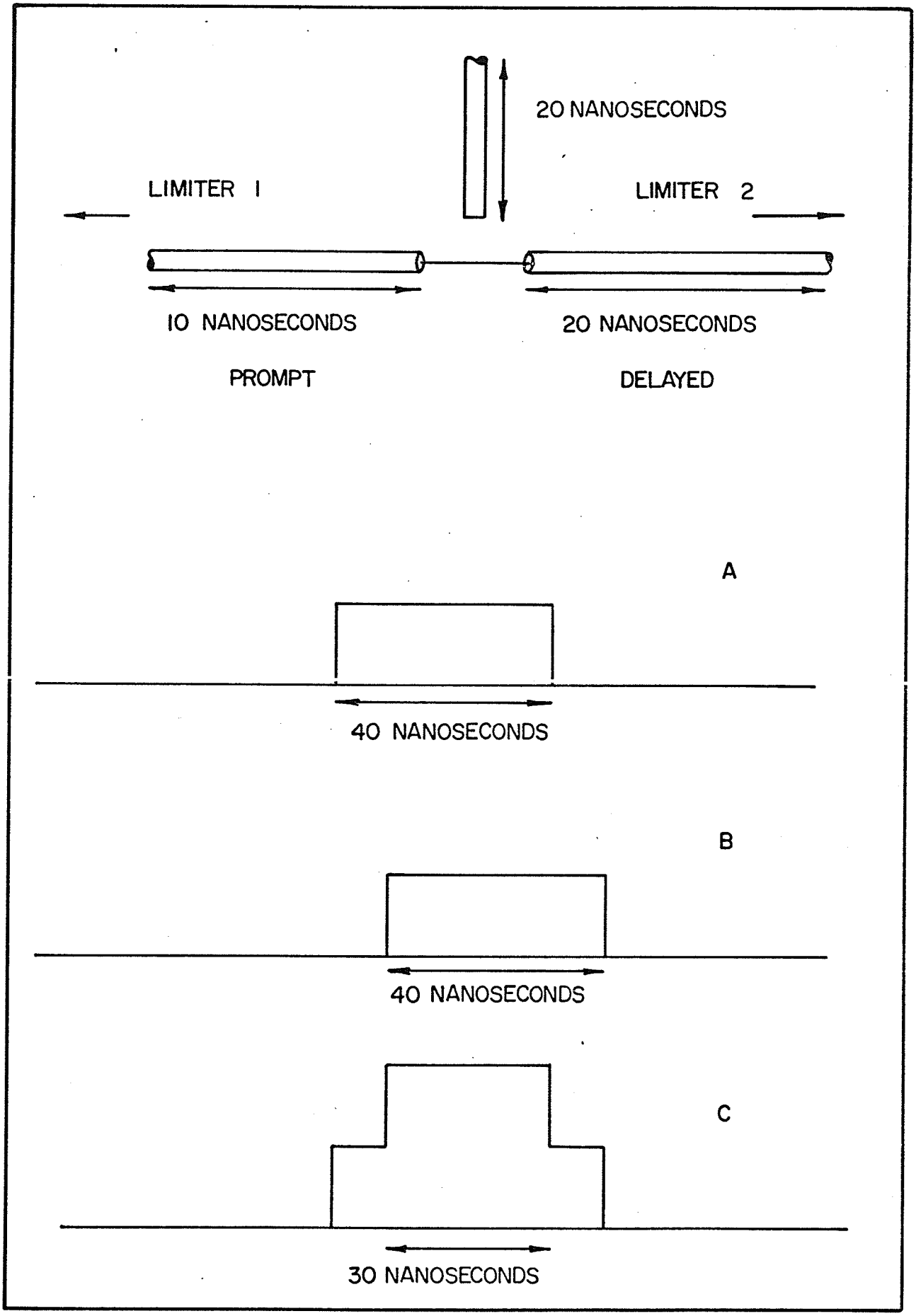
20 NANOSECONDS
LIMITER 1
LIMITER 2
10 NANOSECONDS
PROMPT
20 NANOSECONDS
DELAYED
A
40 NANOSECONDS
B
40 NANOSECONDS
C
30 NANOSECONDS

T.A.C. output and as the delay time between the prompt radiation and the delayed radiation increases, the output from the T.A.C. circuit decreases. To get the maximum useable linear range one can choose to follow the procedure outlined here or alternately have the prompt pulses only slightly overlapped and have them move together as the delay time increases. The latter causes the analogue output from the T.A.C. to increase with increasing delay. The former method was chosen in this work since for reasons not fully understood the performance of the apparatus was significantly better when run in this mode.

The circuit diagram of the T.A.C. is shown in Fig. 2-5. In the T.A.C. the actual time to amplitude conversion is performed by the two diodes D1 and D2 and by the capacitor C1. In the quiescient state the 100 kilohm resistor feeds 3 mA of current through diode D1 to ground through the shorted end of the clipping cable. Therefore the common point of diodes D1 and D2 sits at about 0.4 volts, the forward drop of D1. Thus when a 1.5 volt singles pulse arrives at the limiter cable junction the common point of the two diodes rises to approximately 1.9 volts. Since singles pulses are not to produce an output the reverse bias on diode D2 is set at 1.9 volts. This is done by adjusting the 500 ohm potentiometer to the correct voltage. Now in the case of an overlap pulse arriving at diode D1 the common point of the two diodes starts to rise towards 3.4 volts. However, when the voltage between

Figure 2-5

Time to Amplitude Converter Circuit

Transistors: PNP 2N4258
NPN 2N4274

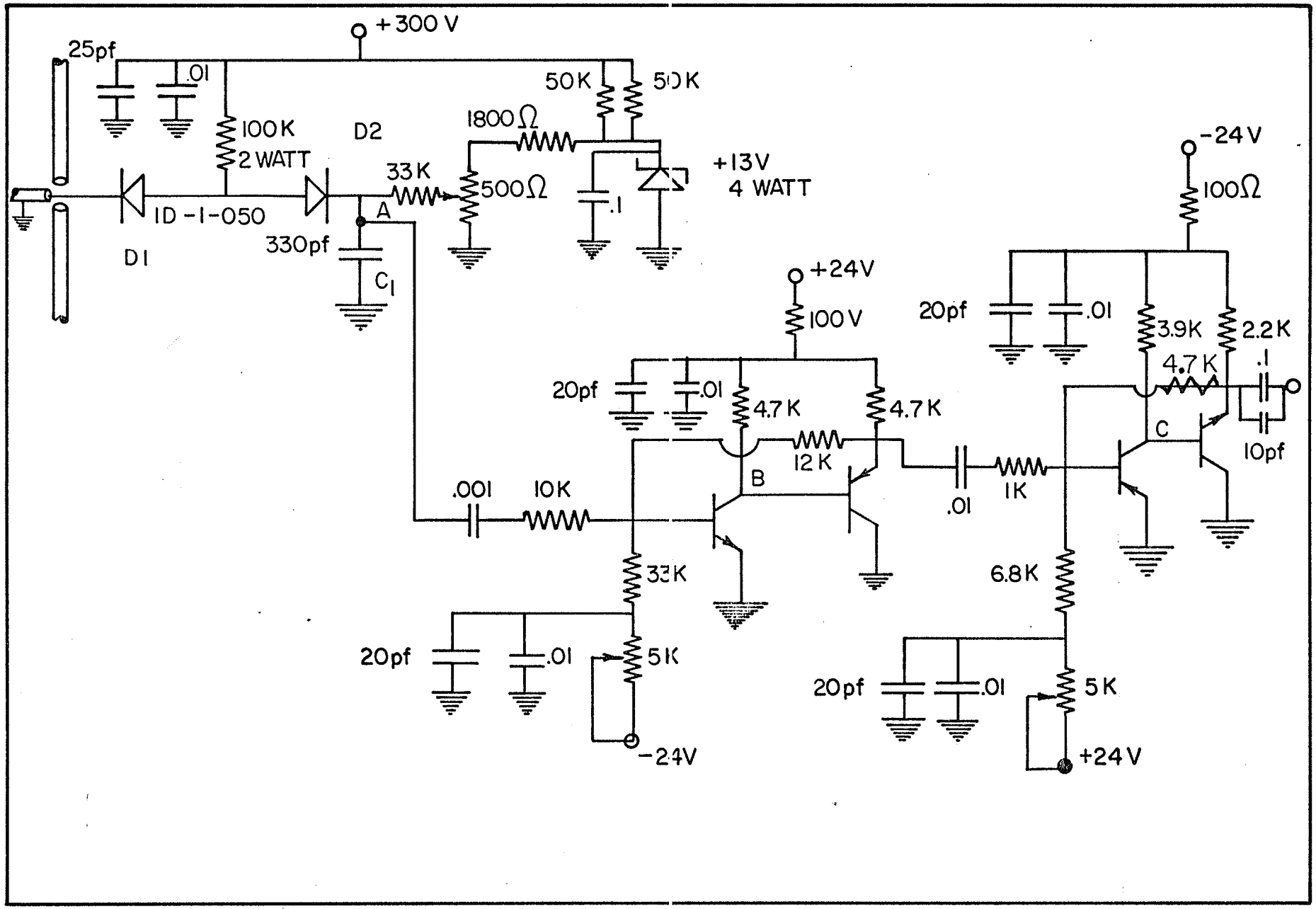
+300 V
25pf
.01
100K
2 WATT
D2
1800Ω
50K
50K
+13V
4 WATT
33K
500Ω
.1
ID-1-050
D1
330pf
C1
A
+24V
100V
20pf
.01
4.7K
4.7K
12K
B
.001
10K
33K
20pf
.01
5K
-24V
-24V
100Ω
20pf
.01
3.9K
2.2K
4.7K
.1
C
10pf
.01
1K
6.8K
20pf
.01
5K
+24V

the two diodes reaches 1.9 volts, current starts to flow through diode D2 and when the current reaches 2.3 volts the full 3 mA of current is flowing through D2. The 3 mA of current flowing through D2 then serves to charge capacitor C1 at a constant charging rate of 9.09×10^6 V/s. Since in this circuit we have a maximum overlap of 30 nsec at time zero, the maximum charge on C1 is .272 volts. When this occurs the common point of D1 and D2 of course rises by the same amount to a value of 2.57 volts. This however still leaves D1 reverse biased by .83 volts which serves as a safety margin under conditions of maximum overlap. The use of a double diode switch in this configuration is advantageous in that a degree of second limiting action is present, such that small changes in the amplitude of the input pulses should not cause any change in the charging rate.

After the capacitor C1 has been charged, the charge leaks off through the 33 kilohm resistor with a time constant of 11 microseconds. The pulse from C1 is then amplified by a factor of 5 through the use of standard circuitry and finally is fed into a commercial amplifier.

2.6 Slow Coincidence Circuitry

The slow portion of the fast-slow coincidence system consists of an amplifier and single channel analyzer for each side of the system, plus the actual slow coincidence unit. Linear pulses from the 10th dynode of each phototube are fed

through emitter followers to their respective amplifiers and from there to the single channel analyzers. If the pulses meet the criteria of the single channel analyzers a positive 3 volt, .5 microsecond logic pulse is then sent to the slow coincidence unit.

The slow coincidence circuit, Fig. 2-6 has two identical input circuits. When a logic pulse from one of the single channel analyzers arrives at one of the inputs it is differentiated and the pulse so formed is then used to trigger the univibrator circuit. The univibrators give out negative square pulses with an amplitude of .5 volts and a duration controlled by capacitor C1. With the 10 pF capacitors used the pulses had a length of approximately 100 nsec. The pulses thus formed were then fed through emitter followers to the parallel diode coincidence element. The coincidence element consists of diodes D1 and D2 through which current from the -24 volt source flowed to ground when no pulses were present. A single negative pulse arriving at either diode effectively cut-off the current in that diode, however since the current was still able to flow through the other diode no potential rise at C occurs. In the case of coincident pulses arriving at diodes D1 and D2 both are cut-off and a negative pulse is formed at C. This pulse is then inverted and fed through an emitter follower to the output univibrator. This output stage produces negative pulses of 1 microsecond duration and of

Figure 2-6

Slow Coincidence Circuit

Transistors: PNP 2N4258
NPN 2N3646

Diodes: Ge 1N3121

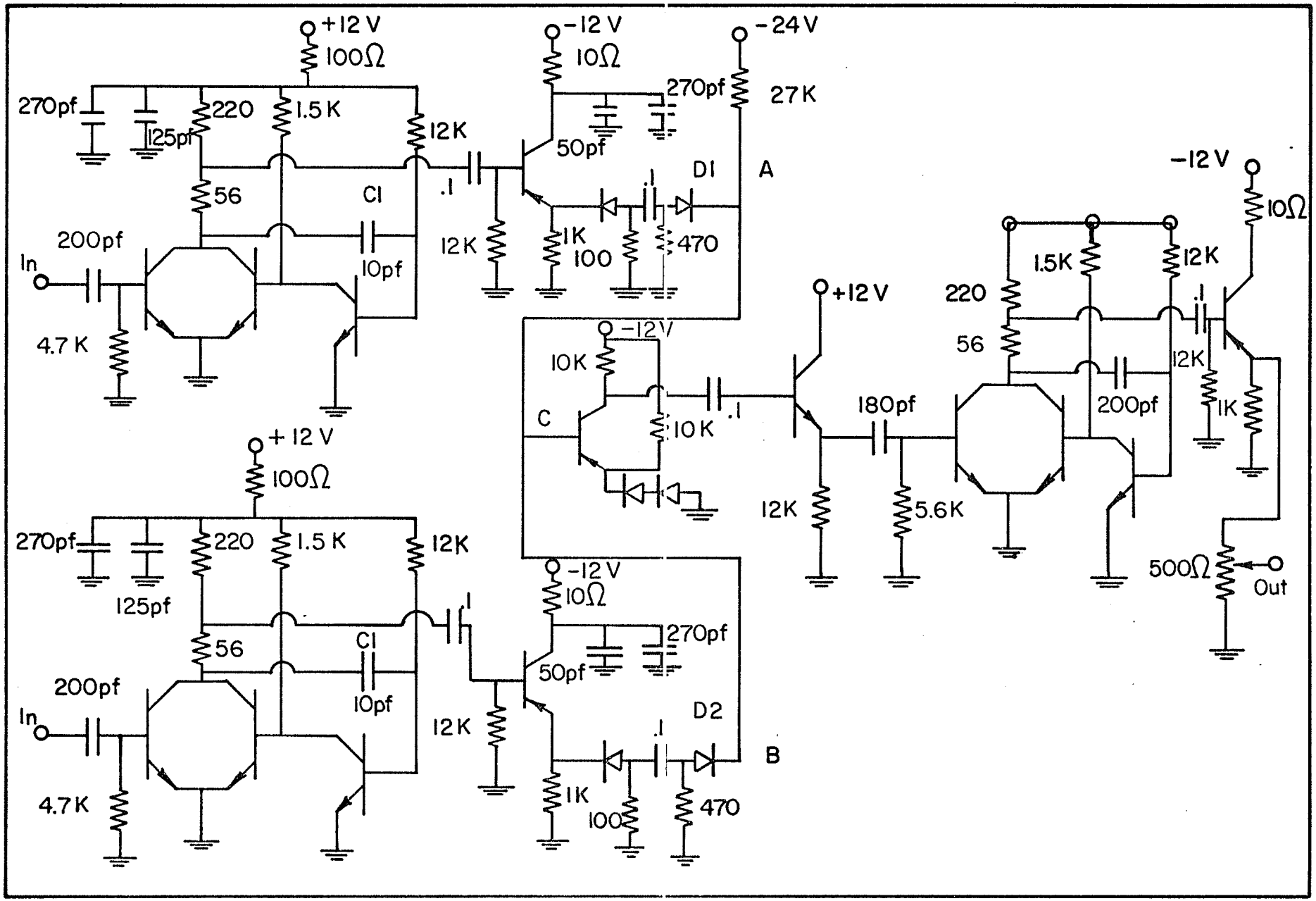
+12 V
100Ω
270pf
125pf
220
1.5 K
12K
56
C1
10pf
200pf
In
4.7 K
.1
12K
-12 V
10Ω
270pf
50pf
27K
-24 V
D1
A
1K
100
470
+12 V
-12V
10K
C
10 K
.1
12K
180pf
5.6K
220
1.5K
56
12K
200pf
1K
-12 V
10Ω
500Ω
Out
+ 12 V
100Ω
270pf
125pf
220
1.5 K
12K
56
C1
10pf
200pf
In
4.7K
.1
12K
-12 V
10Ω
270pf
50pf
D2
B
1K
100
470

variable amplitude. These pulses are then used to activate the linear gate incorporated in the multichannel analyzer.

The overall time resolution of the slow coincidence unit was approximately 200 nsec as determined through the use of uncorrelated γ ray sources, and this agrees with what would be expected from the square pulses arriving at the coincidence element.

2.7 Pulse Height Compensation

a) Effect of Window Width on Time Resolution

In a system using photomultipliers to provide timing information a problem arises due to the fact that the current pulse arriving at the anode has a finite rise time. This is caused by the scintillator's finite decay time and the inherent transit time jitter of the photomultipliers. Now since the rise time of the plate signal is independent of the pulse amplitude and the limiters are run at a cut-off voltage which is an appreciable fraction of the total pulse height, the limiters can only, to a first approximation, remove the effect of varying pulse heights. Fig. 2-7 illustrates the time jitter introduced by varying pulse heights. If in Fig. 2-7 we approximate the rising edges of the anode pulses by straight lines we can then perform a calculation which will give a rough estimate of the magnitude of this effect. In the diagram V is the median voltage of the anode pulses, W is the width in volts of the window, T is the rise time of the pulse at the anode and

Figure 2-7

Schematic of Photomultiplier Anode Pulses

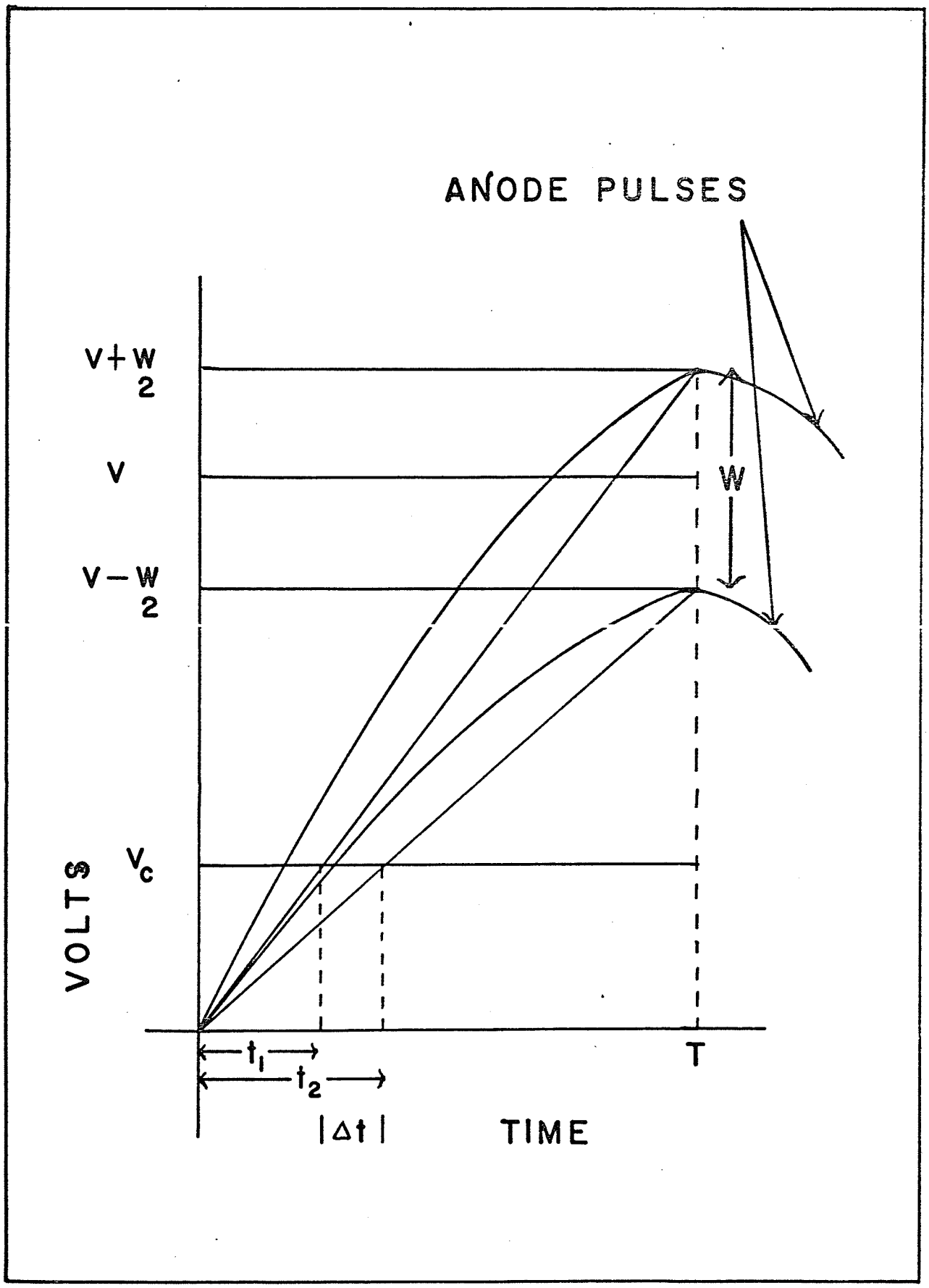
ANODE PULSES
V+W/2
V
V−W/2
W
VOLTS
Vc
t1
t2
T
|Δt|
TIME

V_c is the limiter cut-off voltage.

From simple geometrical considerations we see that:

$$t_1 = \frac{V_c\ T}{V+\frac{W}{2}} \qquad t_2 = \frac{V_c\ T}{V-\frac{W}{2}}$$

Then:

$$\Delta t = t_2 - t_1 = V_c\ T\left(\frac{1}{V-\frac{W}{2}} - \frac{1}{V+\frac{W}{2}}\right)$$

Therefore $\Delta t = V_c\ T\left(\frac{V + \frac{W}{2} - V + \frac{W}{2}}{V^2 - \frac{W^2}{4}}\right)$

and if we neglect $\frac{W^2}{4}$

$$\Delta t = V_c\ T\left(\frac{W}{V^2}\right)$$

Now typical values of the above parameters would be:

V_c = .8 volts

T = 10 x 10^{-9} sec

V = 10 volts

W = 5 volts

and if we insert these in the expression for Δt we find:

Δt = 400 picoseconds

Thus we can see that under reasonably typical operating conditions with a window width of 50% we could expect a time jitter due to the varying pulse heights of the order of 400 psec. The obvious way to minimize this effect is of course

to use narrow energy analyzing windows; During many experiments this is impractical since, as the windows are decreased the counting rate is correspondingly decreased. Also in the case of experiments employing the centroid shift method, in which the position of the centroid channel is measured for a prompt source and for a source containing a lifetime, it is obvious that even with narrow windows the shape of the spectrum over the window can seriously affect the centroid position. Thus unless identically shaped spectra can be obtained from both the prompt and experimental sources large systematic errors may occur.

The method used to overcome this effect in this system is outlined in the next section.

b) Pulse Height Compensator

The P.H.C. used in this apparatus is functionally the same as the one first described by Bell and Jorgensen (1960) in which some fraction of the signals from each of the slow side amplifiers is added to the T.A.C. pulse. Since on the delayed side a larger pulse gives a larger T.A.C. pulse the signal must be phase inverted so that the actual process in the P.H.C. is a subtraction. The process of compensation can easily be explained by considering Fig. 2-8 which plots the centroid channel position of a prompt curve as the single channel analyzer windows are varied across the spectrum. If we now assume that both of the lines in Fig. 2-8 can be

Figure 2-8

Effect of Pulse Height on Centroid Channel Position

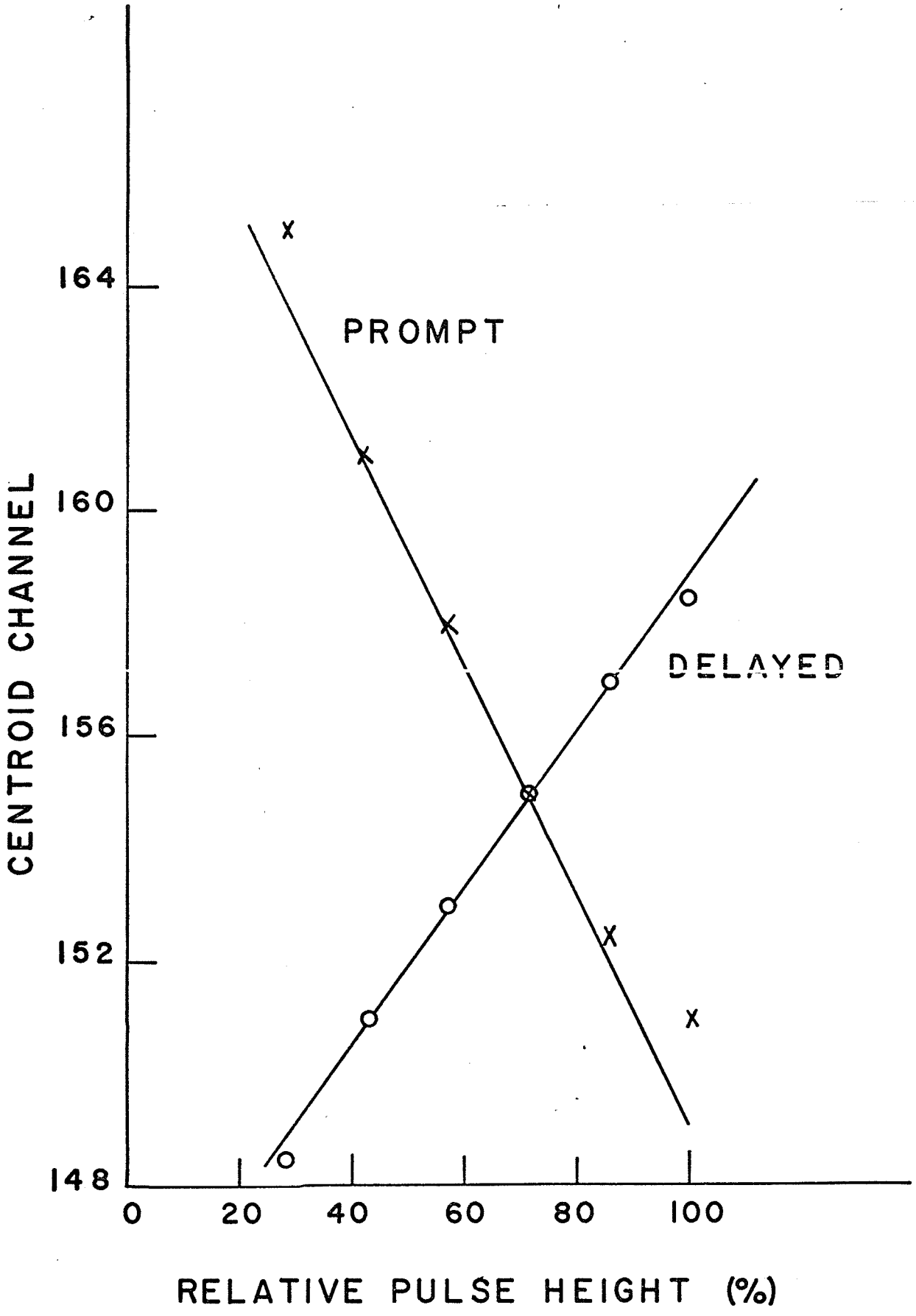
CENTROID CHANNEL
164
160
156
152
148
PROMPT
DELAYED
0
20
40
60
80
100
RELATIVE PULSE HEIGHT (%)

considered as straight lines we can use an analysis similar to that employed by Schwarzschild (1963) to describe what happens. For any particular coincidence the apparent time as detected by the coincidence circuit may be written as:

$$C(t) = T_o + k_D V_D - k_p V_p$$

where T_o is the intersection point of Fig. 2-8, k_p and k_D are respectively the slopes of the prompt and delayed lines and V_p and V_D are the amplitudes of the plate signals.
Now if we form the sum:

$$C^1(t) = C(t) - k_D V_D + k_p V_p$$

then we see that $C^1(t)$ is no longer a function of V_p or V_D. It is precisely this operation that the P.H.C. performs.

The circuit used to perform this operation in the system is shown in Fig. 2-9. The two constants k_1 and k_2 are found empirically by varying the two 1 kilohm input potentiometers until both lines become sensibly flat over the region of interest for a given experiment. The performance of this circuit in eliminating the effect of varying pulse heights is outlined in Section 2.9.

2.8 Calibration Apparatus

The method of calibration used with the time sorting system is based on that described by Graham et al. (1962). In this procedure an air-cored helical delay line is used to provide spaced markers of constant time differences over the

Figure 2-9

Pulse Height Compensator Circuit

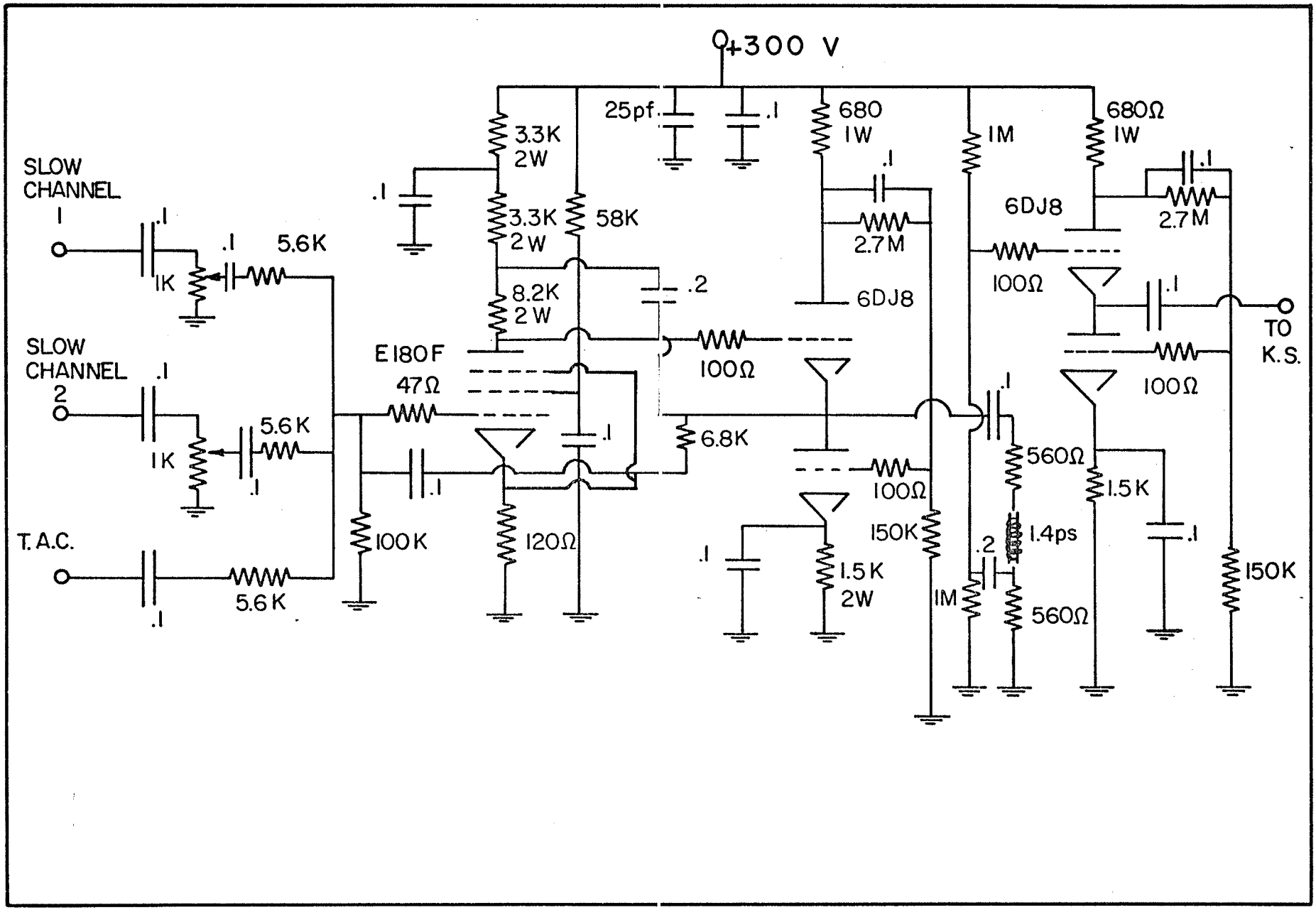
+300 V
SLOW CHANNEL 1
SLOW CHANNEL 2
T. A. C.
.1
1K
5.6K
3.3K 2W
3.3K 2W
8.2K 2W
58K
25pf
.2
E180F
47Ω
100K
120Ω
6.8K
680 1W
2.7M
6DJ8
100Ω
150K
1.5K 2W
1M
680Ω 1W
560Ω
1.4ps
1.5K
150K
TO K.S.

range to be studied. A schematic showing the basic features of the calibration circuitry is shown in Fig. 2-10. Pulses from a Mercury pulser are fed through 50 ohm cable to the moveable carriage. The carriage which has a contact to the center wire and two contacts to the outer ridges of the slotted drum serves to transmit the signals into the delay line. The signals arriving at the delay line are then split and travel to the two opposite ends of the drum. Thus by varying the position of the carriage along the drum one changes the relative time of arrival of the two signals. The signals are then led co-axially out through each end of the drum and through wiper arrangements fed into 100 ohm cables. The signals are then split once again with part passing through the fast test network of the limiters as previously described, and the remainder passing through phase inverters and activating the slow portion of the system. The phase inversion is necessary due to the opposite polarity requirements of the fast and slow sides of the equipment. Fig. 2-11 shows the phase inverters and the trimming capacitors used as variable voltage dividers which allow the pulse heights to be adjusted to fit the window requirements of the system. Set up in this manner the calibration system was able to activate and test both halves of the system simultaneously. Also since calibration could be carried out while actual photomultiplier pulses are activating the limiters the system could be calibrated and checked under

Figure 2-10

Schematic of Calibration Circuitry

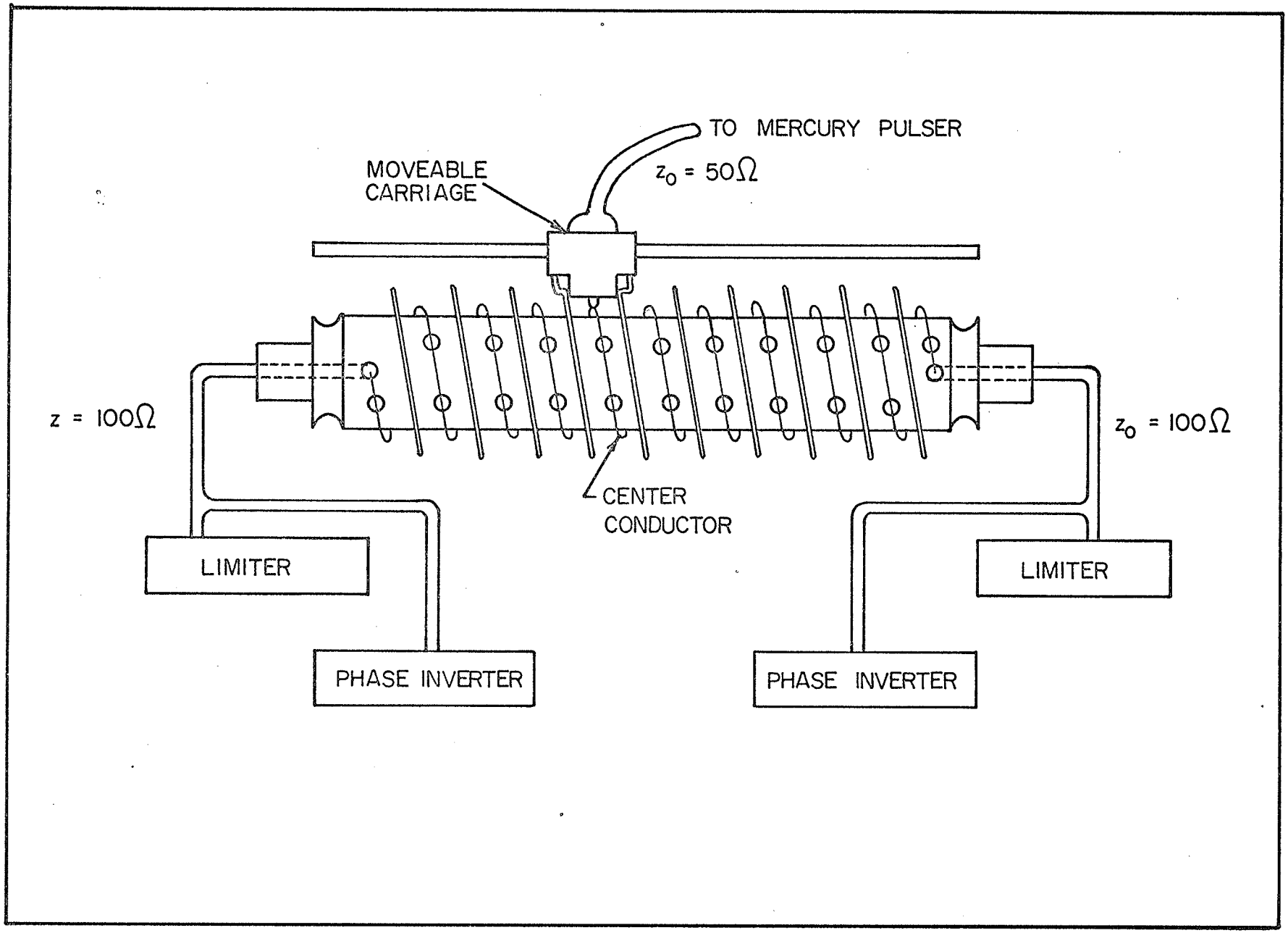
TO MERCURY PULSER
$z_0 = 50\Omega$
MOVEABLE CARRIAGE
$z = 100\Omega$
$z_0 = 100\Omega$
CENTER CONDUCTOR
LIMITER
LIMITER
PHASE INVERTER
PHASE INVERTER

The Helical Delay Line

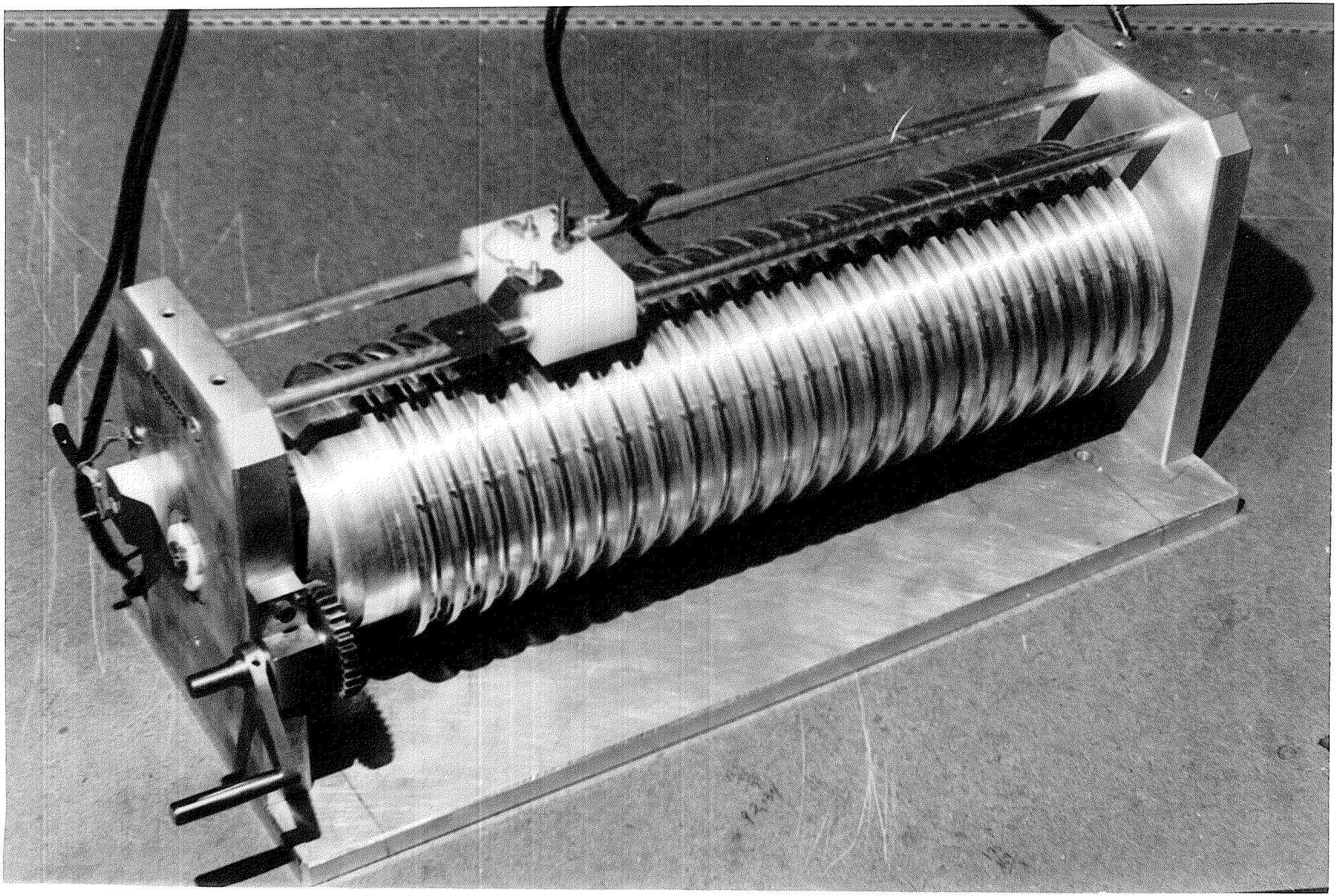

Figure 2-11

Phase Inverter Circuit

Transistors: PNP 2N4258
NPN 2N4274

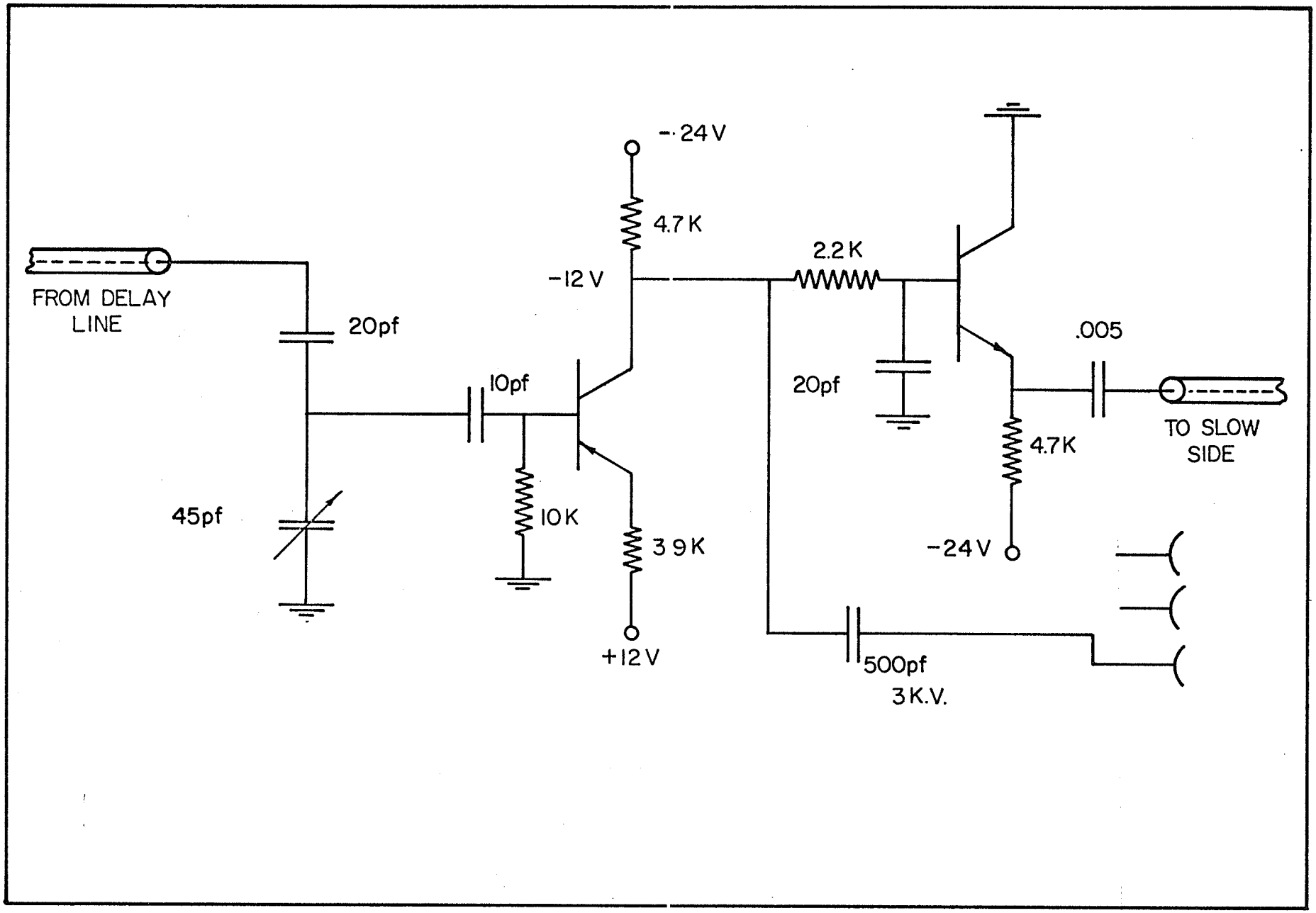
FROM DELAY LINE
20pf
45pf
10pf
10K
-24V
4.7K
-12V
39K
+12V
2.2K
20pf
.005
4.7K
-24V
TO SLOW SIDE
500pf
3K.V.

actual operating conditions.

The mechanical and electrical properties of the drum are similar to those described by Graham et al. (1962). The drum has a characteristic impedance of 100 ohms and like one of the systems they describe is turned manually. Calibration of the drum was achieved by marking equally spaced reference points along the length of the delay line and then calibrating these points by comparison with cables whose delay times were accurately known.

2.9 Circuit Calibration and System Performance

a) Linearity

In a time-sorting apparatus the two system parameters which are of greatest interest are the resolution and the linearity. In this system the linearity was good throughout the range necessary for the experiments conducted. It would however have been limited if experiments concerning longer lifetimes had wished to be attempted. During the construction of the system the linear ranges varied in length as the various models of the equipment were introduced, with the maximum linear range achieved being about 20 nsec. This was more than adequate for the experiments performed. Fig. 2-12 shows an integral linearity curve obtained by use of the helical delay line. In this curve time zero occurs at channel 202 and the sensitivity as found from the curve is .175 nsec per channel. As can be seen a certain amount of non-linearity occurs at

Figure 2-12

Integral Linearity Curve

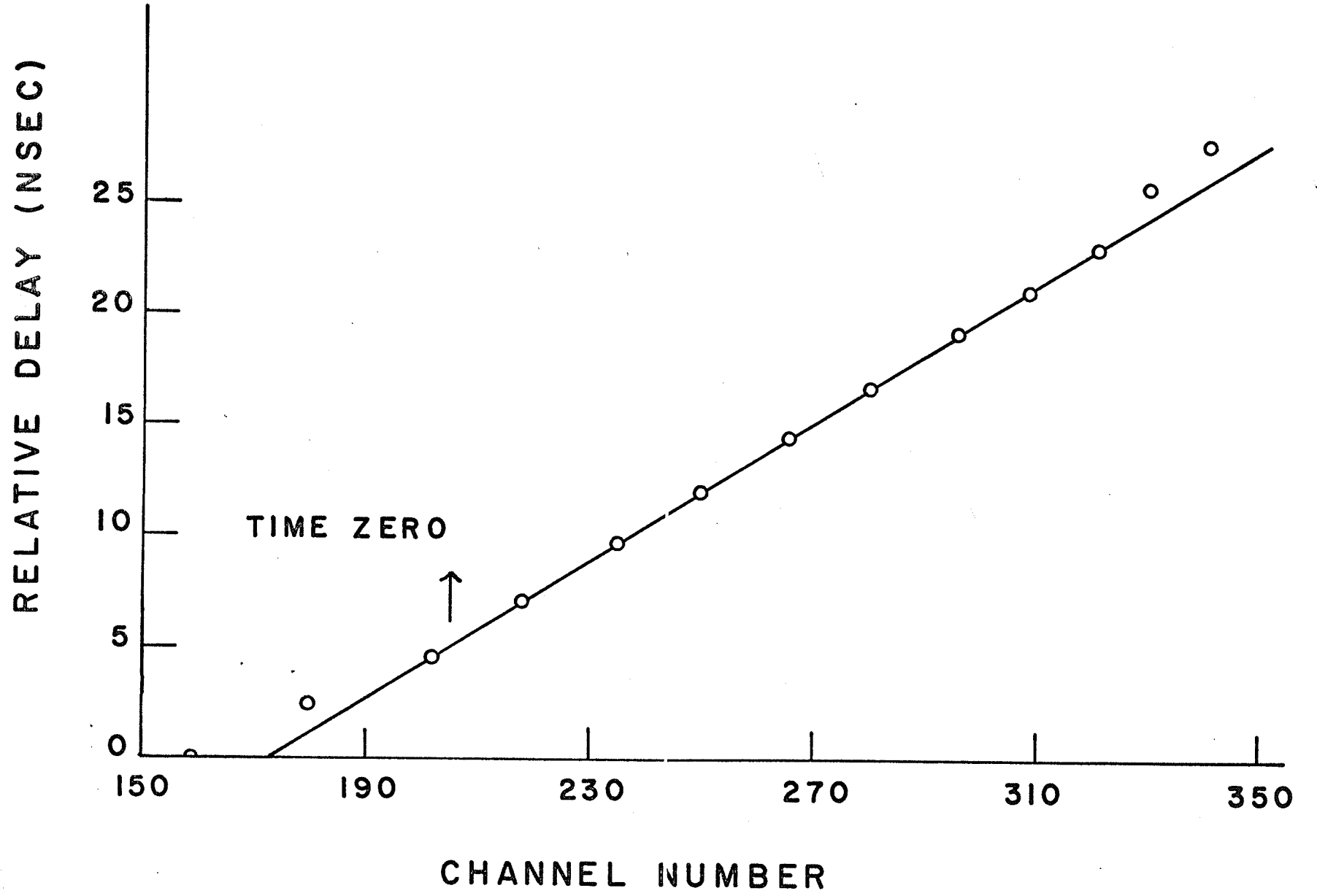
RELATIVE DELAY (NSEC)
25
20
15
10
5
0
TIME ZERO
150
190
230
270
310
350
CHANNEL NUMBER

both ends of the curve limiting the useful region to approximately 20 nsec. A second curve which plots the differential linearity of the system under the same conditions is shown in Fig. 2-13. This curve was obtained by isolating the two photomultipliers of the system and then activating them with uncorrelated γ ray sources. Differential linearity curves of this type are important in that they tend to illustrate any detailed non-linearities which the system may possess. As can be seen in Fig. 2-13 the curve is essentially flat over the useable region. To test whether any variations which may have been present in the curve affected the experimental data, a point by point correction from the differential linearity curve was applied to some of the experimental data. Since it was found this procedure produced no significant changes in the results obtained no corrections of this type were carried out on most of the data.

b) Resolution

The resolution obtainable with the apparatus which has been described was approximately 300 psec. Fig. 2-14 shows a spectrum of Co^{60} obtained under normal operating conditions with fairly wide windows and employing the P.H.C. As can be seen the curve falls almost linearly on the right hand side but shows a certain amount of tailing on the left. Various attempts were made to correct this effect, however no satisfactory solution to this problem was discovered. Since

Figure 2-13

Differential Linearity Curve

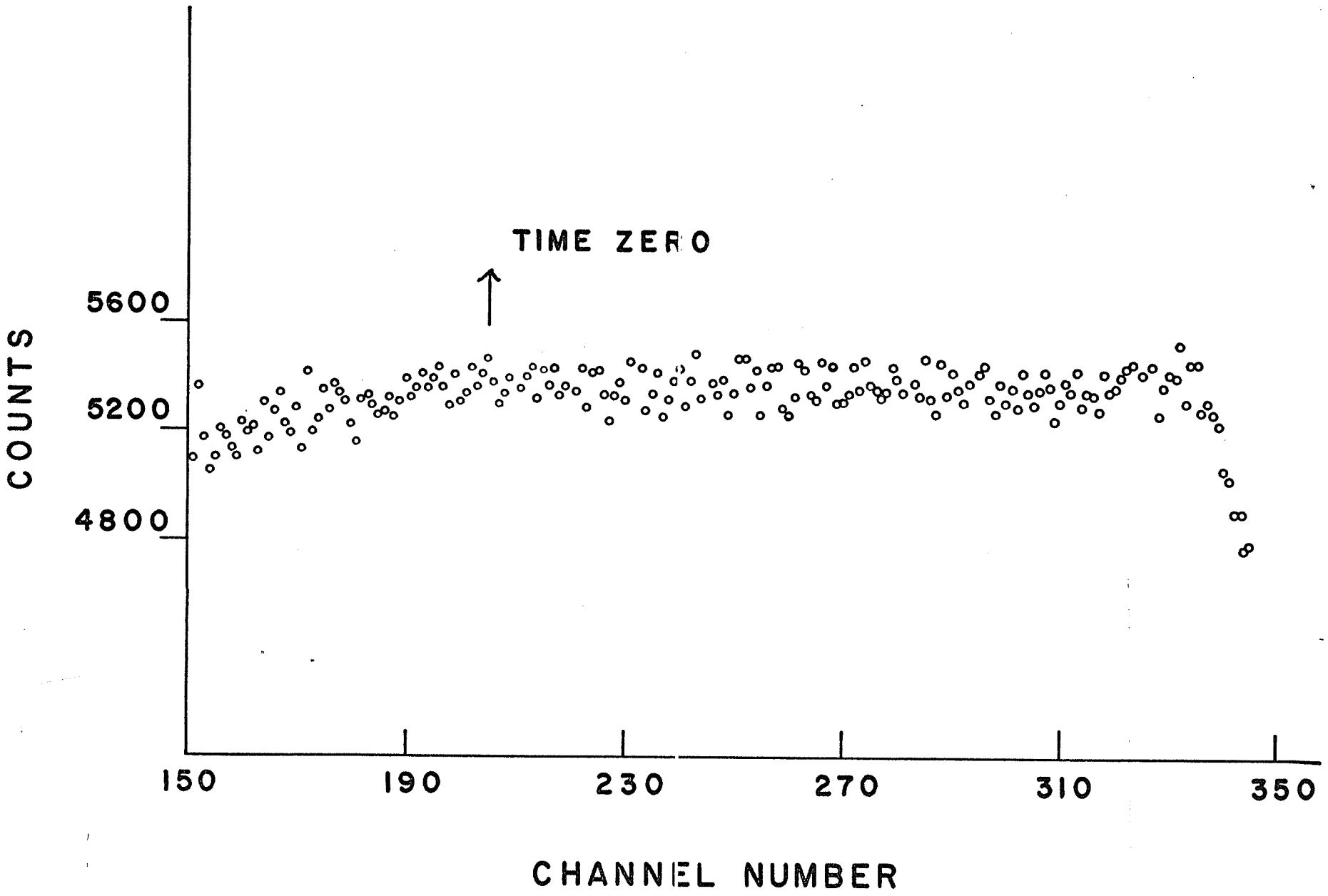
TIME ZERO
5600
5200
4800
COUNTS
150
190
230
270
310
350
CHANNEL NUMBER

Figure 2-14

Co^{60} Resolution Curve

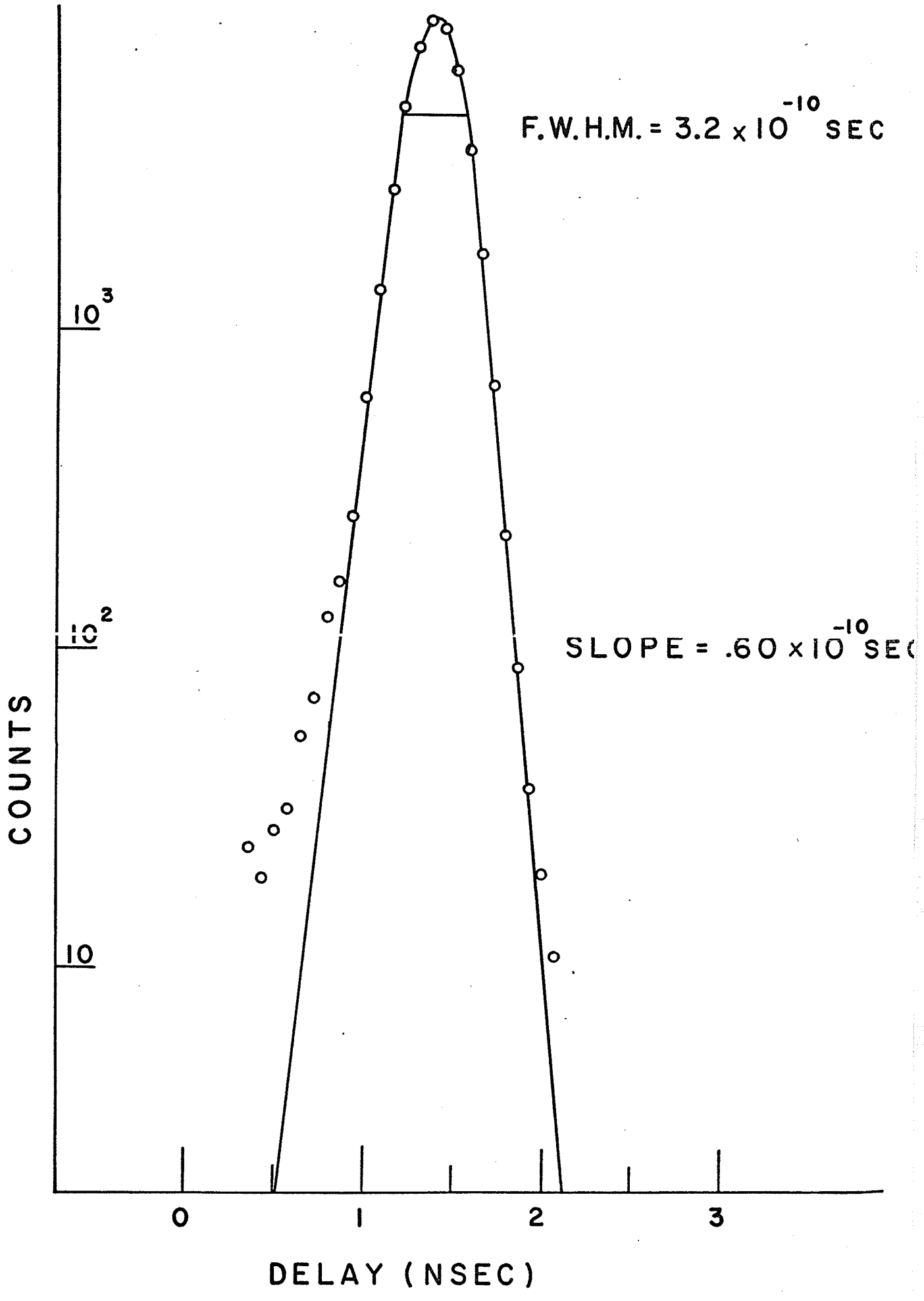
F.W.H.M. = 3.2 x 10^-10 SEC
SLOPE = .60 x 10^-10 SEC
10^3
10^2
10
COUNTS
0
1
2
3
DELAY (NSEC)

lifetimes were measured from the right side of the curve this tailing would not affect the experimental results. Fig. 2-15 shows the effect of the P.H.C. on the resolution. As can be seen with the window widths used during the experiments an improvement in resolution of greater than 2 was obtained by use of this method. Again, on these curves, one can notice the tailing which was present on the left hand side of the curves.

c) Stability

The final parameter which affects the usefulness of a system of this type is the stability against drifts which the apparatus exhibits over periods of time. In this system the stability was very good if the ambient temperature was constant to three or four degrees. Under normal operating conditions typical centroid shifts during given runs were found to be of the order of 50 psec or less since generally the temperature regulation in the labratory was good to 1 or 2°C.

2.10 Temperature Regulation Apparatus

During the course of the experiments performed runs were taken at temperatures ranging from approximately +50°C to -196°C. To achieve temperature regulation during these runs two basic methods were used. The first of the arrangements is shown schematically in Fig. 2-16. This consisted of a liquid nitrogen reservoir which cooled, through a series of

Figure 2-15

Co^{60} Resolution Curve Showing Effect of Pulse Height Compensation

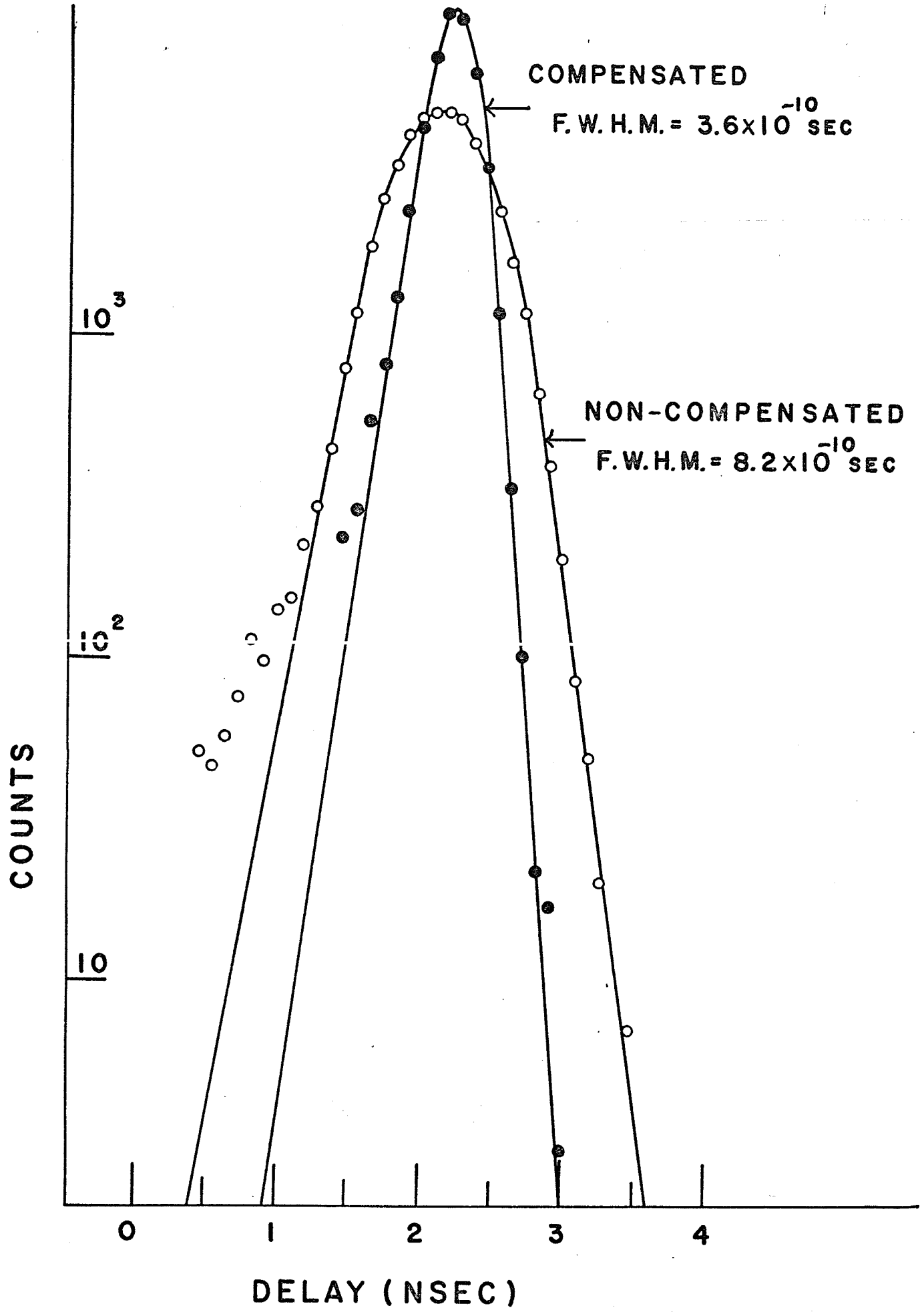
COMPENSATED
F.W.H.M. = 3.6x10^-10 SEC
NON-COMPENSATED
F.W.H.M. = 8.2x10^-10 SEC
10^3
10^2
10
COUNTS
0
1
2
3
4
DELAY (NSEC)

Figure 2-16

Temperature Regulation Apparatus

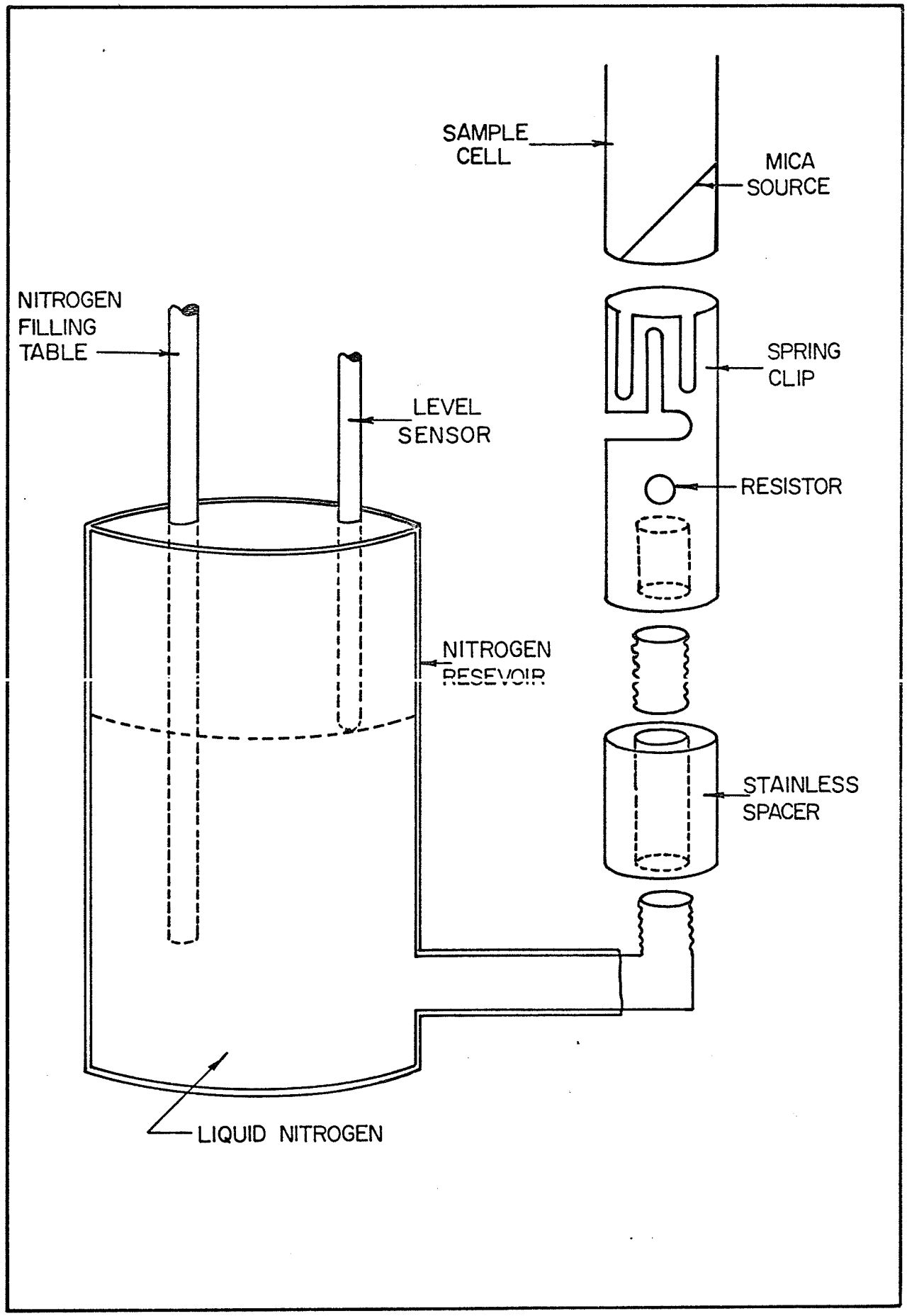
SAMPLE CELL
MICA SOURCE
NITROGEN FILLING TABLE
SPRING CLIP
LEVEL SENSOR
RESISTOR
NITROGEN RESEVOIR
STAINLESS SPACER
LIQUID NITROGEN

spacers, a spring clip made of aluminum. The glass sample cell fitted tightly into the spring clip and thus was cooled to the desired temperature. Temperature readings were made from a thermocouple attached to the outside of the glass cell. While it was felt at first that the outside and inside temperature of the sample cell may not have been the same, tests utilizing a low temperature thermometer inside the sample cell indicated that if a sufficient cooling period was allowed the temperatures were identical. To achieve temperature variation larger and smaller stainless steel spacers were employed and to achieve fine variations the required power was fed into the resistor in the spring clip. Using this method temperature variations during a run were typically less than $1^{o}C$. The filling device for the nitrogen resevoir consisted of a level sensing mechanism (Fig. 2-17), which opened and closed a solenoid valve on the transfer line, allowing nitrogen to transfer from a 25 litre dewar whenever the level dropped below a predetermined point. Nitrogen consumption varied with the various configurations employed but was typically of the order of 1 litre per hour. Since this arrangement achieved a minimum temperature of only $-150^{o}C$ a second method had to be employed at lower temperatures. This consisted of inserting an aluminum rod into the spring clip and then immersing the rod into a dewar of liquid nitrogen to the depth necessary to achieve the required temperature. The

Figure 2-17

Liquid N_2 Level Control Circuit

Transistors: PNP 2N3702

Diodes: Ge 1N3121

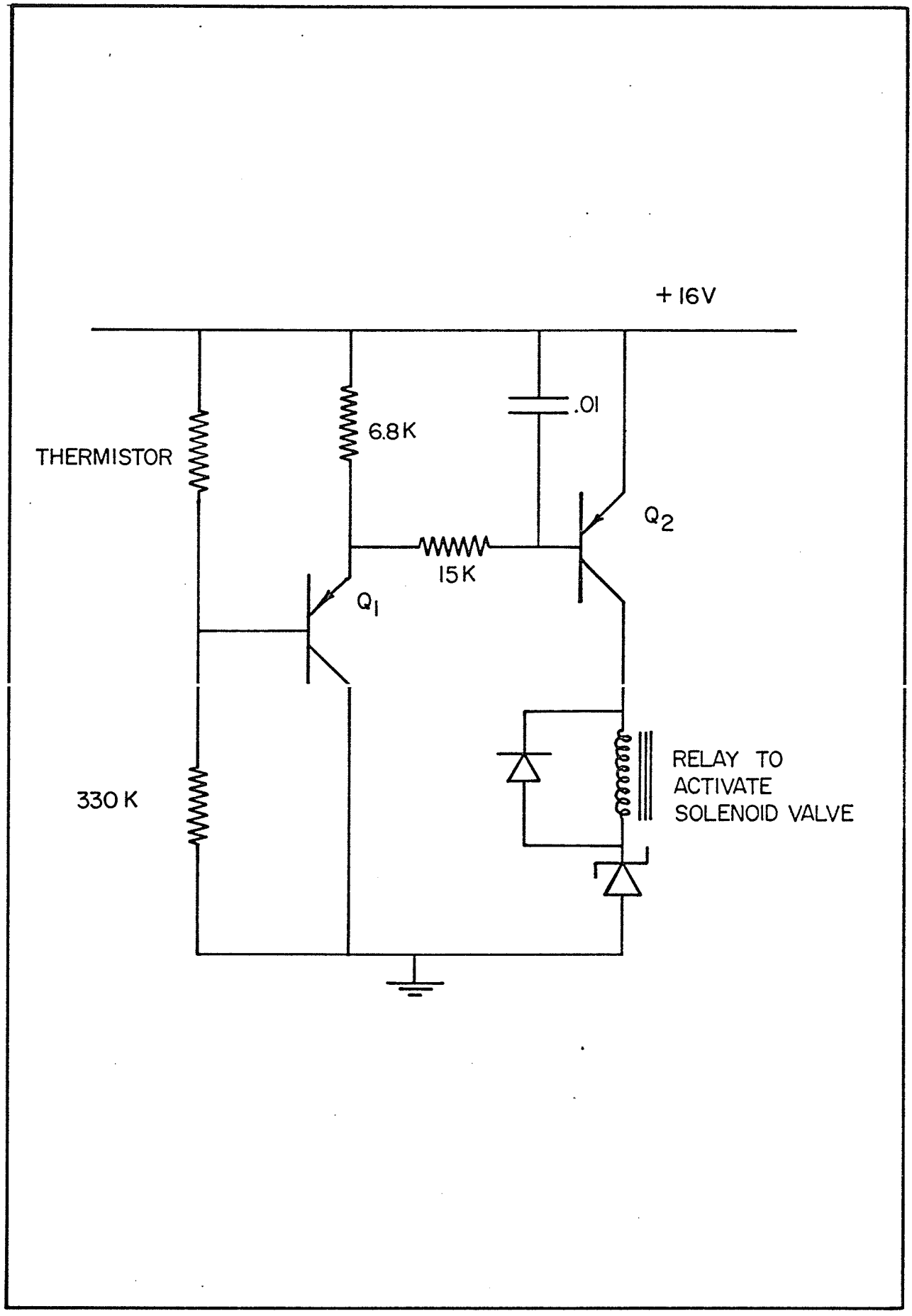
+16V
THERMISTOR
6.8K
.01
Q2
15K
Q1
330 K
RELAY TO
ACTIVATE
SOLENOID VALVE

nitrogen level was then held constant by use of the level controller and filling system. With this arrangement temperatures down to liquid nitrogen could be achieved. The temperature regulation was good to only $\pm 4^{o}C$ due to the response time of the filling system. Fortunately it was not a major problem as the experimental parameters being measured were found to be fairly insensitive at these temperatures so no attempt was made to improve this part of the system.

CHAPTER III

EXPERIMENTAL PROCEDURE AND DATA ANALYSIS

3.1 Source Preparation

The radioactive source used throughout the experiments consisted of Na^{22}, which is a positron emitter with a half-life of 2.58 years. Na^{22} has the property that when it emits a positron it forms Ne^{22} in an excited state which subsequently de-excites by emission of a 1.28 MeV γ ray. Since the time lapse between the appearance of the positron and the subsequent emission of the nuclear γ ray is short (less than 10^{-11} sec) compared to the resolving time of the time-sorting system (3×10^{-10} sec) experimentally we consider the two events to be coincident.

In the course of the experiments performed two types of sources were used. The first type was that in which the radioactive material was deposited on a supporting backing, while in the second type the radioactivity was diffused equally throughout the media under study.

Since $Na^{22}Cl$ was not soluble in most of the substances studied, open faced mica layers were used as source backings. The sources were prepared by evaporating aqueous $Na^{22}Cl$ solution on to thin sheets of mica (2 mg/cm^2) over an area of approximately 1 cm^2. Mica was chosen for the source backings since it does not exhibit any long lifetime in its time

spectrum and also since if thin backings are used it absorbs only a small fraction of the positrons emitted. Bertolaccini and Zappa (1967) conducted experiments to ascertain the fraction of positrons decaying in a mica source and found that for a sandwich source employing mica of the thickness which we used, approximately 6% of the positrons decay in the source backings. Therefore in an open source of the type we employed probably not more than three or four percent of the positrons annihilated in the mica. Since these events all register in the prompt peak they would not affect the lifetimes obtained. They would however tend to introduce a small uncertainty of the order of .5% into the intensity measurements obtained. This effect was therefore corrected for in cases where it was significant.

For the experiments in which the $Na^{22}Cl$ was soluble in the media under investigation two types of sources were employed. In the first method the $Na^{22}Cl$ was simply dissolved in the medium. This had the advantage that no supporting foils were present, however it had the disadvantage that annihilations could take place in the walls of the containing vessel and also that the $Na^{22}Cl$ might itself effect the substance under study. The first effect could be minimized by having a sufficient volume of the substance under study to minimize the percentage of annihilations taking place in the walls of the vessel and then by correcting the data if necessary for those

that remained. The second effect was tested for by employing a sealed Havar source to test for any differences in the spectra. The Havar source, which used polyethelene 'O' rings for sealing, was used since it was found difficult to seal mica sources sufficiently well for use in the substances tested.

3.2 Sample Preparation

During the course of the experimental work a number of different substances were studied. Since these substances varied in their physical characteristics different ways had to be evolved to handle the various types. The first general class of substances studied could be characterized as organic liquids which were liquid at room temperature. Samples of this type presented no problem in their preparation since all that was necessary was to acquire samples of research grade purity and place them in clean test-tubes. In the experiments performed on these samples, runs were taken on degassed as well as normal air-saturated ones. The degassing was achieved by use of the vacuum freeze-thaw technique in which the sample was repeatedly frozen and then pumped on. By employing this technique a low concentration of oxygen in the sample was achieved. To measure the amount of oxygen remaining in the sample after degassing some samples were analyzed mass spectroscopically and were found to contain less than 1% of the amount of oxygen present in an air-

saturated sample.

The second class of substances studied were condensed gases which exhibited high vapor pressures at room temperature. These substances therefore had to be kept cooled at all times and had to be contained in a closed vacuum system. The basic distillation and transfer apparatus used in these experiments is shown in Fig. 3-1. The distillation system was used in two different ways. For the experiments concerning NH_3, Ammonia gas was first transferred from its container into the storage cell of the system. The storage cell contained Sodium metal which trapped any impurities present in the Ammonia. The NH_3 was then transferred from the storage cell into the sample cell. The sample cell was then removed from the distillation apparatus and placed in the Aluminium clip as described previously. The Mercury Manometer served as both a safety valve in case the pressure in the system became too great and as a way of monitoring the pressure in the system during transferring operations. A thin layer of vacuum pump oil was introduced above the Mercury column to prevent the diffusion of Mercury vapor into the apparatus.

For the experiments employing other condensed gases besides NH_3, the appropriate substance was let into the sample cell directly from the other input to the system. Once filled

Figure 3-1

Distillation and Transfer Apparatus

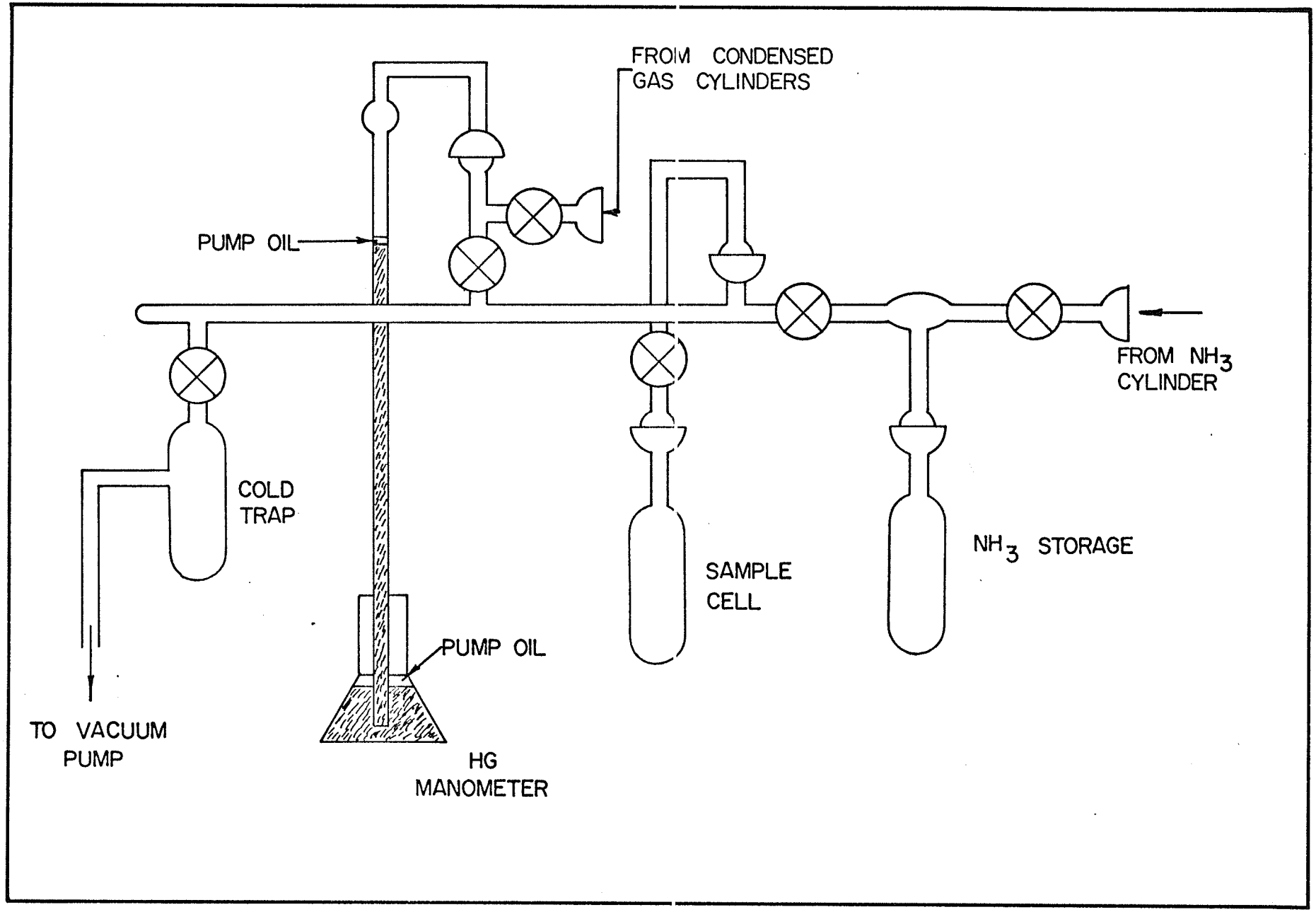
FROM CONDENSED
GAS CYLINDERS
PUMP OIL
FROM NH_3
CYLINDER
COLD
TRAP
SAMPLE
CELL
NH_3 STORAGE
PUMP OIL
TO VACUUM
PUMP
HG
MANOMETER

to the correct level the sample cell was again removed from the distillation system and placed in the Aluminium clip.

3.3 Data Accumulation

During the course of the experiments performed, runs lasting anywhere from a few hours to a few days in length were recorded. During these times from a few thousand to one-hundred thousand counts were accumulated in the peak channel of the spectrum. After each run a background was noted from a portion of the spectrum not affected by true coincidences. Also after almost all runs a time calibration curve for the system was recorded.

Data Analysis

In positron annihilation lifetime work the parameters of interest which one finds experimentally are the lifetimes and intensities of the various decay modes. In cases where no positronium is formed the spectra exhibit a single decay mode. In cases where positronium is formed, however, theory predicts that at least three different modes of decay should be operative. These are decay due to the pick-off of triplet positronium, decay of free positrons and decay of singlet positronium. The problem in analyzing the experimental spectra is then one of finding the parameters of the various exponential terms which make up the spectra.

To analyze the data use was made of an I.B.M. 360-65

computer and a multi-exponential curve fitting program developed by W. R. Wall (1968).

The program assumes that the experimental spectra can be represented by a sum of exponential terms such that:

$$3\text{-}1 \qquad f_i = \sum A_k \, e^{\frac{-t_i}{\tau_k}}$$

where $k = 1 \ldots n$ and $i = 1 \ldots N$

$$3\text{-}2 \text{ or} \qquad f_i = f(i; q_j)$$

where $j = 1 \ldots 2n$

where n is the number of components in the spectra and N is the number of data points.

The program employs a least-squares approach in which the parameters q_j are chosen to minimize the sum of the weighted squares of the deviations of the data from the assumed function such that a minimum value is sought for:

$$3\text{-}3 \qquad R^2 = \sum w_i \, (r_i - f_i)^2$$

where $i = 1 \ldots N$

where r_i is the ith data point and w_i are the weights associated with r_i.

Since the assumed function $f(i; q_j)$ is not linear the Gauss method of linearization is employed. In this method initial guesses of the parameters are made q_j° and Eq. 3-1 is expanded in a truncated Taylor series:

$$3\text{-}4 \qquad f_i \approx f(i; q_j^{\circ}) + \sum \left(\frac{Jf}{Jq_j} \right)_{\circ} \delta q_j$$

where $j = 1 \ldots 2n$.

Since this equation is then linear with respect to the parameter changes δ_j, standard techniques can then be used to determine the changes. These changes are then used to determine better initial guesses and by iteration the process is continued until predetermined convergence criteria for the parameters are met.

A problem arises in analyzing experimental positron lifetime spectra in that rather than being a pure sum of exponentials the spectra is made up of a system response function, plus the sum of exponentials. Wall (1968) has performed a detailed analysis of the effects on the exponential parameters of folding a gaussian system response function with a sum of exponentials. His analysis shows that the exponential time behavior of the input function is accurately reproduced in the output at times larger than four or five standard deviations of the gaussian system response function. Also he shows that the error in the projected amplitude will be less than 1% if:

$a\delta \leq 0.1$ where

a-is the inverse of the exponential time constant

δ -is the standard deviation of the system response function.

Since $a\delta$ was less than 0.1 for our spectra no attempt was made to correct for this effect. Also to avoid distortion

of the exponential portion of the spectra by the system response function, analysis was always started a sufficient number of channels away from time zero such that no distortion should occur.

The computer program also included in it a correction for the finite channel width of the experimental data. This is necessitated since the experimental data obtained is not a smooth sum of exponentials but rather a histogram in which pulses in adjacent ranges of heights are stored in consecutive channels. To study the effect this will have on the derived parameters we consider the case where the width of the time channel is λ seconds. Then if we denote the time spectra of interest by f(t) the number of counts in channel i, r_i will be given by:

$$3\text{-}5 \qquad r_i = \int_{(i-1)\lambda}^{i\lambda} f(t)\, dt$$

and in our case since we are dealing with a sum of exponentials we let

$$3\text{-}6 \qquad f(t) = Ae^{-t/\tau} .$$

Then:

$$3\text{-}7 \qquad r_i = A\tau e^{\frac{-i\lambda}{\tau}} (e^{\lambda/\tau} - 1)$$

where i = 1, 2, 3, ...

or $r_i = A^1 e^{\frac{-i\lambda}{\tau}}$ where:

$$3\text{-}8 \qquad A^1 = A\tau(e^{\lambda/\tau} - 1)$$

Thus we see that the fact that the experimental data is

in the form of a histogram does not change the time constant τ but does effect the amplitude of the distribution. Therefore the computer program utilizes Eq. 3-8 to correct for this fact.

Since in positron annihilation studies the results are quoted as lifetimes and intensities rather than lifetimes and amplitudes the computer program carries out a further procedure. This procedure produces the intensity of a given component in the following way:

The number of counts in the component under consideration are found from the equation:

$$S = \int_{i_o}^{N\lambda} A_k \, e^{\frac{-t}{\tau_k}} \, dt$$

where: k - denotes the component

N - denotes the number of data points

λ - denotes the channel width

i_o - denotes the time-zero of the system.

This value is then divided by the total number of counts in the spectrum to give the intensity I_k. The positron of time-zero for the system was determined experimentally through the use of a Co^{60} source.

Finally the computer program produced least-squares standard deviations for each of the parameters and also a chi-squared variance which was a test of the goodness of fit of the

data.

To check how well the program worked test data was constructed with the computer using as the working function the equation:

$$r_i = A\tau e^{-\frac{i\lambda}{\tau}} (e^{\lambda/\tau} - 1)$$

The points found by utilizing various parameters in this equation were then randomized according to a $1/r_i^2$ procedure which should produce spectra very close to the type of experimental spectra we were working with. The test data so constructed was then fed into the multi-exponential curve fitting program and in all cases the fits obtained were within the standard deviations.

In the actual analysis of the experimental data the initial estimates were found from graphs of the spectra. In all cases two component fits were applied to the data since it was found impossible to separate the shortest lived component from the system response function meaningfully.

The errors quoted throughout the work are either the standard deviations produced by the computer program or in the cases where a number of runs were taken for the same quantity the standard deviations of the various runs.

CHAPTER IV

EXPERIMENTAL RESULTS

4.1 Ammonia

For the work on Ammonia the samples were prepared by vacuum distilling the Ammonia from a Sodium Ammonia solution in order to remove any water present. This procedure was carried out in the distillation apparatus previously described. The Ammonia was then degassed by repeated freezing and pumping, after which it was transferred into the temperature regulating equipment.

Since $Na^{22}Cl$ is soluble in Ammonia most of the runs were taken with the source of $Na^{22}Cl$ in solution with the Ammonia. The experimental curves were then checked for any extra components in the spectra which may have arisen from the annihilation of positrons in the glass walls of the sample cell. None was found so no correction for this effect was attempted. Also to check whether the small amount of $Na^{22}Cl$ source dissolved in the Ammonia sample had any effect on the results, a number of runs were taken using a sealed Havar source. Since these runs gave results consistent with the first method it was concluded that the dissolved $Na^{22}Cl$ had no significant effect on the experimental results.

Figures 4-1 to 4-5 show some typical lifetime curves obtained for Ammonia at various temperatures. These curves

have been plotted directly from the experimental points after subtraction of background. The straight lines drawn through the points are visual fits to the data. From the plotted curves initial estimates for the computer analysis could be calculated. Computer analysis for each of the curves obtained was then carried out and Table 4-1 gives a complete list of the decay parameters found for Ammonia at the various temperatures.

Figures 4-6 to 4-9 illustrate the temperature dependence of the decay parameters. The solid lines drawn through the experimental points are simply best fits and the arrows indicate the temperature at which the liquid-solid phase change takes place.

Table 4-1

Ammonia

Temp (°C)	τ_2 (nsec)	τ_1 (nsec)	I_2 (%)	I_1 (%)
-196	.88 ± .01	.35 ± .01	25 ± 2	62 ± 6
-174	.87 ± .03	.26 ± .02	27 ± 2	61 ± 7
-151	.88 ± .04	.32 ± .03	28 ± 4	59 ± 12
-131	.92 ± .04	.31 ± .03	26 ± 4	64 ± 11
-129	.95 ± .03	.34 ± .03	26 ± 4	64 ± 10
-115	.90 ± .04	.35 ± .03	29 ± 5	59 ± 12
-100	1.00 ± .04	.34 ± .03	28 ± 4	63 ± 13
- 98.5	1.29 ± .04	.40 ± .02	24 ± 3	64 ± 6
- 96.5	1.35 ± .04	.44 ± .03	27 ± 4	71 ± 7
- 88	1.42 ± .04	.45 ± .03	22 ± 1	64 ± 6
- 85	1.57 ± .03	.36 ± .02	22 ± 2	71 ± 6
- 83	1.67 ± .03	.36 ± .02	22 ± 2	74 ± 6
- 67	1.78 ± .03	.36 ± .02	25 ± 2	69 ± 6
- 65	1.81 ± .04	.37 ± .03	25 ± 2	66 ± 7
- 49	1.96 ± .03	.38 ± .02	24 ± 1	63 ± 6
- 46	2.05 ± .04	.41 ± .03	23 ± 3	71 ± 8

Figure 4-1

Time Spectra of Ammonia at -49°C

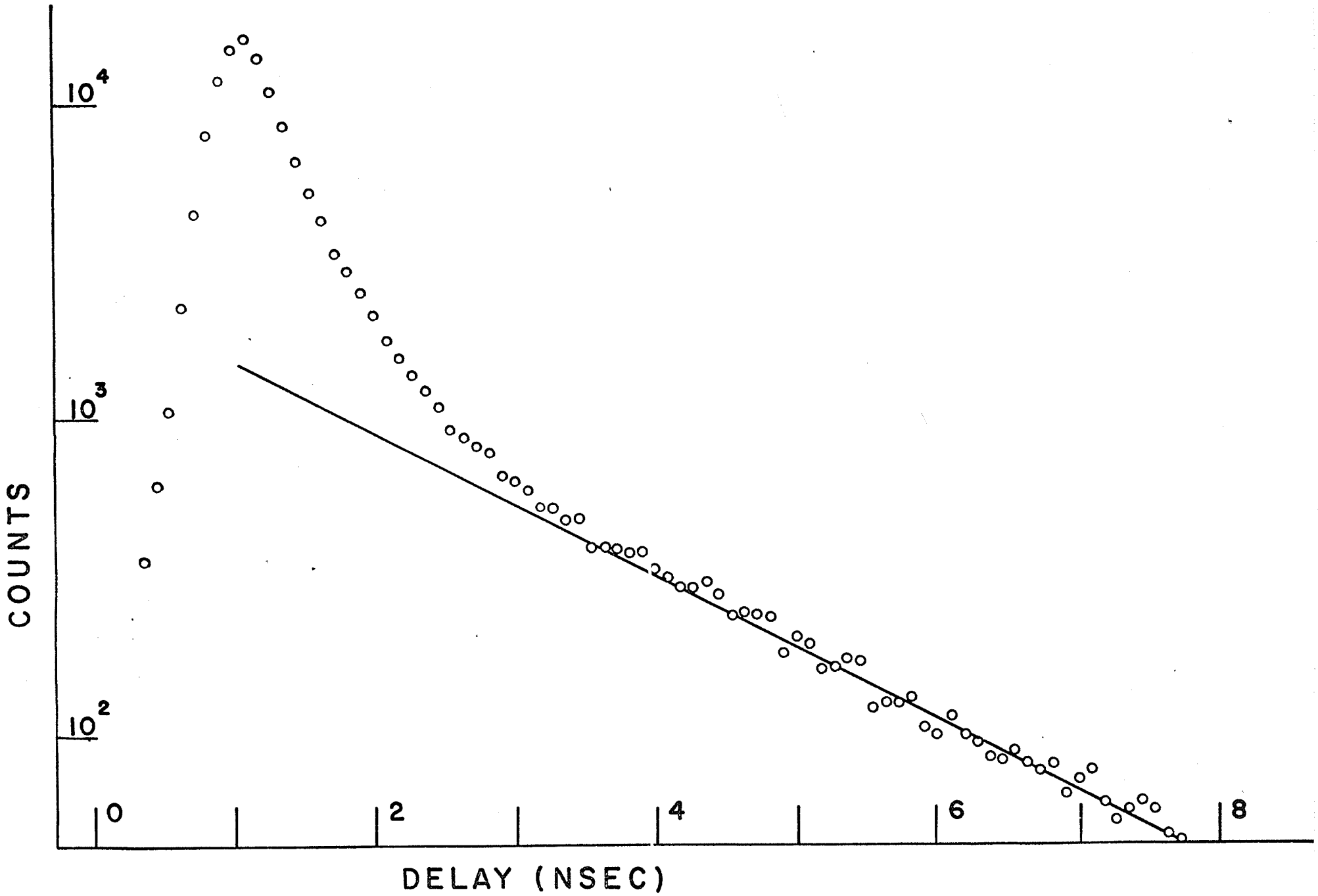
10^4
10^3
10^2
COUNTS
0
2
4
6
8
DELAY (NSEC)

Figure 4-2

Time Spectra of Ammonia at -67°C

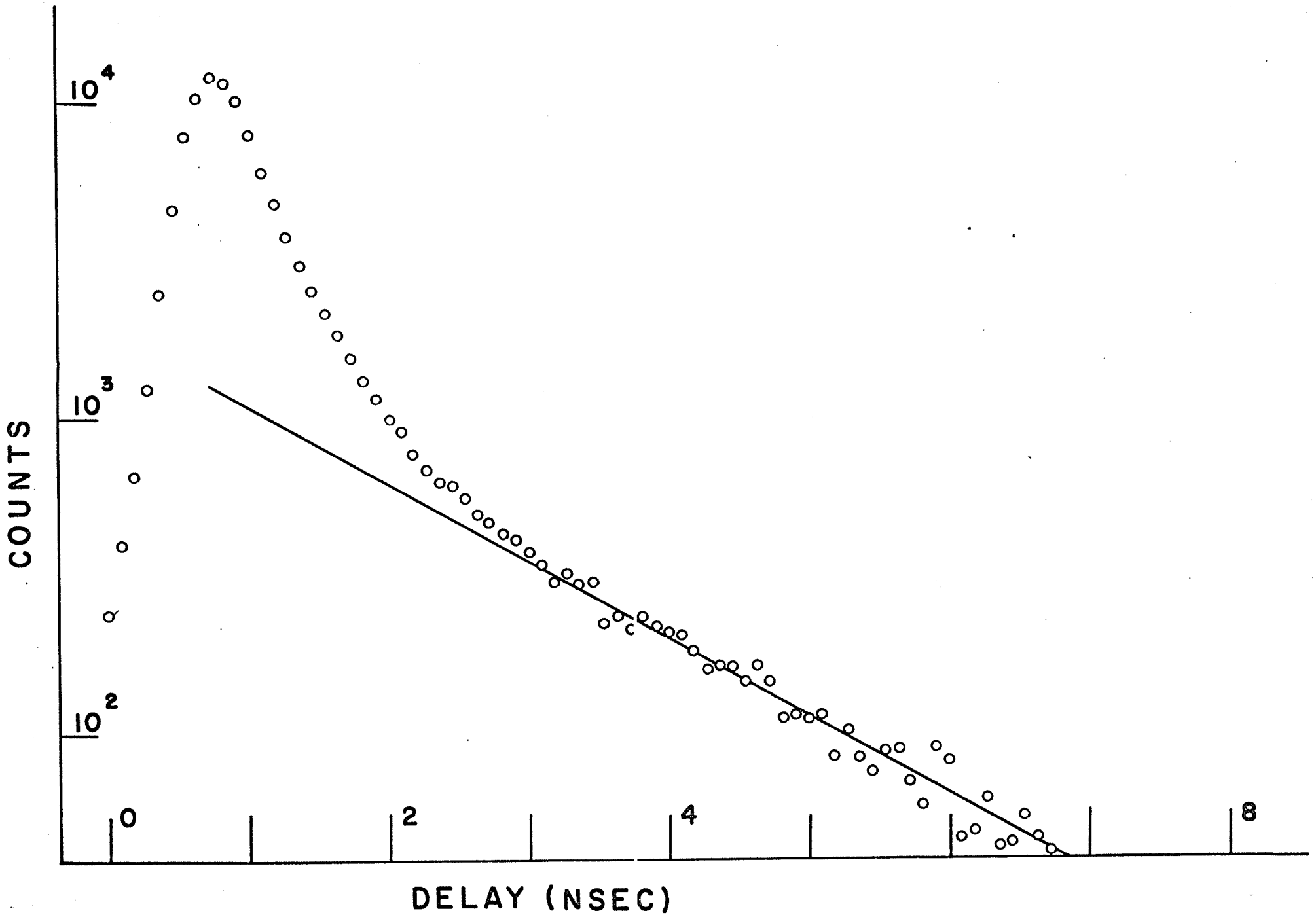
COUNTS
10^4
10^3
10^2
0
2
4
8
DELAY (NSEC)

Figure 4-3

Time Spectra of Ammonia at -98.5°C

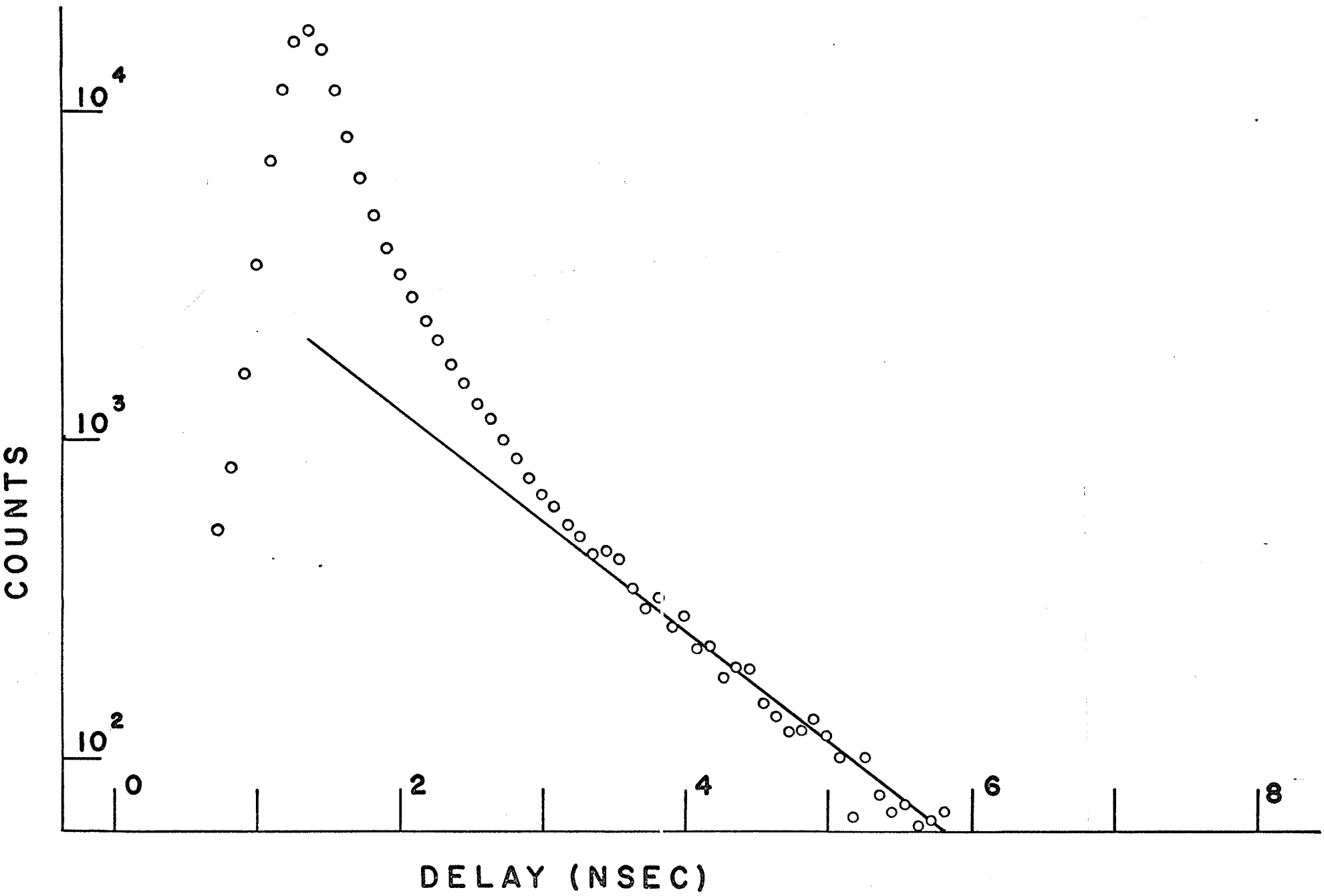
COUNTS
10^4
10^3
10^2
0
2
4
6
8
DELAY (NSEC)

Figure 4-4

Time Spectra of Ammonia at -131°C

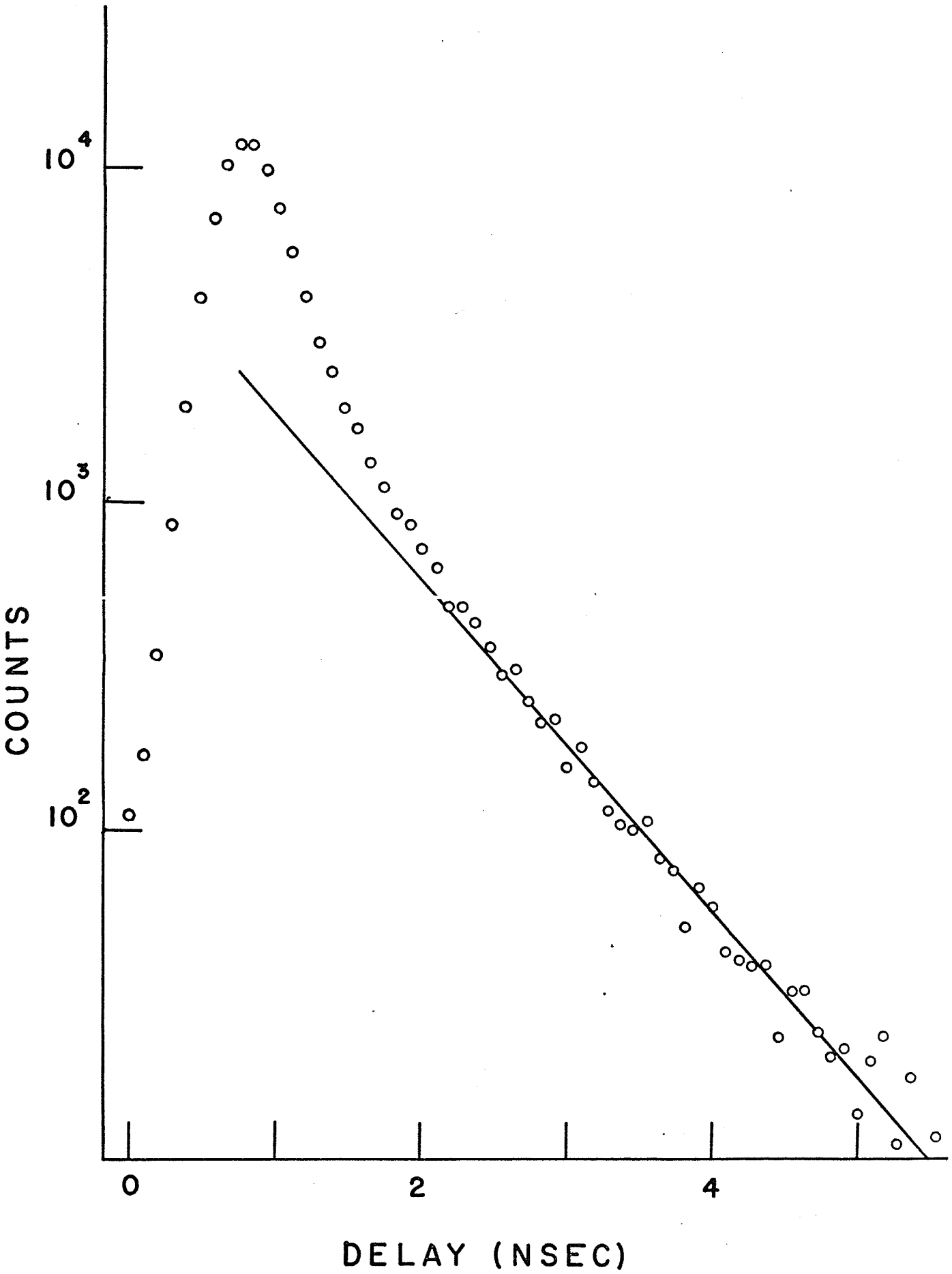
10^4
10^3
10^2
COUNTS
0
2
4
DELAY (NSEC)

Figure 4-5

Time Spectra of Ammonia at $-174^{\circ}C$

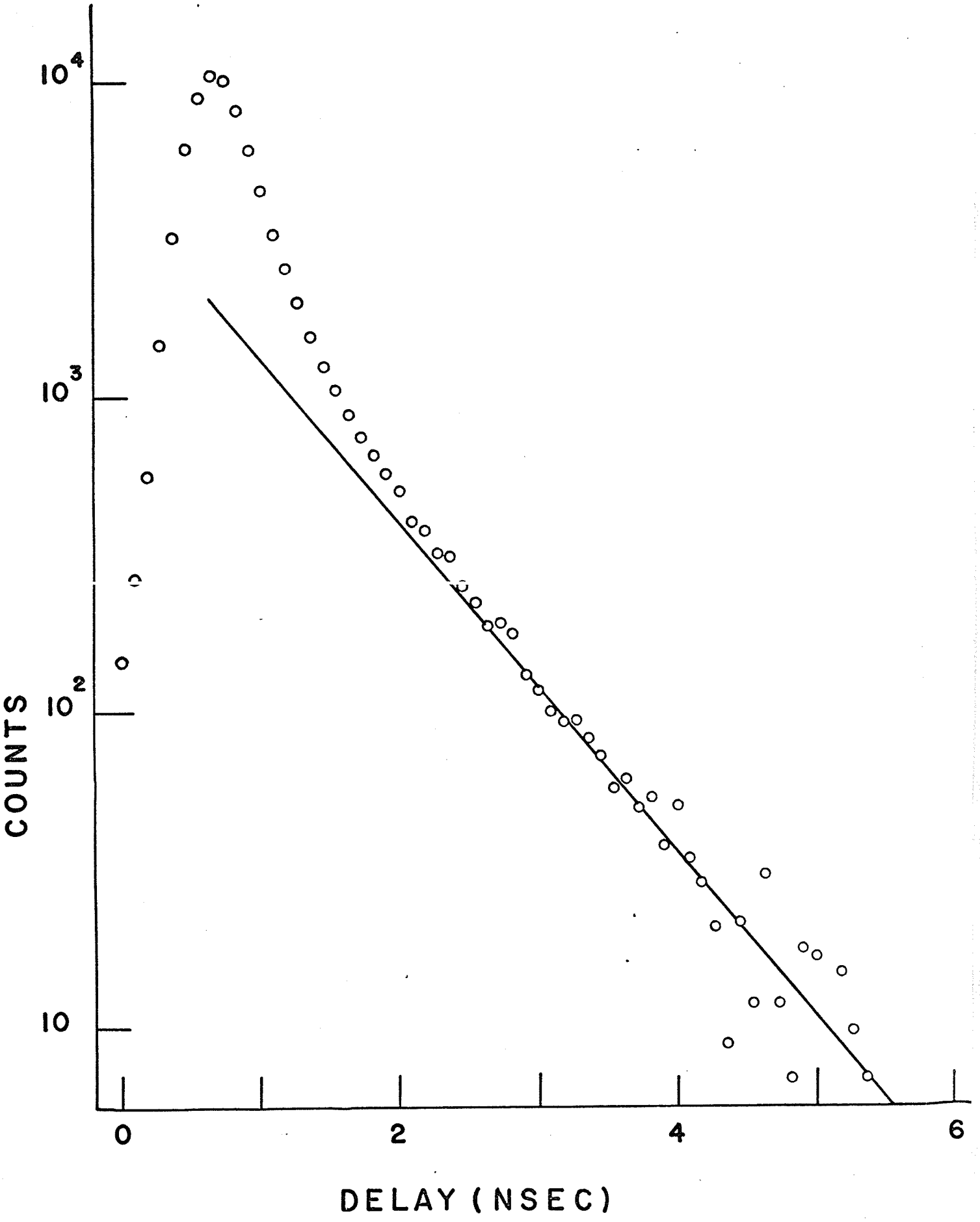
10^4
10^3
10^2
10
COUNTS
0
2
4
6
DELAY (NSEC)

Figure 4-6

Temperature Dependence of T_2 for Ammonia

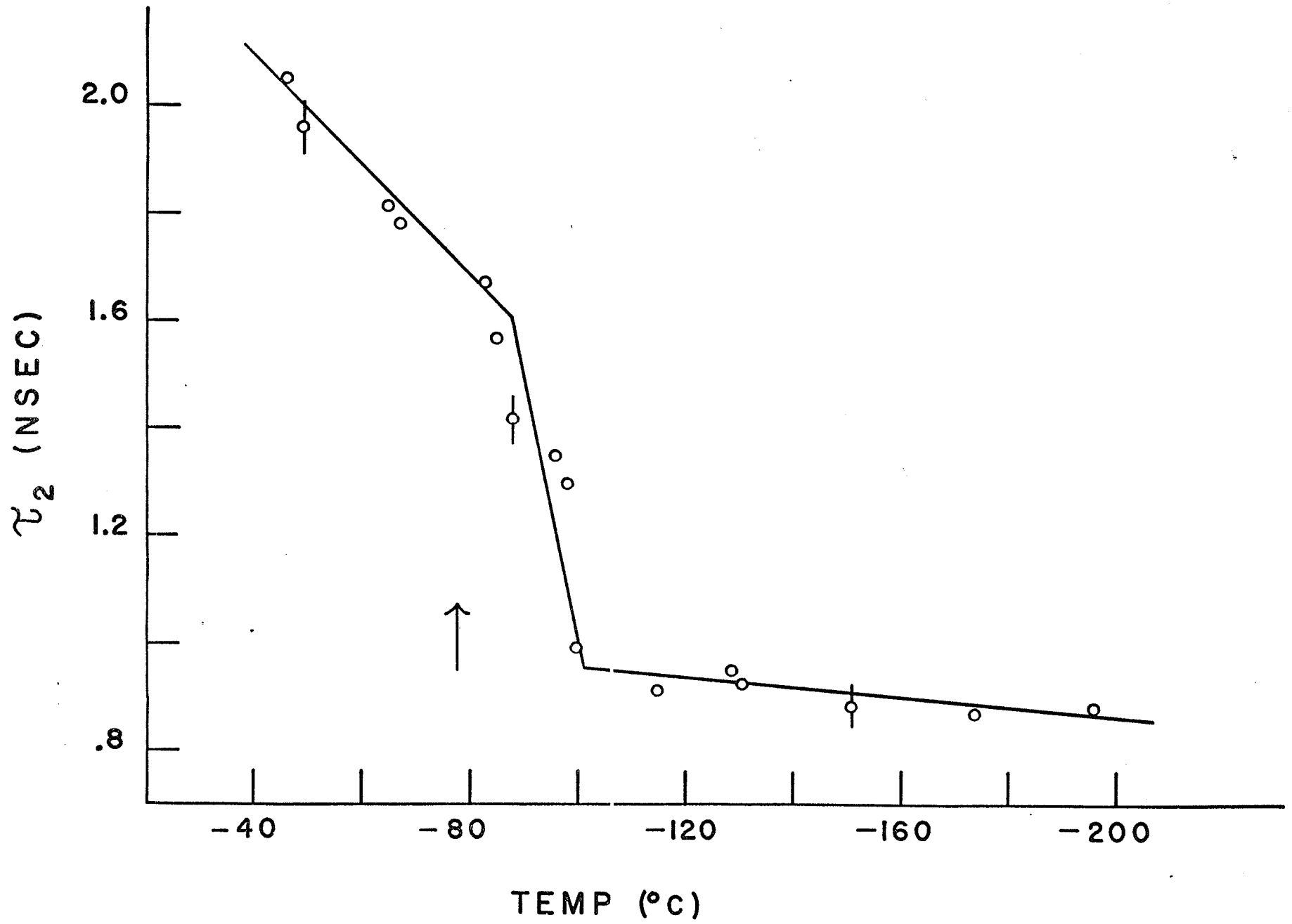
2.0
1.6
1.2
.8
τ_2 (NSEC)
-40
-80
-120
-160
-200
TEMP (°C)

Figure 4-7

Temperature Dependence of γ_1 for Ammonia

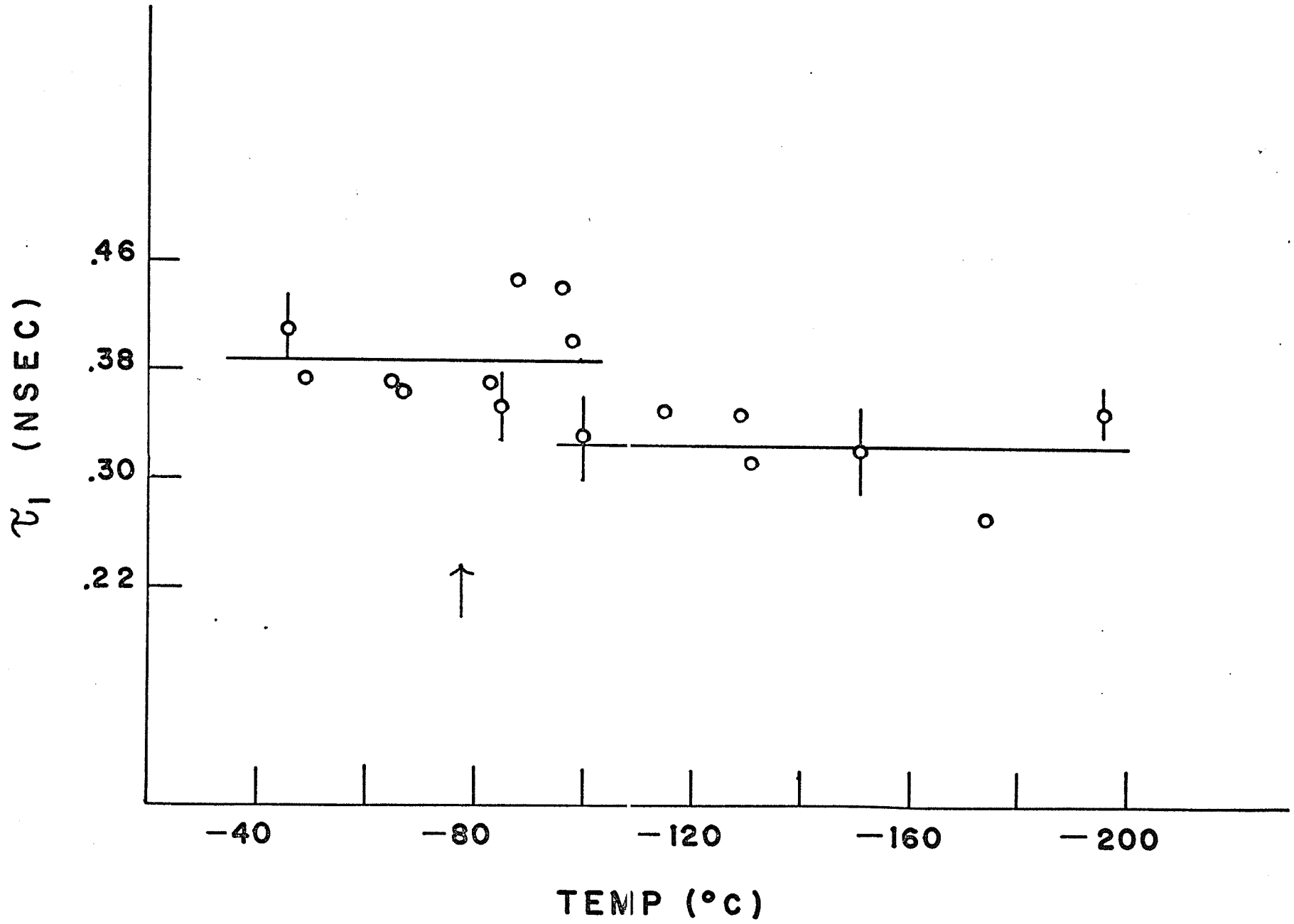
.46
.38
.30
.22
τ_1 (NSEC)
-40
-80
-120
-160
-200
TEMP (°C)

Figure 4-8

Temperature Dependence of I_2 for Ammonia

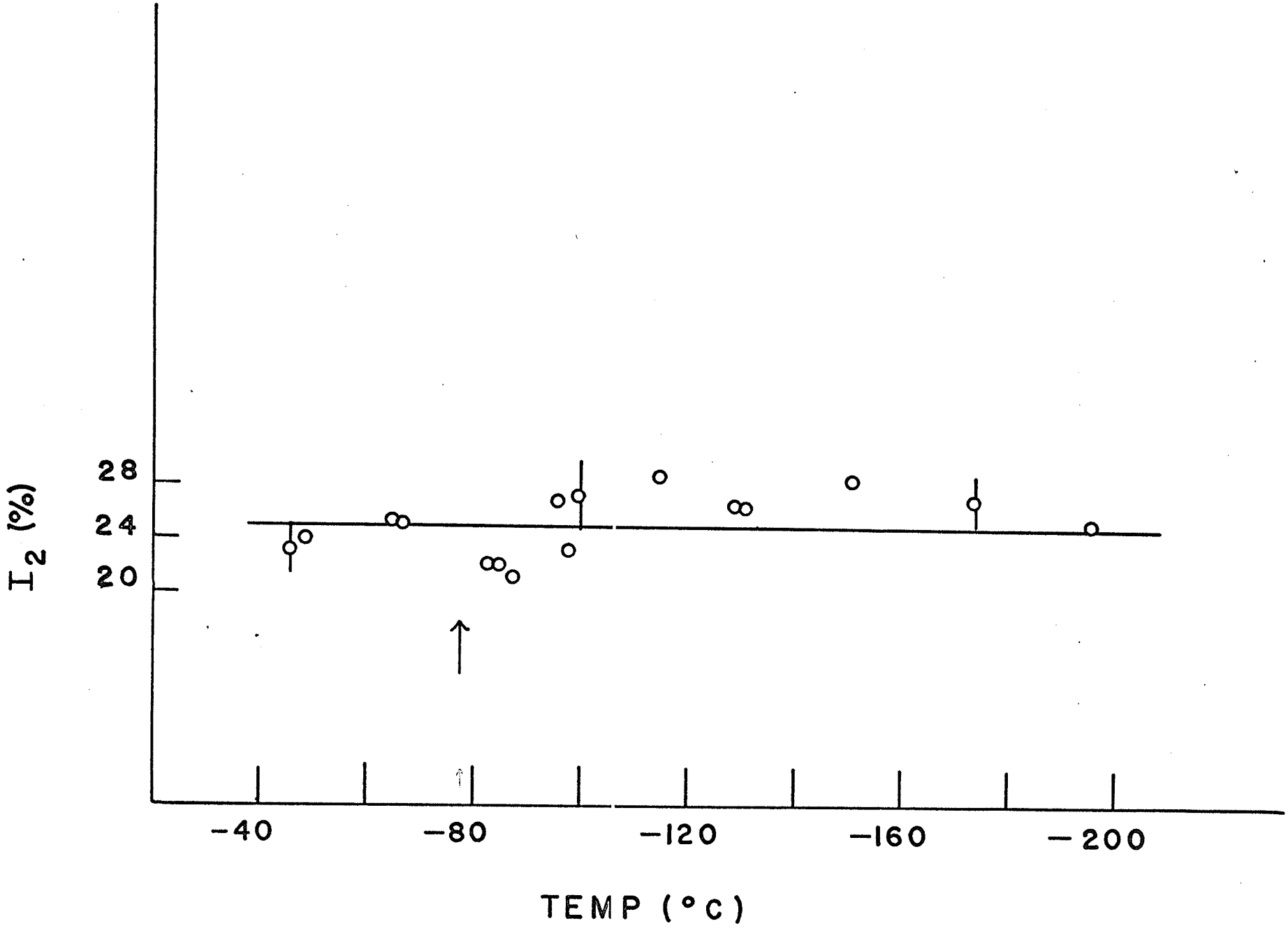
I_2 (%)
28
24
20
-40
-80
-120
-160
-200
TEMP (°C)

Figure 4-9

Temperature Dependence of I_1 for Ammonia

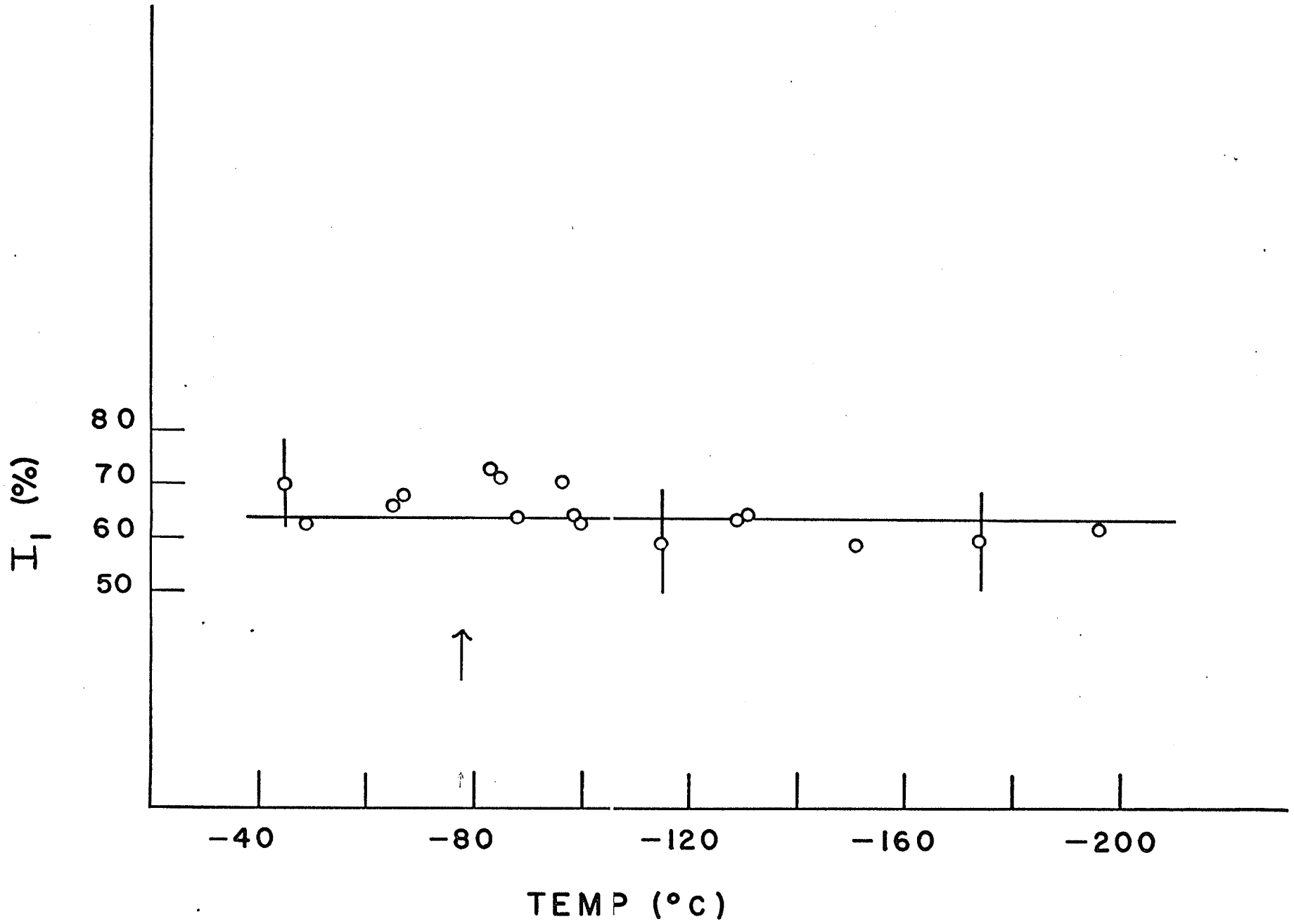
80
70
60
50
I_1 (%)
−40
−80
−120
−160
−200
TEMP (°C)

4.2 Cyclohexane

In the experimental work on Cyclohexane 99 mole % pure C_6H_{12} from the Fisher Scientific Company was used. Time runs were taken at various temperatures using both normal air-saturated samples and samples which had been degassed. A mica source as described previously was used and after preparation the Cyclohexane was placed in the temperature regulating apparatus.

Figures 4-10 to 4-15 illustrate some typical lifetime decay curves for Cyclohexane at various temperatures for both some air-saturated and degassed samples.

Tables 4-2 and 4-3 list the various decay parameters found for Cyclohexane.

Figures 4-16 to 4-19 illustrate the temperature dependence of the decay parameters of Cyclohexane for both the air-saturated and degassed cases. The arrows indicate the liquid-solid phase transition and the solid-solid phase transition found in Cyclohexane.

Table 4-2

Cyclohexane (Degassed)

Temp (°C)	τ_2 (nsec)	τ_1 (nsec)	I_2 (%)	I_1 (%)
-196	1.04 ± .02	.31 ± .01	26 ± 1	76 ± 3
-160	1.08 ± .03	.35 ± .03	22 ± 2	80 ± 4
-128	1.17 ± .03	.34 ± .03	17 ± 1	80 ± 6
-118	1.21 ± .02	.33 ± .03	20 ± 2	79 ± 6
- 90	1.28 ± .03	.33 ± .02	17 ± 1	80 ± 4
- 88	1.28 ± .03	.38 ± .02	18 ± 2	89 ± 3
- 83	1.53 ± .03	.33 ± .02	16 ± 1	80 ± 3
- 78	1.14 ± .06	.35 ± .04	20 ± 3	82 ± 15
- 75	1.32 ± .03	.34 ± .02	17 ± 2	82 ± 3
- 73	2.05 ± .04	.36 ± .02	19 ± 1	76 ± 3
- 68	1.90 ± .04	.36 ± .03	19 ± 2	76 ± 8
- 65	2.26 ± .04	.39 ± .02	21 ± 1	77 ± 3
- 45	2.28 ± .05	.37 ± .02	21 ± 1	75 ± 5
- 32	2.41 ± .04	.40 ± .02	23 ± 2	78 ± 3
0	2.60 ± .04	.37 ± .03	25 ± 1	74 ± 7
+ 5	2.66 ± .04	.35 ± .02	22 ± 1	72 ± 3
+ 9	3.00 ± .04	.37 ± .02	31 ± 1	70 ± 3
+ 20	3.08 ± .04	.39 ± .03	34 ± 2	58 ± 4
+ 32	3.15 ± .07	.36 ± .02	31 ± 1	65 ± 5
+ 44	3.26 ± .05	.36 ± .02	31 ± 1	67 ± 5

Table 4-3

Cyclohexane (Non-Degassed)

Temp (°C)	τ_2 (nsec)	τ_1 (nsec)	I_2 (%)	I_1 (%)
-196	1.07 ± .02	.35 ± .02	19 ± 1	69 ± 5
-174	1.07 ± .02	.31 ± .03	15 ± 3	76 ± 10
-114	1.18 ± .04	.37 ± .04	17 ± 2	73 ± 11
-102	1.25 ± .04	.39 ± .04	18 ± 2	67 ± 10
- 86	1.26 ± .04	.33 ± .03	18 ± 2	81 ± 8
- 84	1.12 ± .02	.30 ± .02	19 ± 1	84 ± 4
- 80	1.71 ± .02	.35 ± .02	19 ± 1	75 ± 3
- 79	1.18 ± .03	.31 ± .02	21 ± 2	73 ± 4
- 78	1.96 ± .04	.39 ± .02	20 ± 1	71 ± 3
- 77	1.88 ± .04	.38 ± .02	20 ± 1	77 ± 5
- 76	1.98 ± .04	.38 ± .03	20 ± 1	75 ± 3
- 75	2.12 ± .02	.37 ± .02	18 ± 1	77 ± 4
- 52	2.11 ± .02	.36 ± .02	20 ± 1	71 ± 3
- 39	2.22 ± .04	.37 ± .01	20 ± 1	69 ± 3
- 7	2.24 ± .04	.34 ± .02	19 ± 2	74 ± 5
0	2.28 ± .04	.35 ± .03	21 ± 1	62 ± 6
+ 6	2.44 ± .04	.37 ± .01	22 ± 1	75 ± 3
+ 12	2.35 ± .02	.34 ± .02	28 ± 1	72 ± 4
+ 20	2.50 ± .04	.38 ± .03	34 ± 1	60 ± 6
+ 33	2.37 ± .02	.33 ± .02	30 ± 1	62 ± 3
+ 49	2.51 ± .02	.34 ± .02	31 ± 1	71 ± 4

Figure 4-10

Time Spectra of Cyclohexane Degassed at +44°C Non-Degassed at +49°C

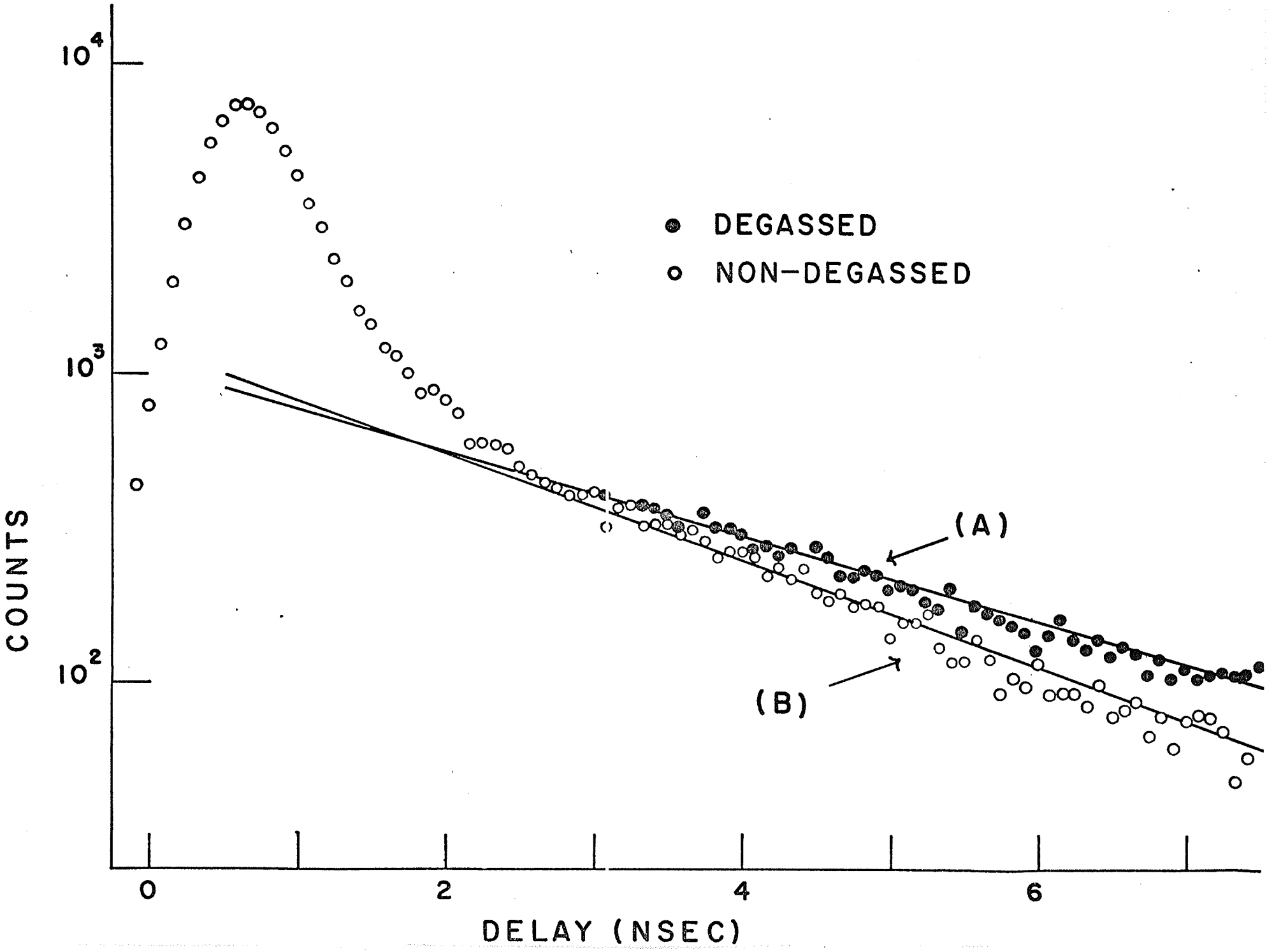
10^4
10^3
10^2
COUNTS
DEGASSED
NON-DEGASSED
(A)
(B)
0
2
4
6
DELAY (NSEC)

Figure 4-11

Time Spectra of Degassed Cyclohexane at +20°C

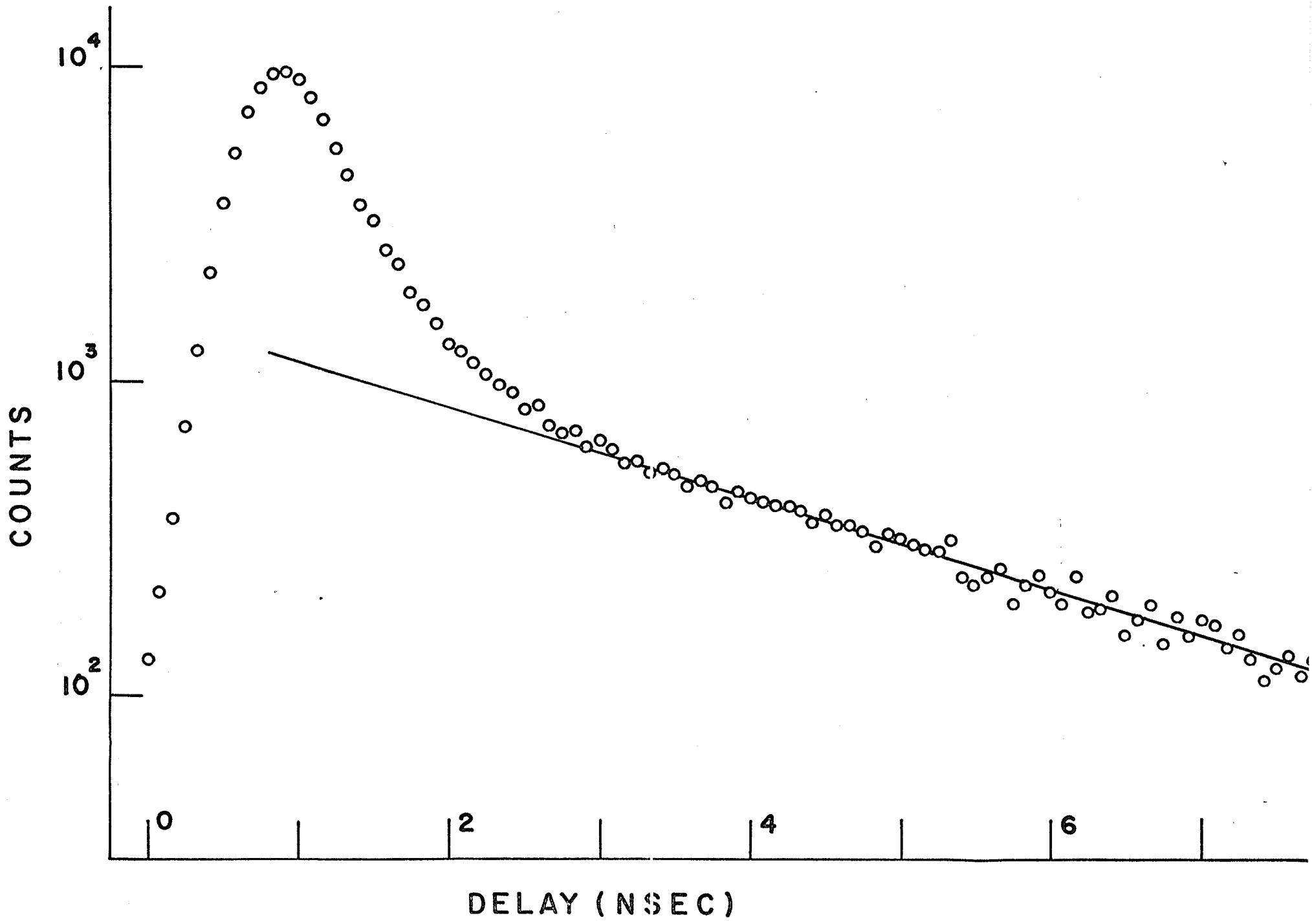
10^4
10^3
10^2
COUNTS
0
2
4
6
DELAY (NSEC)

Figure 4-12

Time Spectra of Cyclohexane Degassed at 4.7°C

Non-Degassed at 0°C

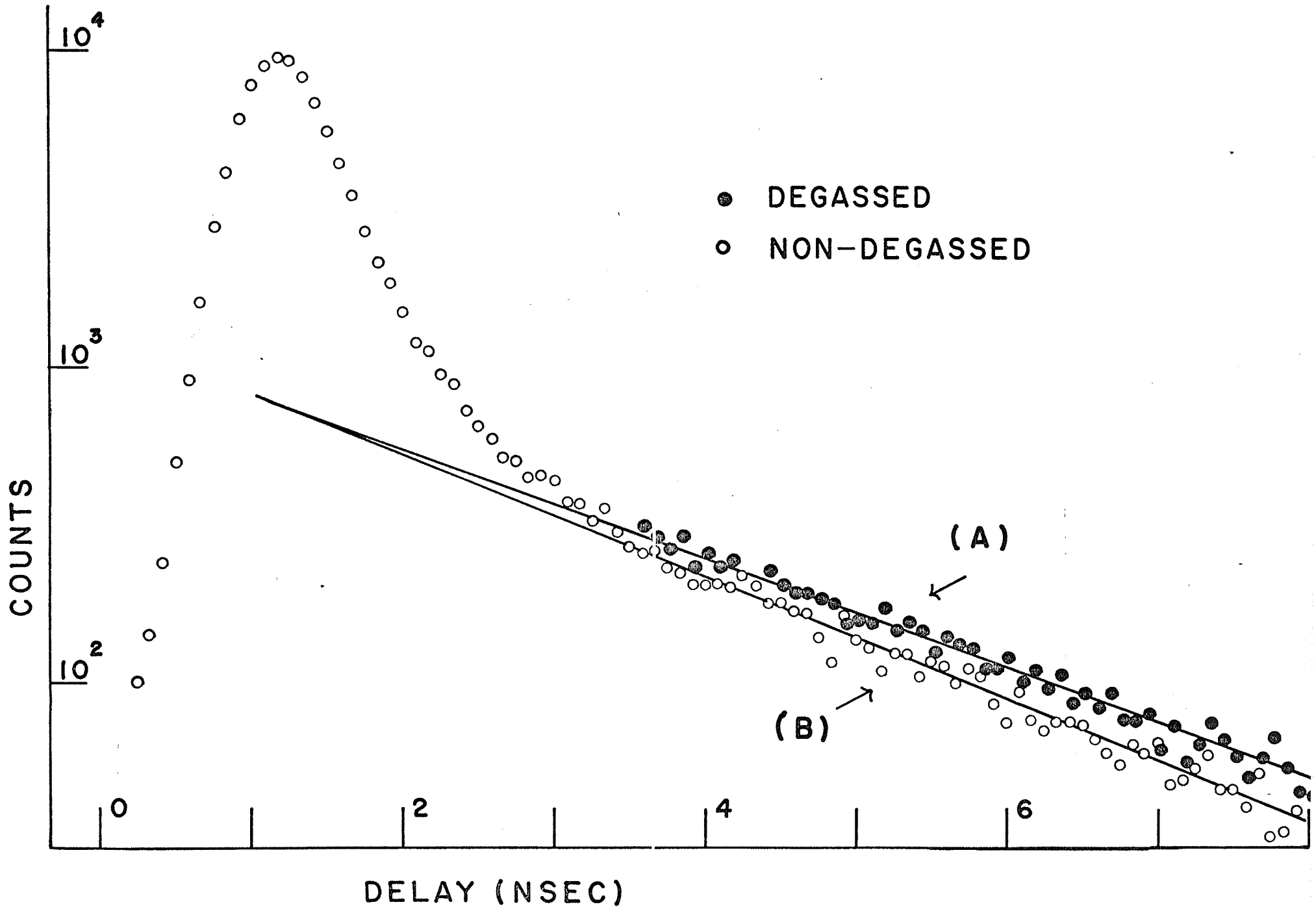
10^4
10^3
10^2
COUNTS
DEGASSED
NON-DEGASSED
(A)
(B)
0
2
4
6
DELAY (NSEC)

Figure 4-13

Time Spectra of Cyclohexane Degassed at -45°C

Non-Degassed at -39°C

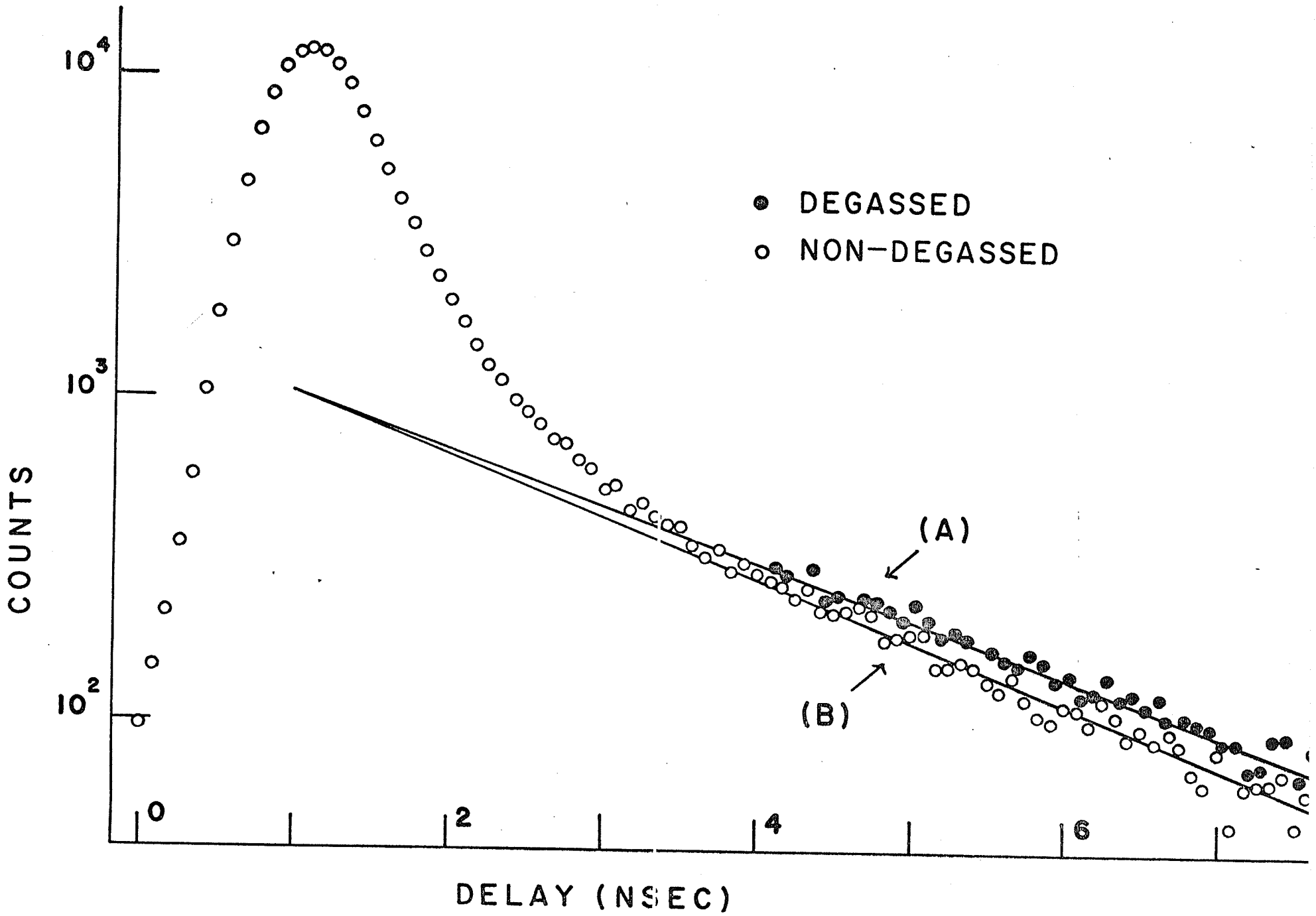
DEGASSED
NON-DEGASSED
(A)
(B)
COUNTS
10^4
10^3
10^2
0
2
4
6
DELAY (NSEC)

Figure 4-14

Time Spectra of Non-Degassed Cyclohexane at -74°C

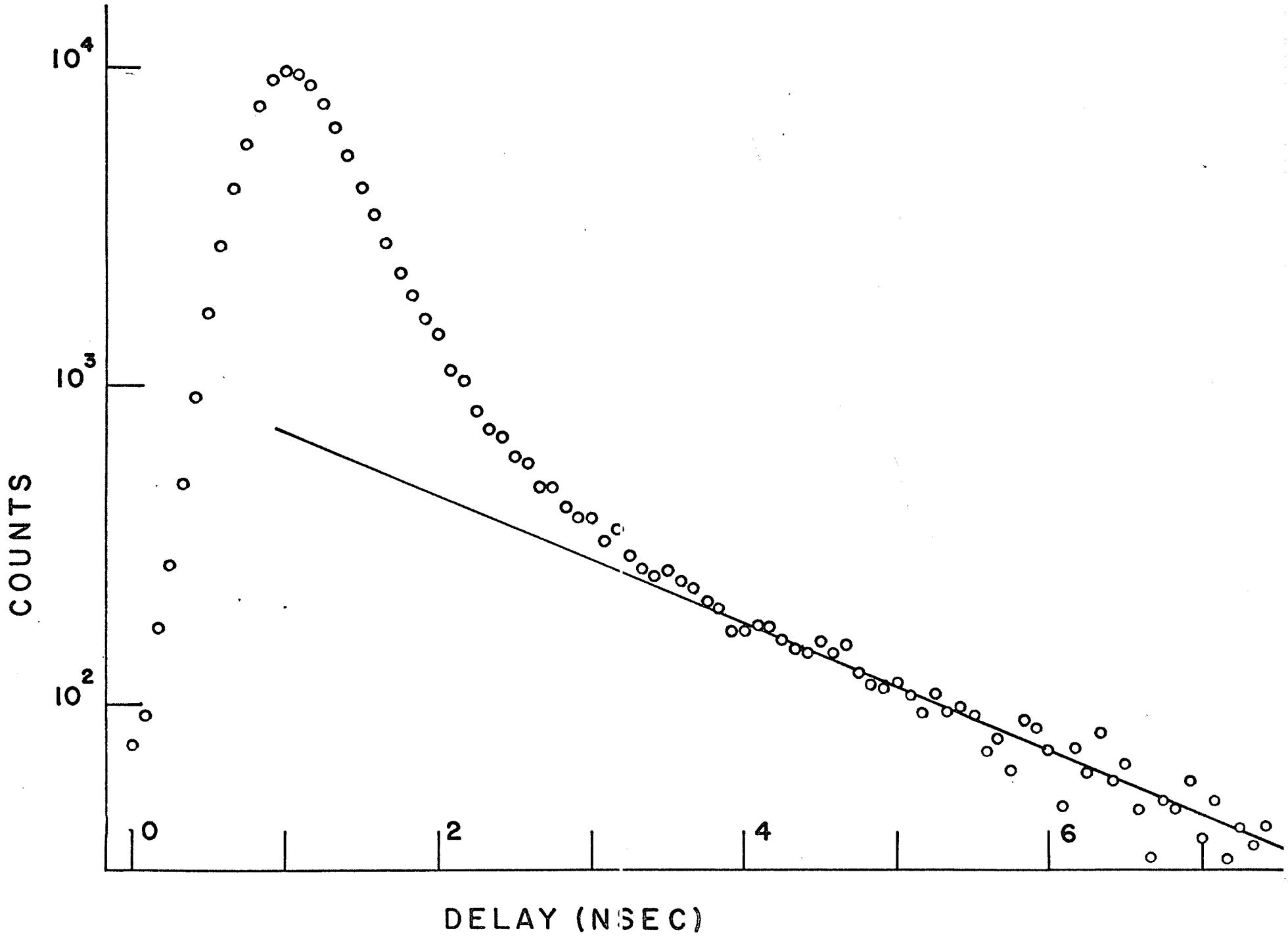
10^4
10^3
10^2
COUNTS
0
2
4
6
DELAY (NSEC)

Figure 4-15

Time Spectra of Degassed Cyclohexane at -118°C

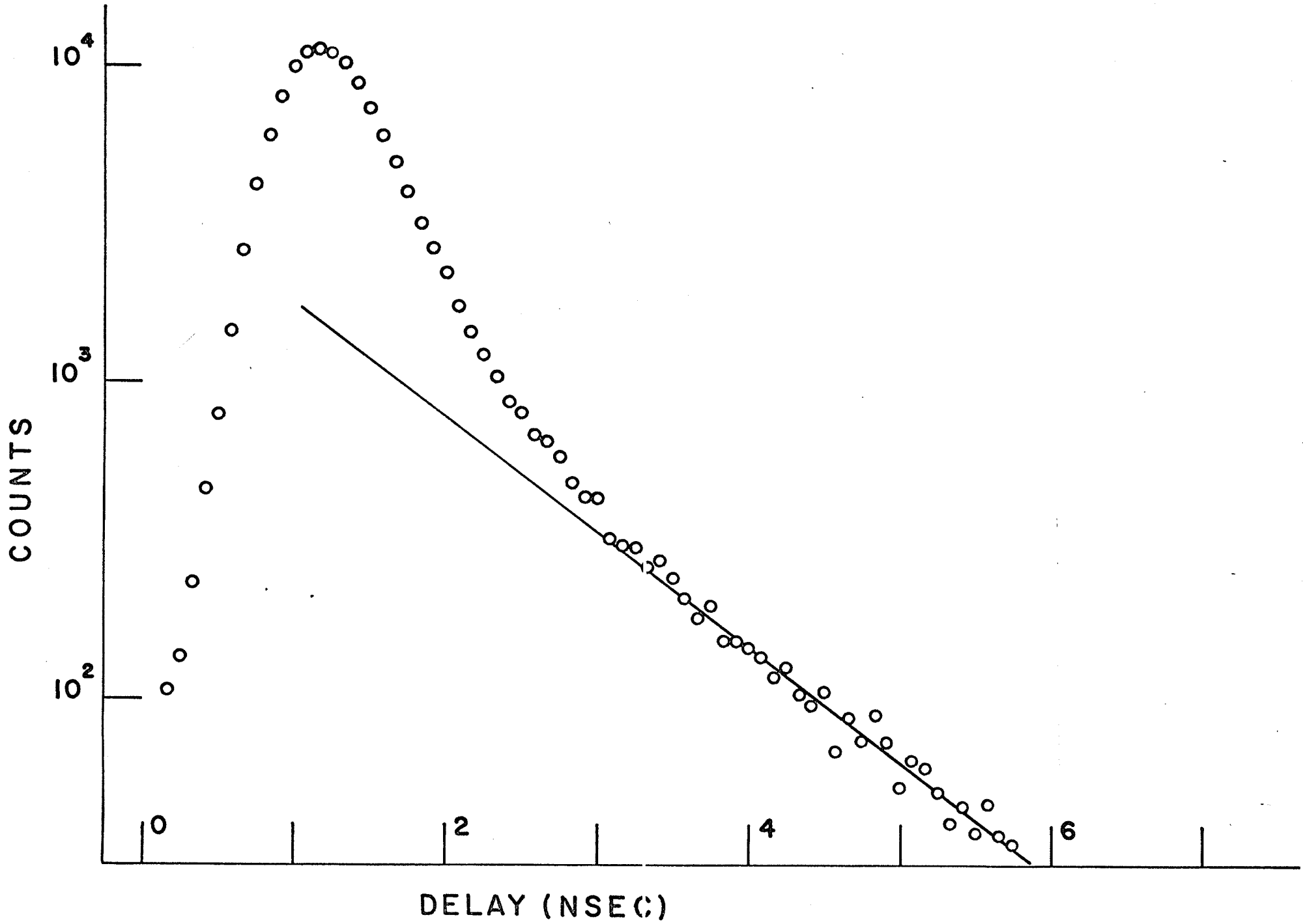
10^4
10^3
10^2
COUNTS
0
2
4
6
DELAY (NSEC)

Figure 4-16

Temperature Dependence of τ_2 for Cyclohexane

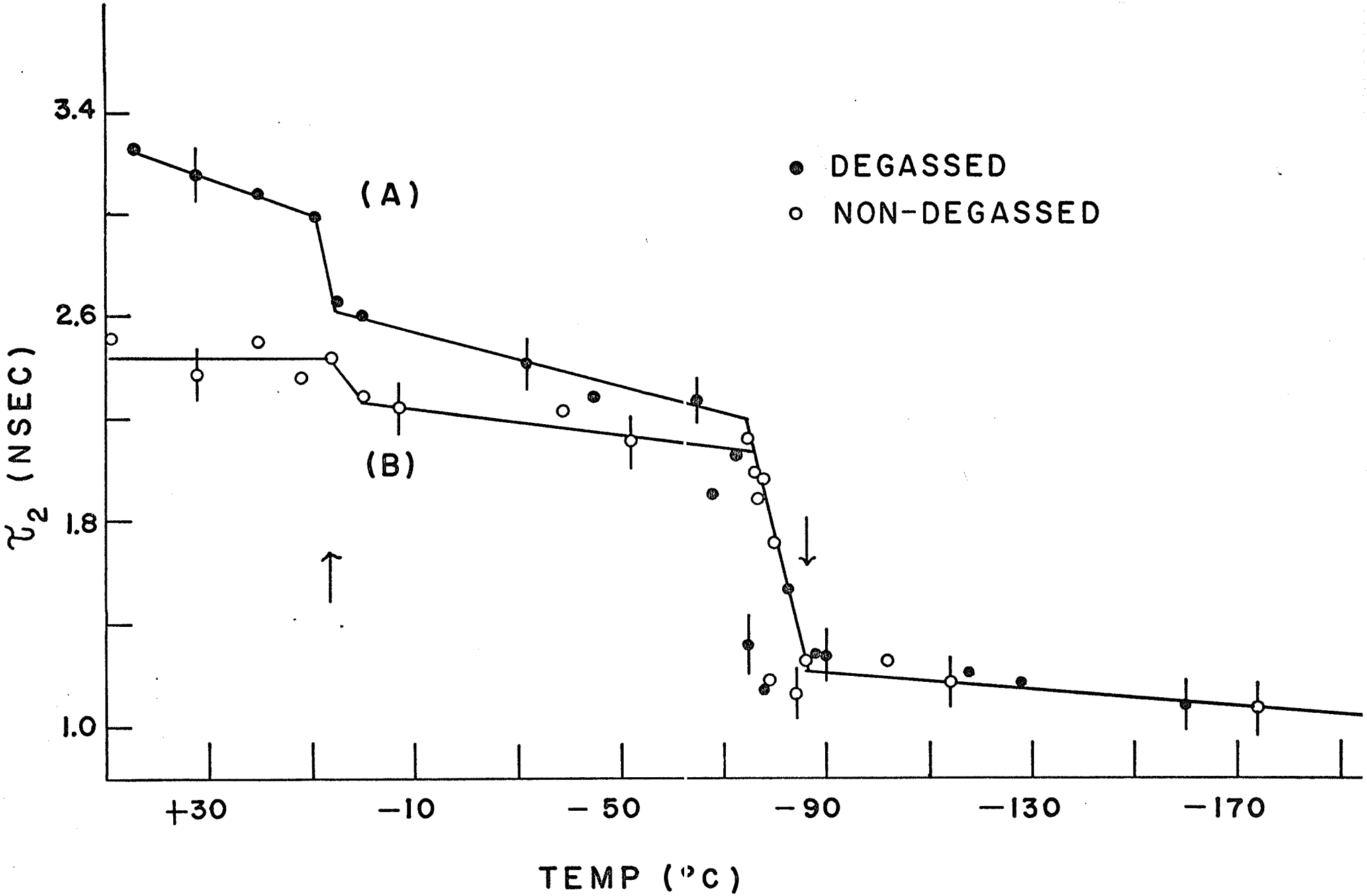
3.4
2.6
1.8
1.0
τ_2 (NSEC)
(A)
(B)
DEGASSED
NON-DEGASSED
+30
−10
− 50
−90
−130
−170
TEMP (°C)

Figure 4-17

Temperature Dependence of τ_1 for Cyclohexane

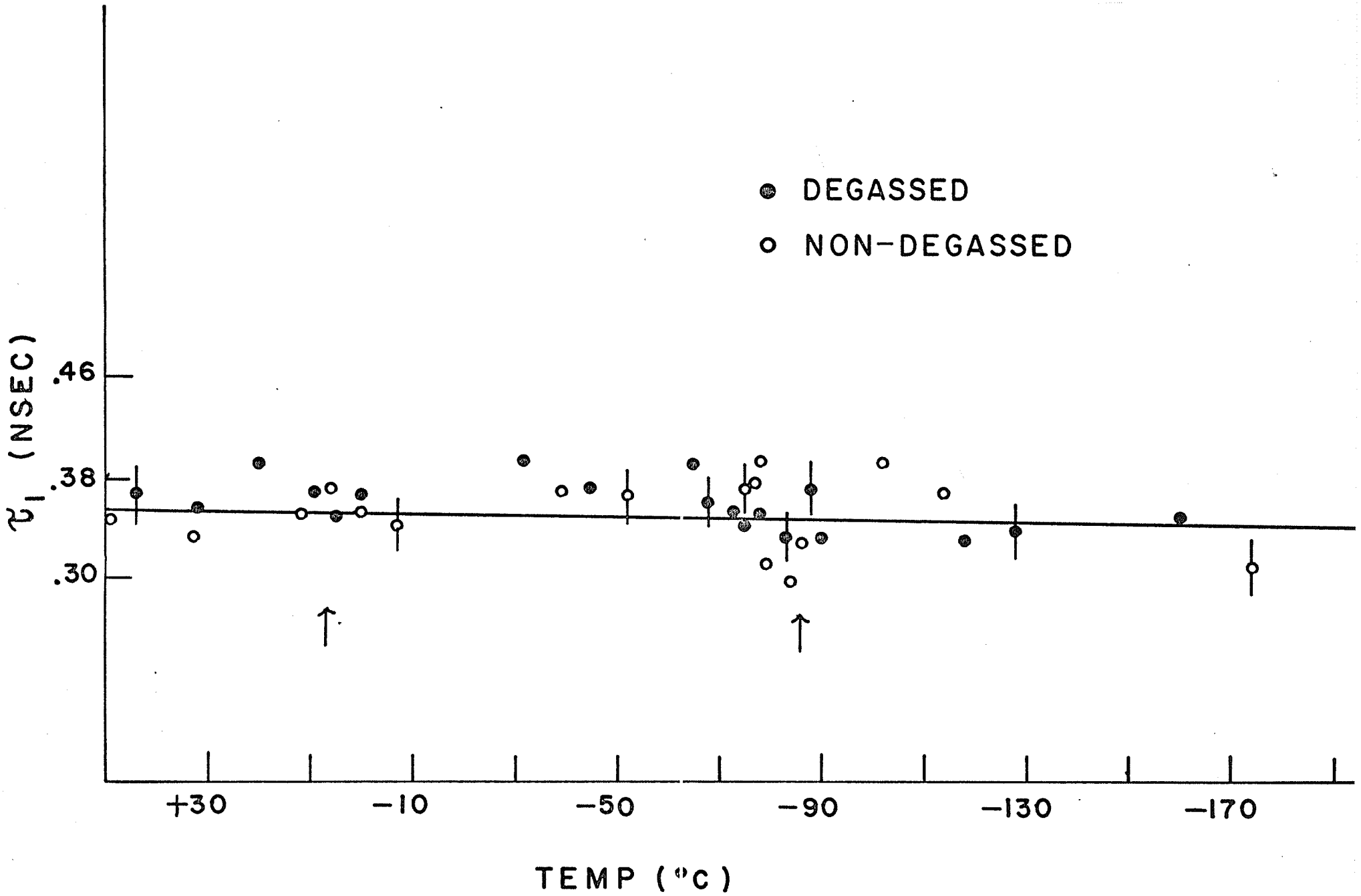
DEGASSED
NON-DEGASSED
τ_1 (NSEC)
.46
.38
.30
+30
−10
−50
−90
−130
−170
TEMP (°C)

Figure 4-18

Temperature Dependence of I_2 for Cyclohexane

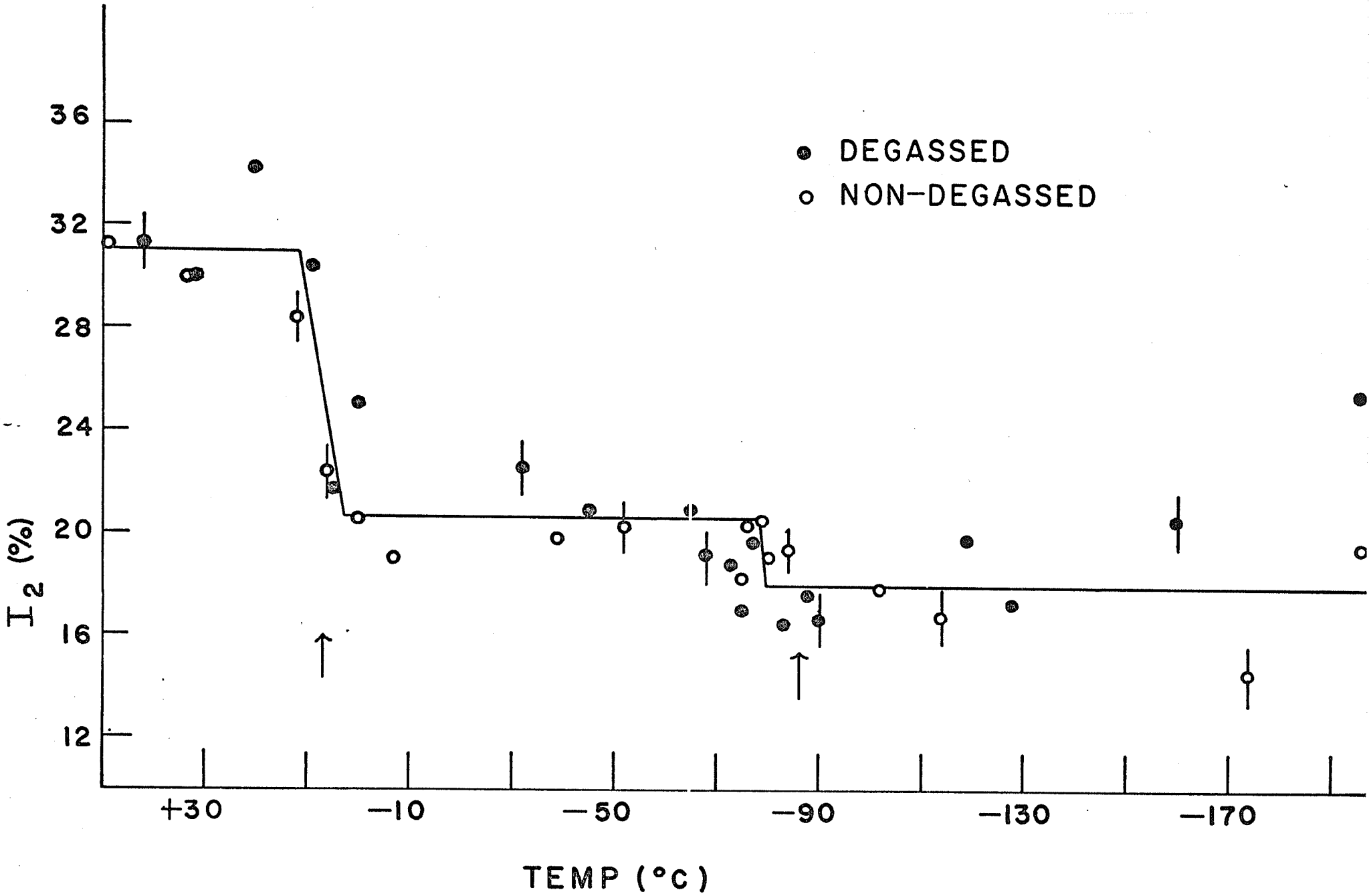
DEGASSED
NON-DEGASSED
36
32
28
24
20
16
12
I_2 (%)
+30
−10
−50
−90
−130
−170
TEMP (°C)

Figure 4-19

Temperature Dependence of I_1 for Cyclohexane

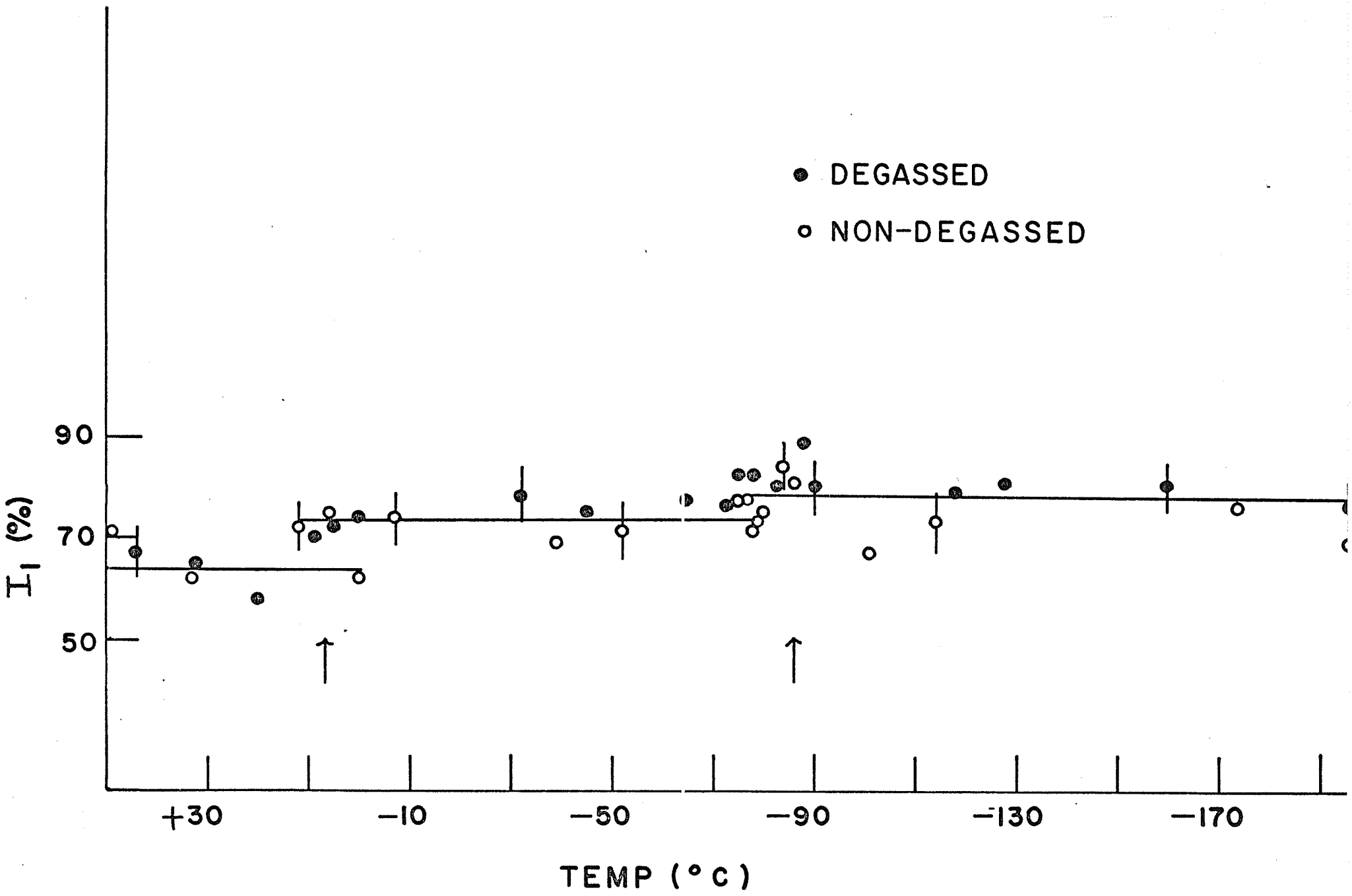
DEGASSED
NON-DEGASSED
90
70
50
I_1 (%)
+30
−10
−50
−90
−130
−170
TEMP (°C)

4.3 Methane

For the work on Methane, research grade CH_4 from The Matheson Company was employed. This type of Methane has a purity of 99.99 mole % with the oxygen contamination being of the order of two parts per million. The Methane was transferred into the sample cell by use of the distillation apparatus which was first evacuated ensuring no contamination of the Methane during the runs. No runs were taken with oxygen present in the sample. A mica source was used during all the experiments.

Figures 4-20 to 4-23 illustrate some decay curves for Methane at various temperatures. Table 4-4 lists the decay parameters found for Methane. Since Methane boils at -161.6°C only a limited range of temperature data could be acquired.

Figures 4-24 to 4-27 illustrate the temperature dependence of the decay parameters of Methane. Again the arrows indicate the liquid-solid phase transition.

Table 4-4

Methane

Temp (°C)	τ_2 (nsec)	τ_1 (nsec)	I_2 (%)	I_1 (%)
-196	2.81 ± .05	.40 ± .01	32 ± 1	57 ± 3
-188	3.25 ± .07	.36 ± .04	31 ± 2	65 ± 11
-183	4.43 ± .06	.41 ± .04	32 ± 2	65 ± 10
-176	5.43 ± .08	.35 ± .03	33 ± 2	59 ± 8
-174	5.72 ± .07	.37 ± .04	34 ± 1	56 ± 7

Figure 4-20

Time Spectra of Methane at -174°C

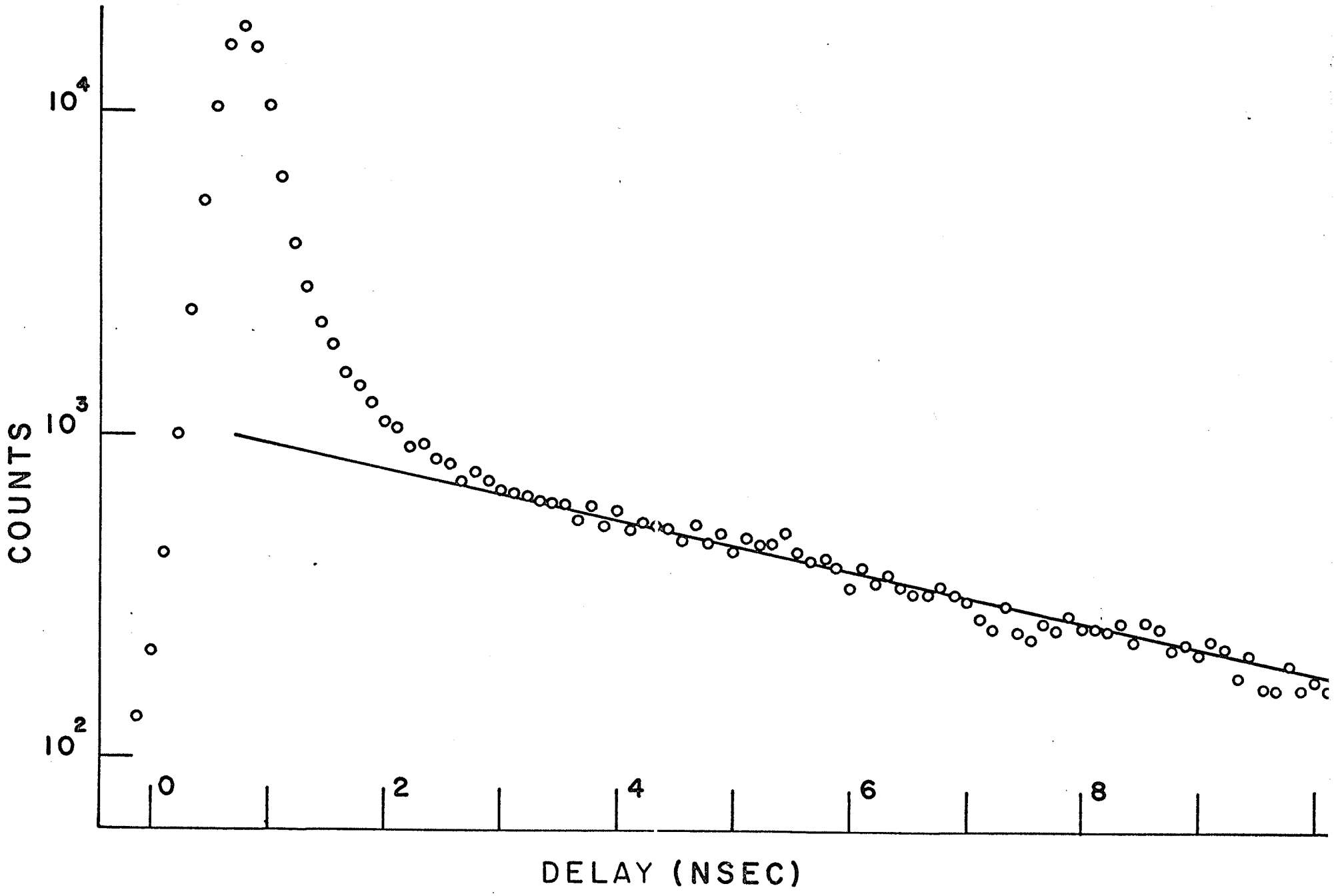
COUNTS
10^4
10^3
10^2
0
2
4
6
8
DELAY (NSEC)

Figure 4-21

Time Spectra of Methane at -183°C

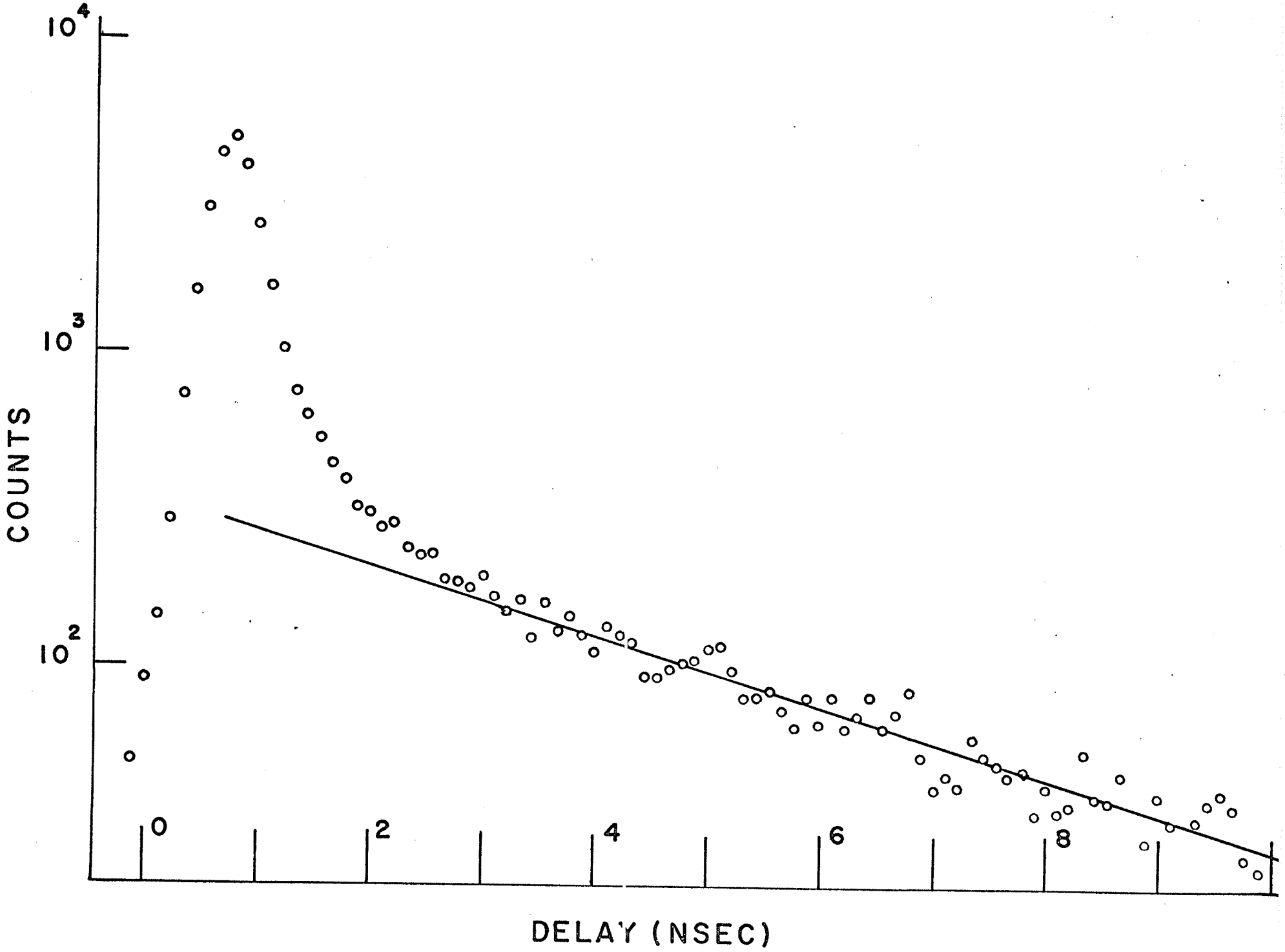
10^4
10^3
10^2
COUNTS
0
2
4
6
8
DELAY (NSEC)

Figure 4-22

Time Spectra of Methane at -188°C

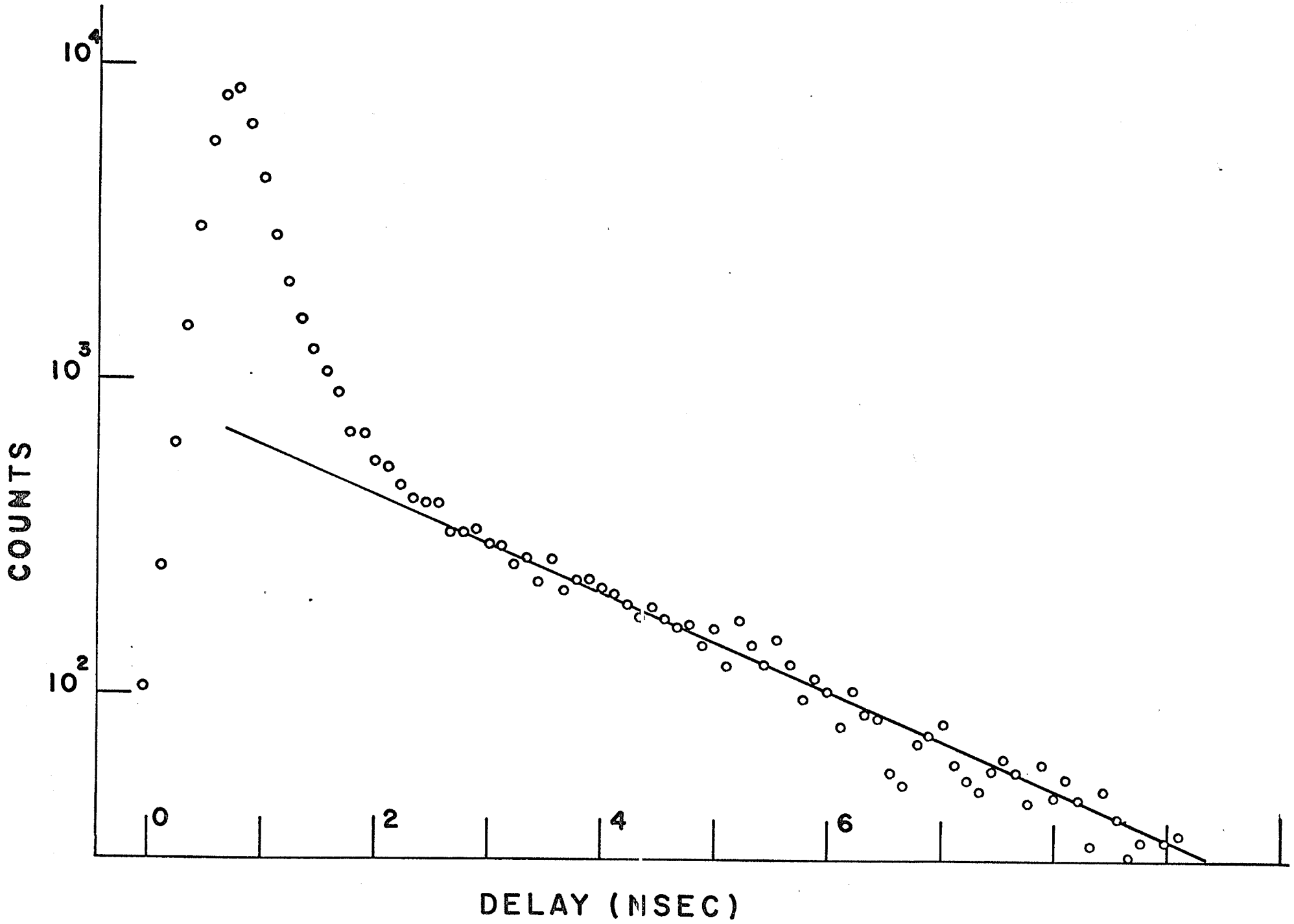
10^4
10^3
10^2
COUNTS
0
2
4
6
DELAY (NSEC)

Figure 4-23

Time Spectra of Methane at -196°C

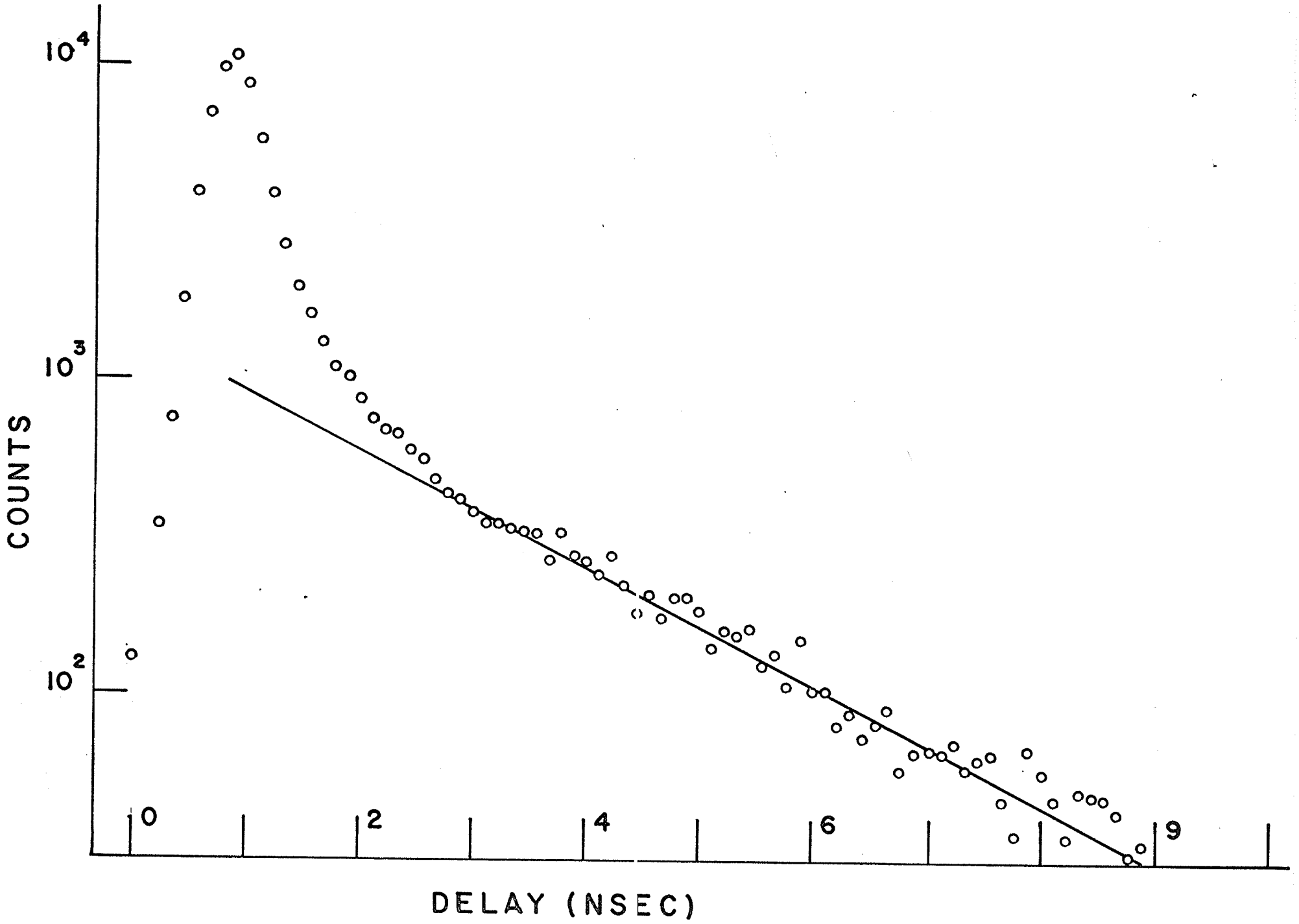
10^4
10^3
10^2
COUNTS
0
2
4
6
9
DELAY (NSEC)

Figure 4-24

Temperature Dependence of τ_2 for Methane

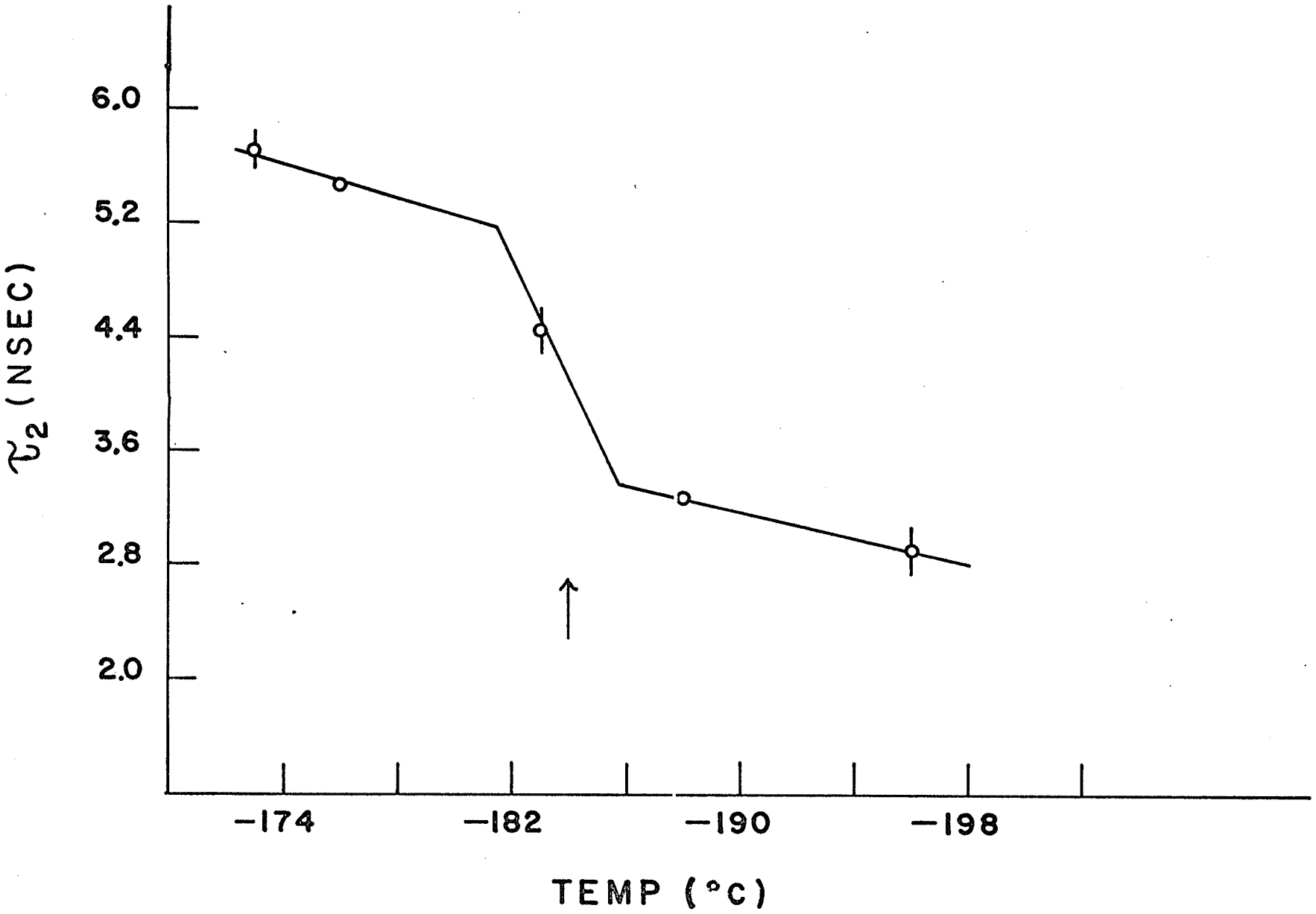
6.0
5.2
4.4
3.6
2.8
2.0
τ_2 (NSEC)
-174
-182
-190
-198
TEMP (°C)

Figure 4-25

Temperature Dependence of τ_1 for Methane

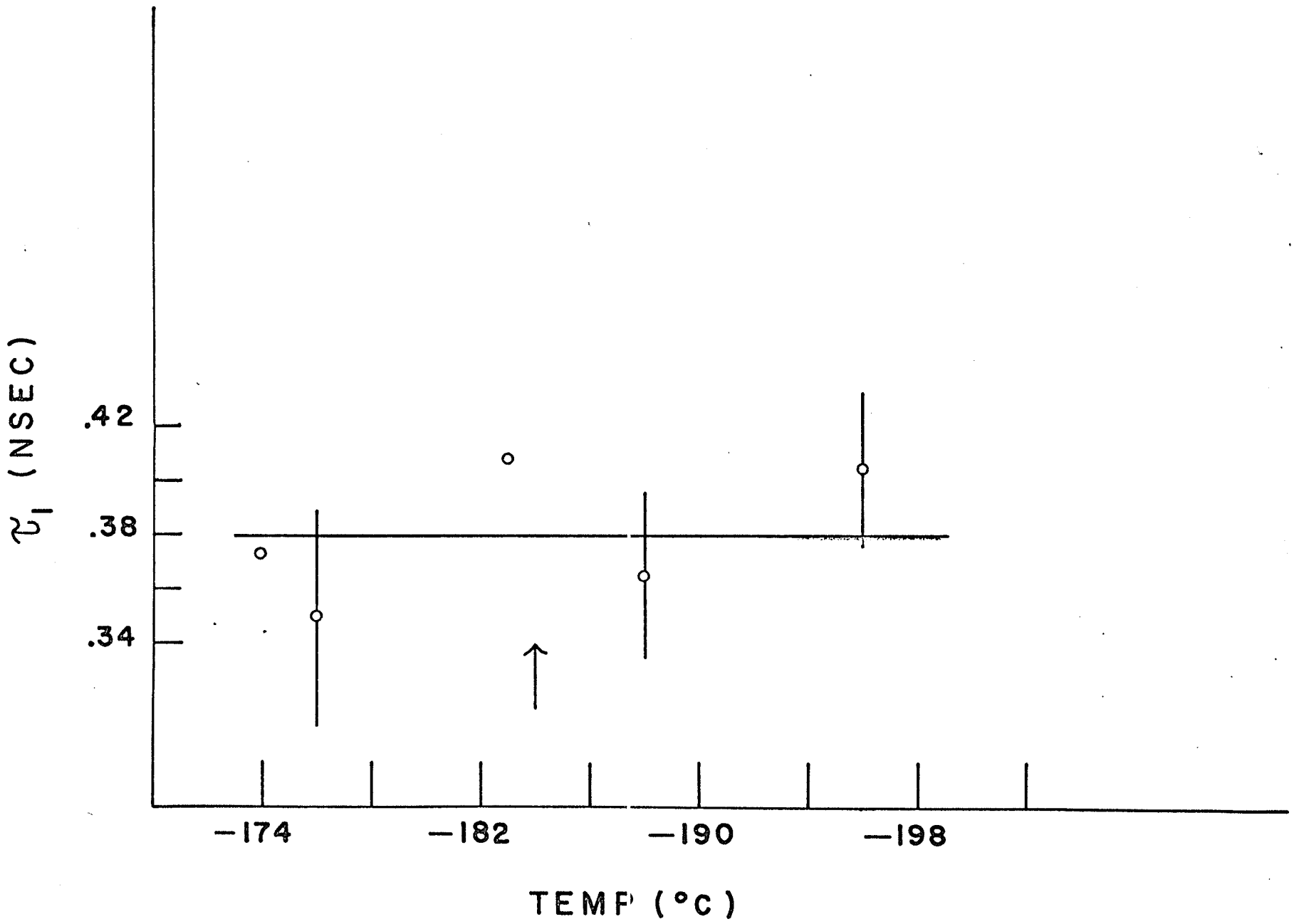
τ_1 (NSEC)
.42
.38
.34
−174
−182
−190
−198
TEMP (°C)

Figure 4-26

Temperature Dependence of I_2 for Methane

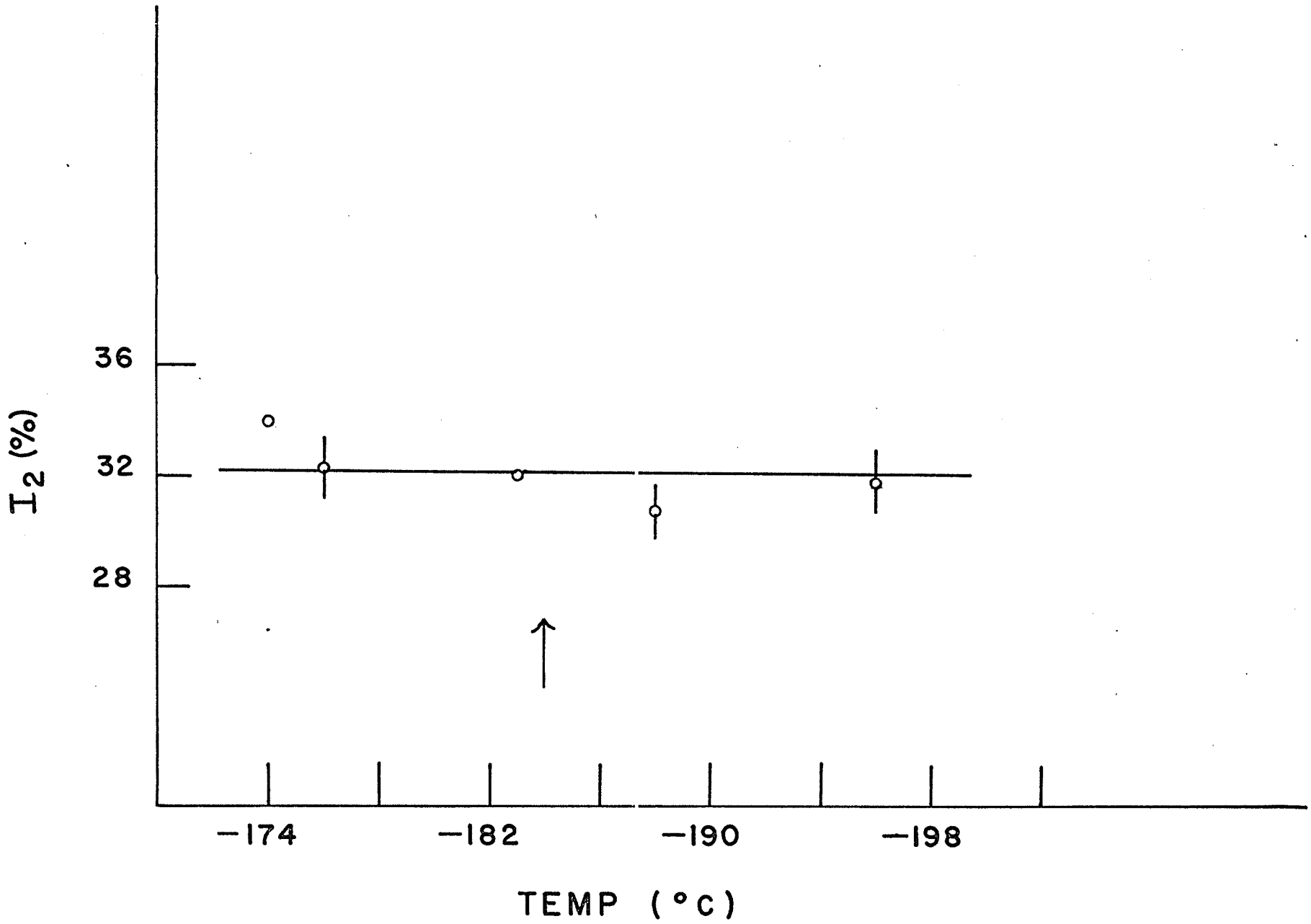
36
32
28
I_2 (%)
−174
−182
−190
−198
TEMP (°C)

Figure 4-27

Temperature Dependence of I_1 for Methane

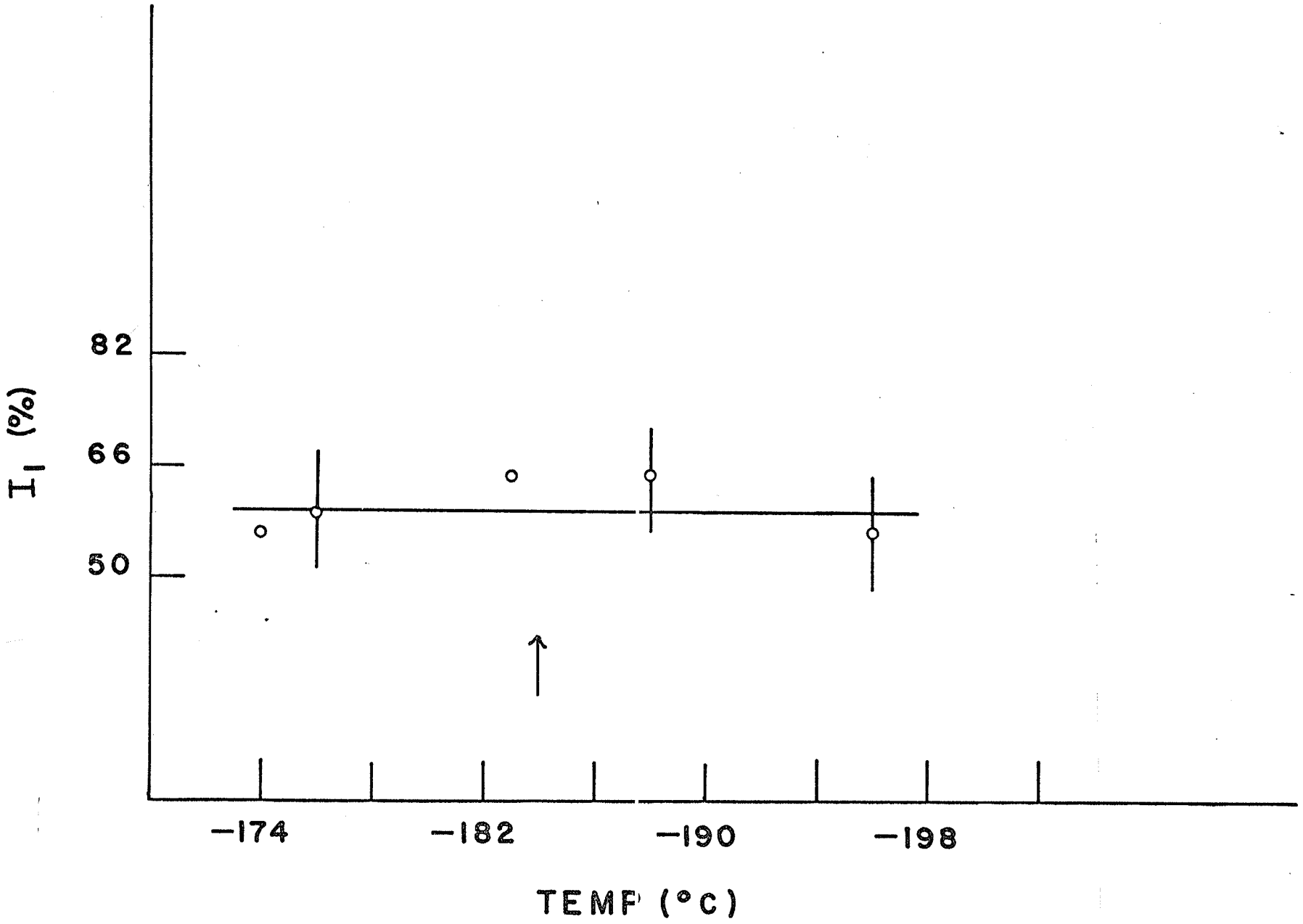
82
66
50
I_1 (%)
−174
−182
−190
−198
TEMP (°C)

4.4 Butane

The Butane used in the experiments was supplied by the Phillips Petroleum Company. This research grade Butane had a purity of 99.99 mole %. As with the Methane it was transferred into the sample cell by use of the distillation apparatus to avoid contamination of the sample. Again runs were taken only with pure samples, no runs were taken on samples containing oxygen. A mica source was used during the experiments.

Figures 4-28 to 4-31 show some typical lifetime curves for Butane at several temperatures. Table 4-5 lists all the decay parameters found for Butane. Figures 4-32 to 4-35 illustrate the temperature dependence of the decay parameters of Butane with the arrows showing the liquid-solid phase transition.

Table 4-5

Butane

Temp (°C)	τ_2 (nsec)	τ_1 (nsec)	I_2 (%)	I_1 (%)
-196	1.27 ± .03	.34 ± .02	12 ± 1	86 ± 2
-144	1.46 ± .04	.34 ± .02	14 ± 2	84 ± 7
-138	1.48 ± .04	.34 ± .02	17 ± 1	85 ± 8
-137	1.53 ± .05	.34 ± .02	14 ± 2	81 ± 8
-136	1.51 ± .04	.34 ± .02	12 ± 1	80 ± 7
-135	1.45 ± .03	.33 ± .01	12 ± 1	79 ± 5
-130	1.79 ± .03	.36 ± .03	13 ± 1	82 ± 7
-123	2.35 ± .04	.37 ± .02	17 ± 1	79 ± 11
- 88	3.23 ± .03	.43 ± .02	17 ± 1	71 ± 8
- 77	3.02 ± .03	.38 ± .02	17 ± 1	78 ± 7
- 75	3.10 ± .03	.42 ± .03	18 ± 1	74 ± 9

Figure 4-28

Time Spectra of Butane at -88°C

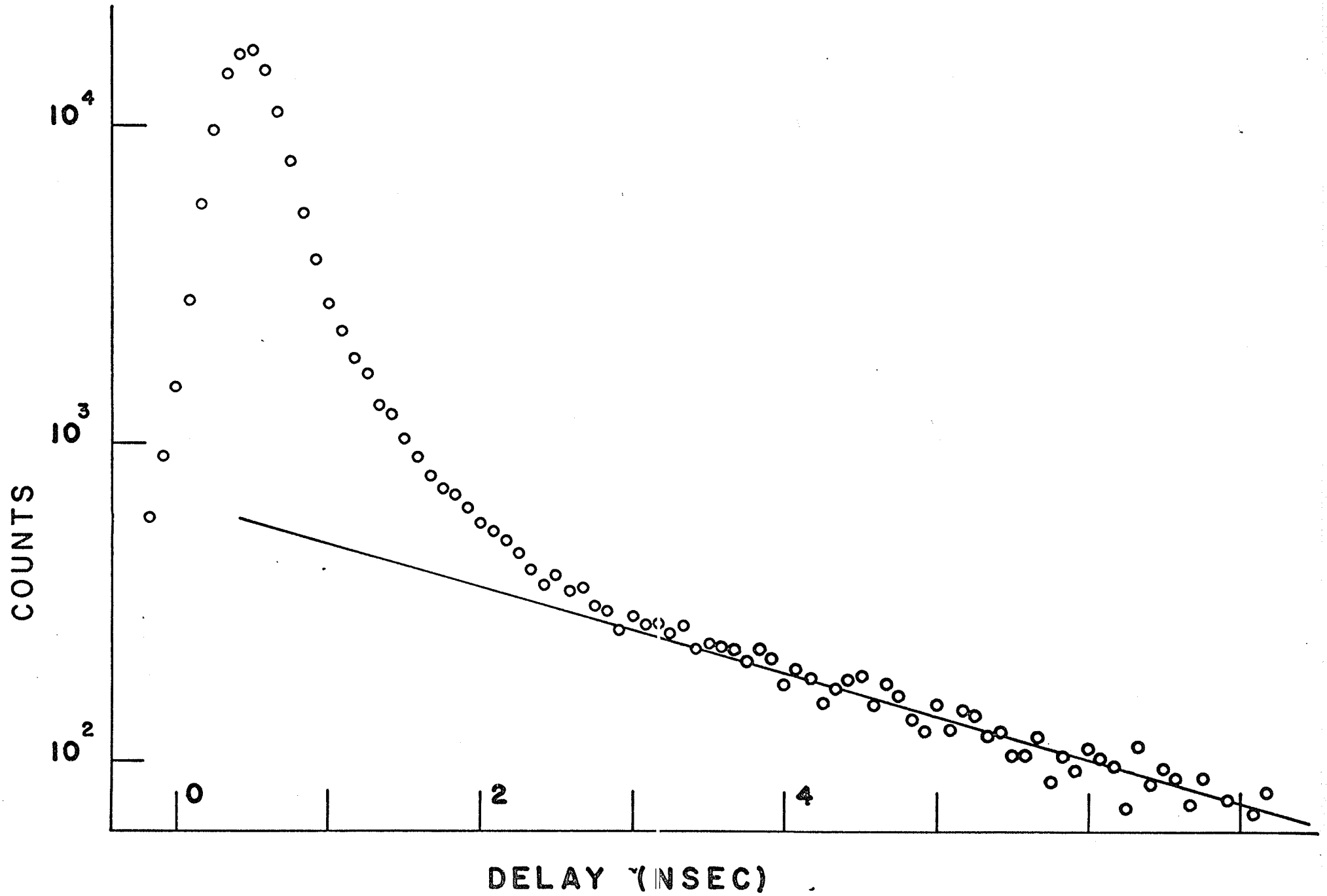
10^4
10^3
10^2
COUNTS
0
2
4
DELAY (NSEC)

Figure 4-29

Time Spectra of Butane at -123°C

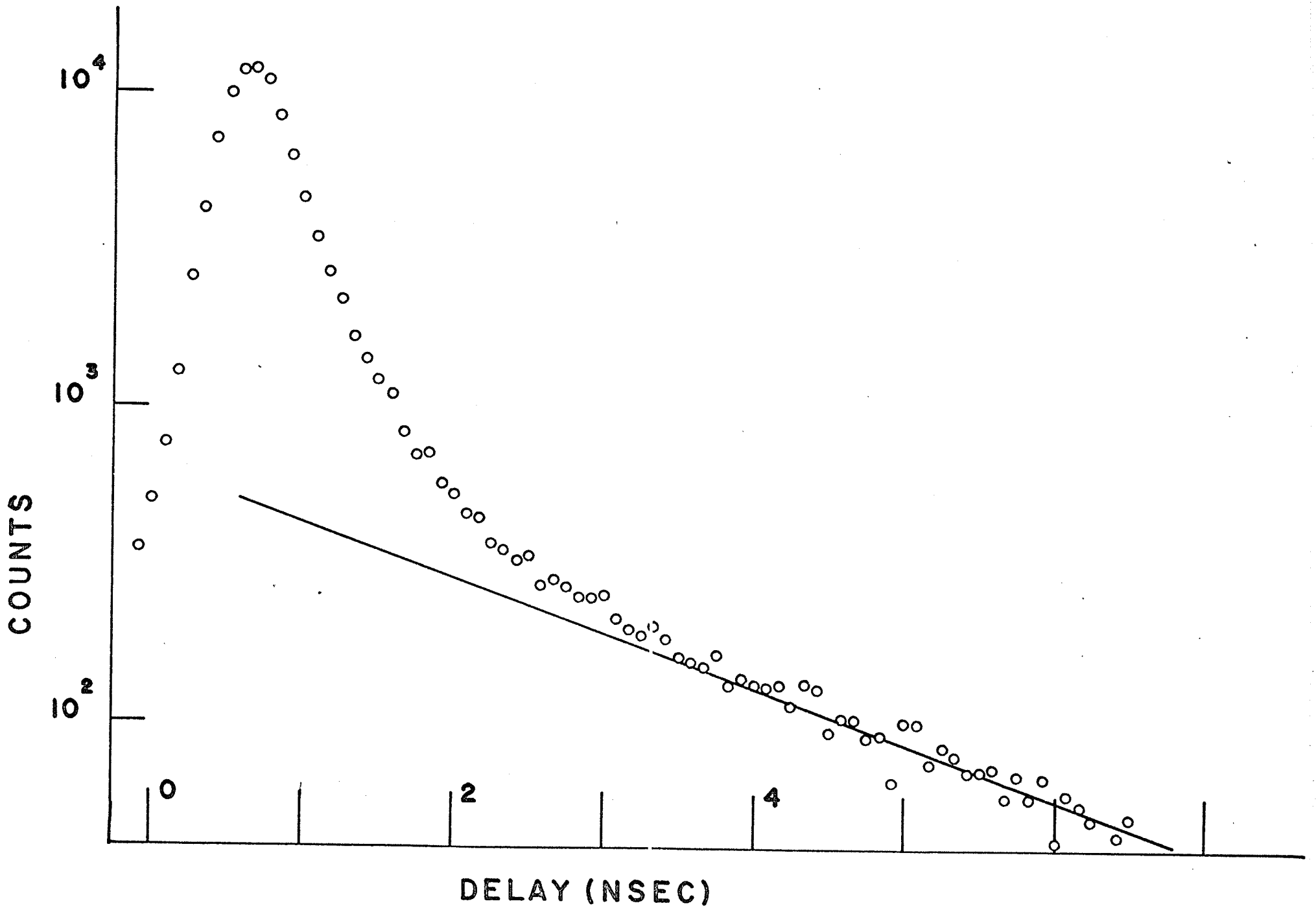
10^4
10^3
10^2
COUNTS
0
2
4
DELAY (NSEC)

Figure 4-30

Time Spectra of Butane at -138°C

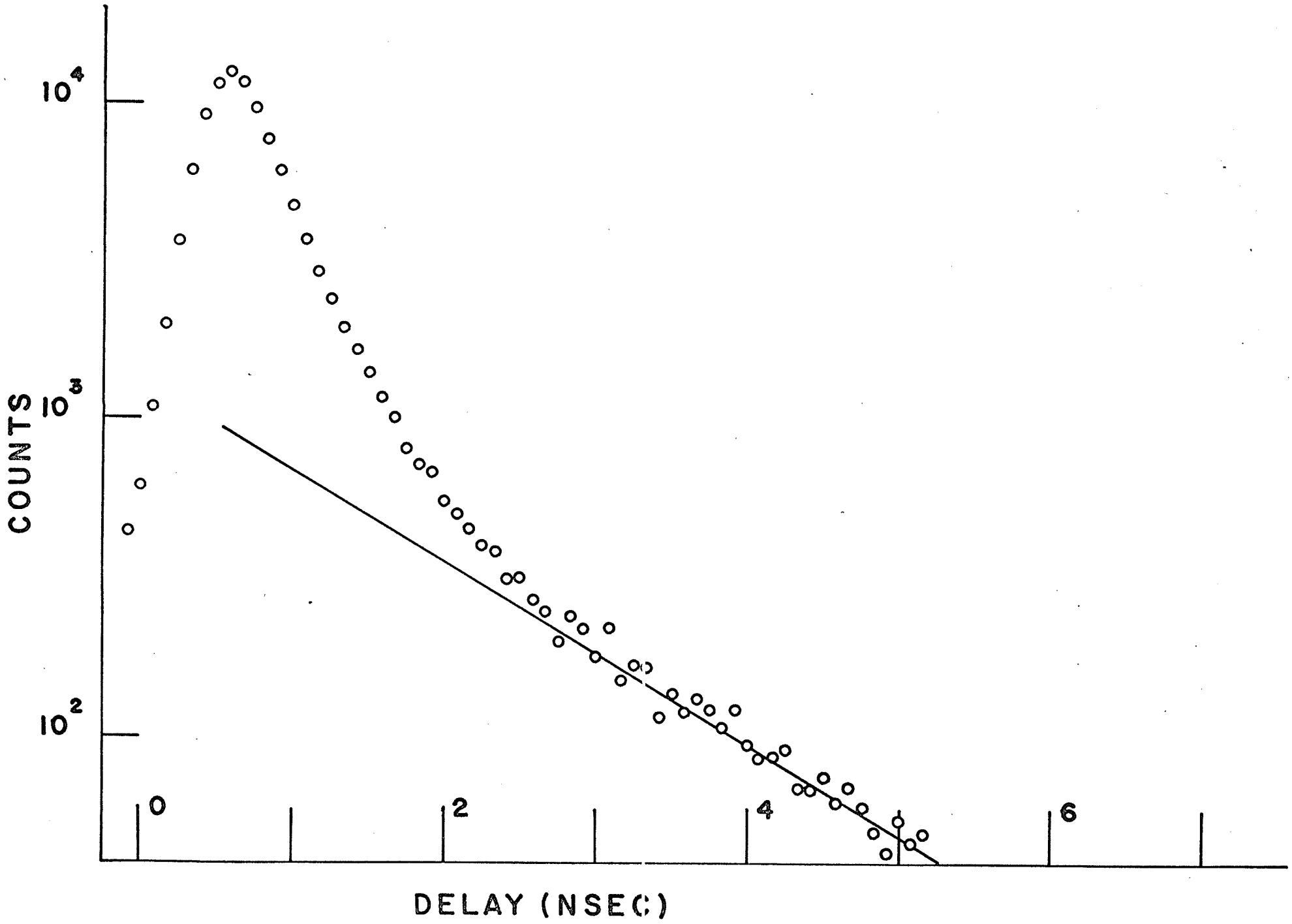
10^4
10^3
10^2
COUNTS
0
2
4
6
DELAY (NSEC)

Figure 4-31

Time Spectra of Butane at -196°C

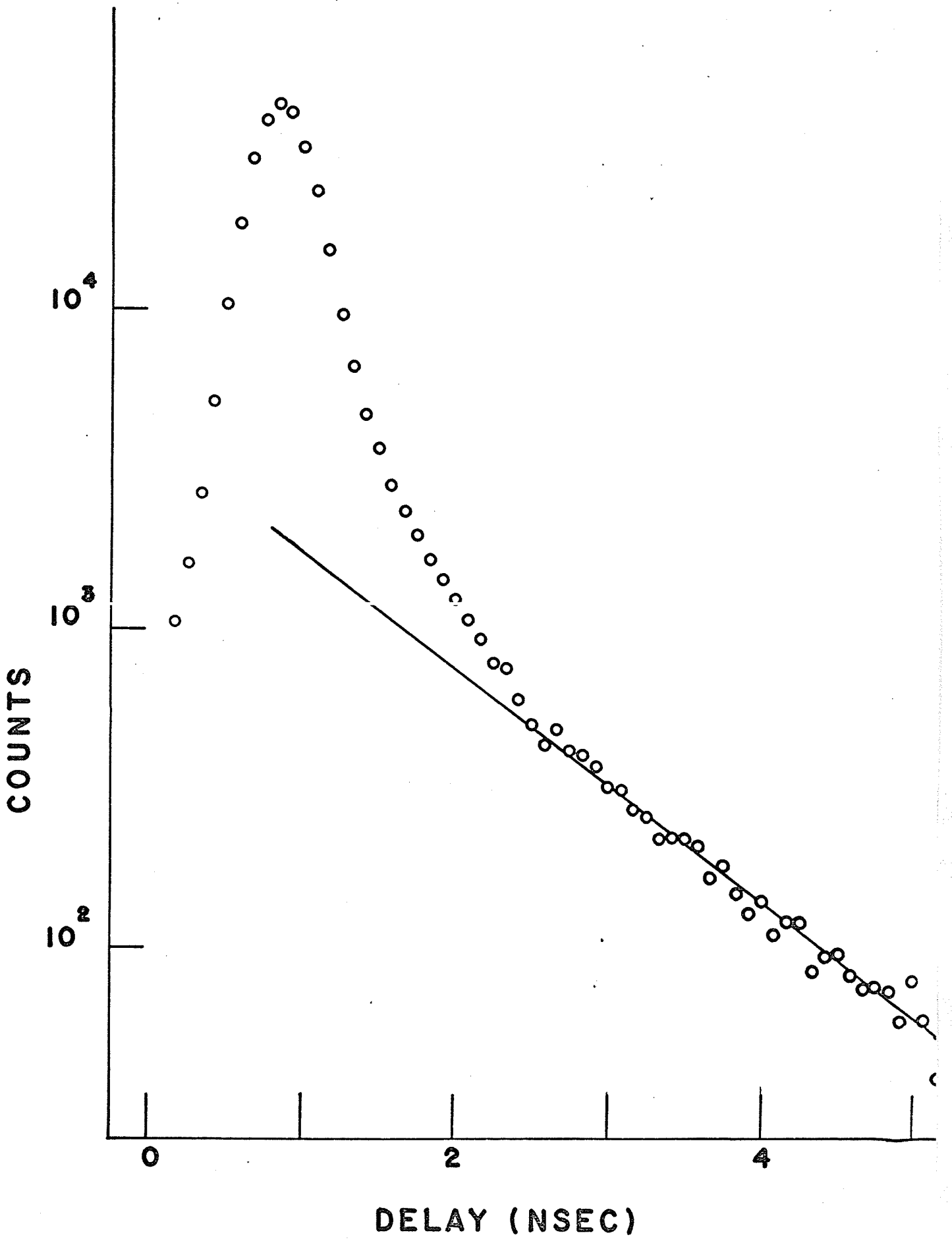
10^4
10^3
10^2
COUNTS
0
2
4
DELAY (NSEC)

Figure 4-32

Temperature Dependence of τ_2 for Butane

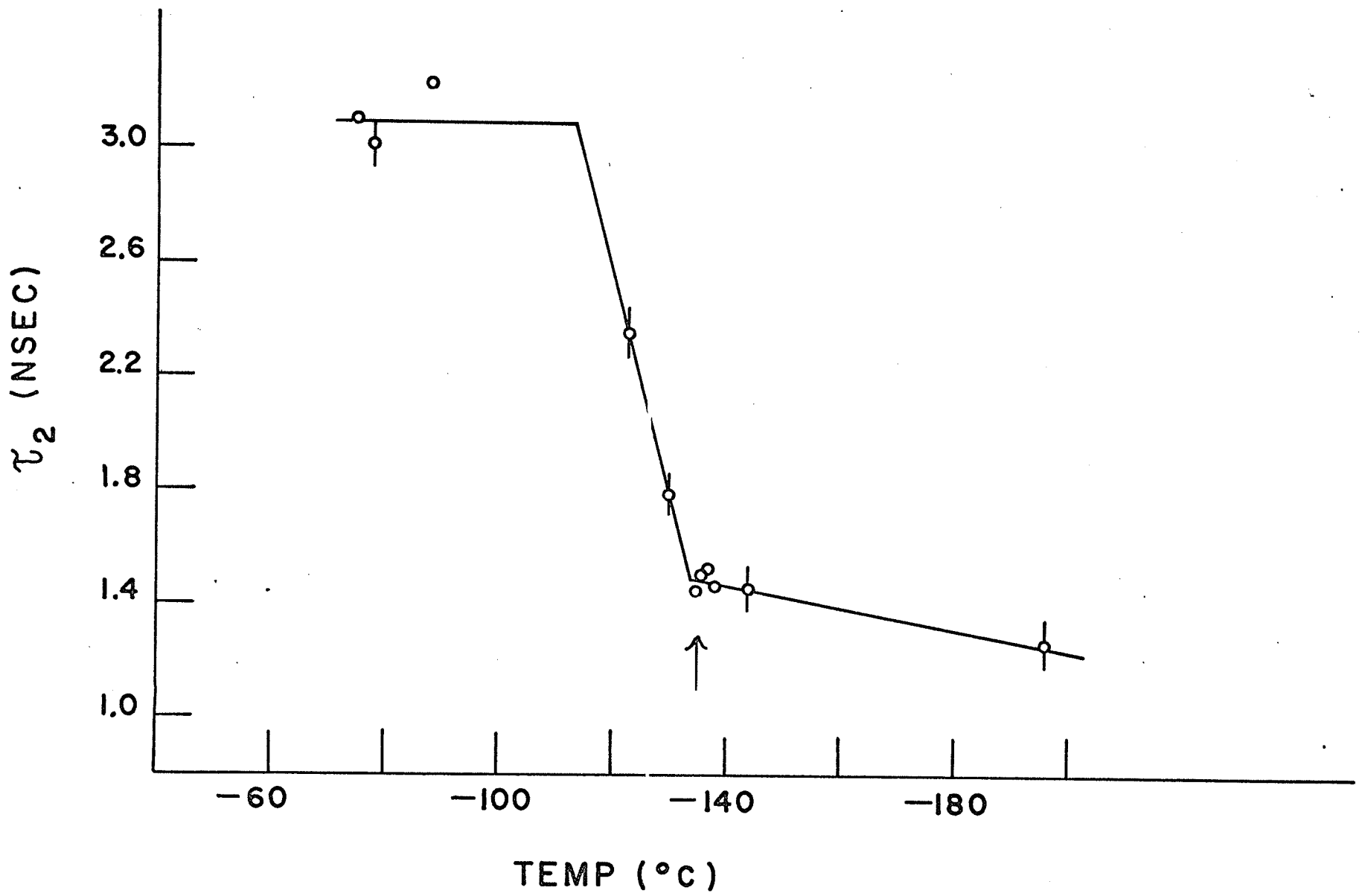
3.0
2.6
2.2
1.8
1.4
1.0
τ_2 (NSEC)
−60
−100
−140
−180
TEMP (°C)

Figure 4-33

Temperature Dependence of τ_1 for Butane

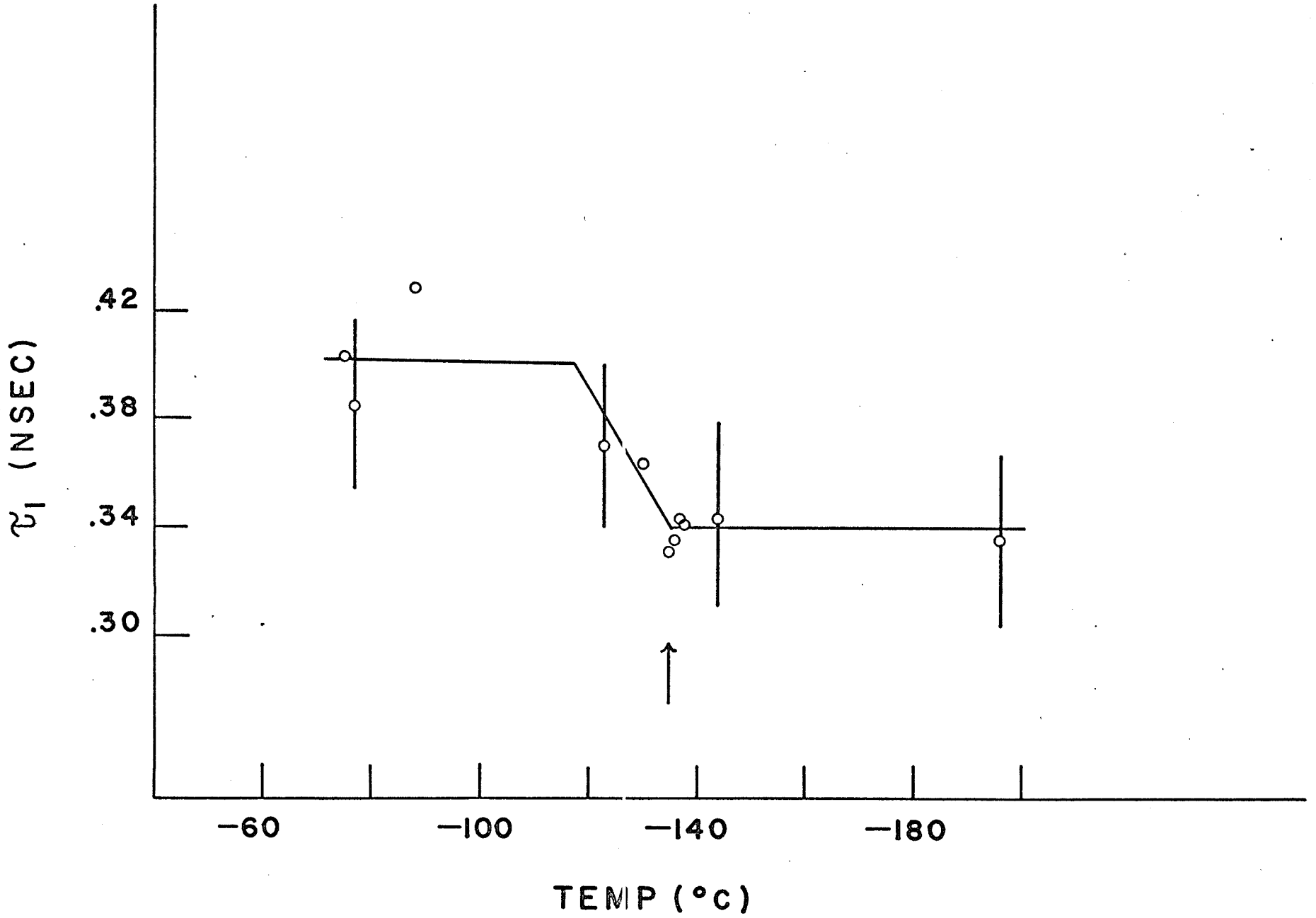
.42
.38
.34
.30
τ_1 (NSEC)
-60
-100
-140
-180
TEMP (°C)

Figure 4-34

Temperature Dependence of I_2 for Butane

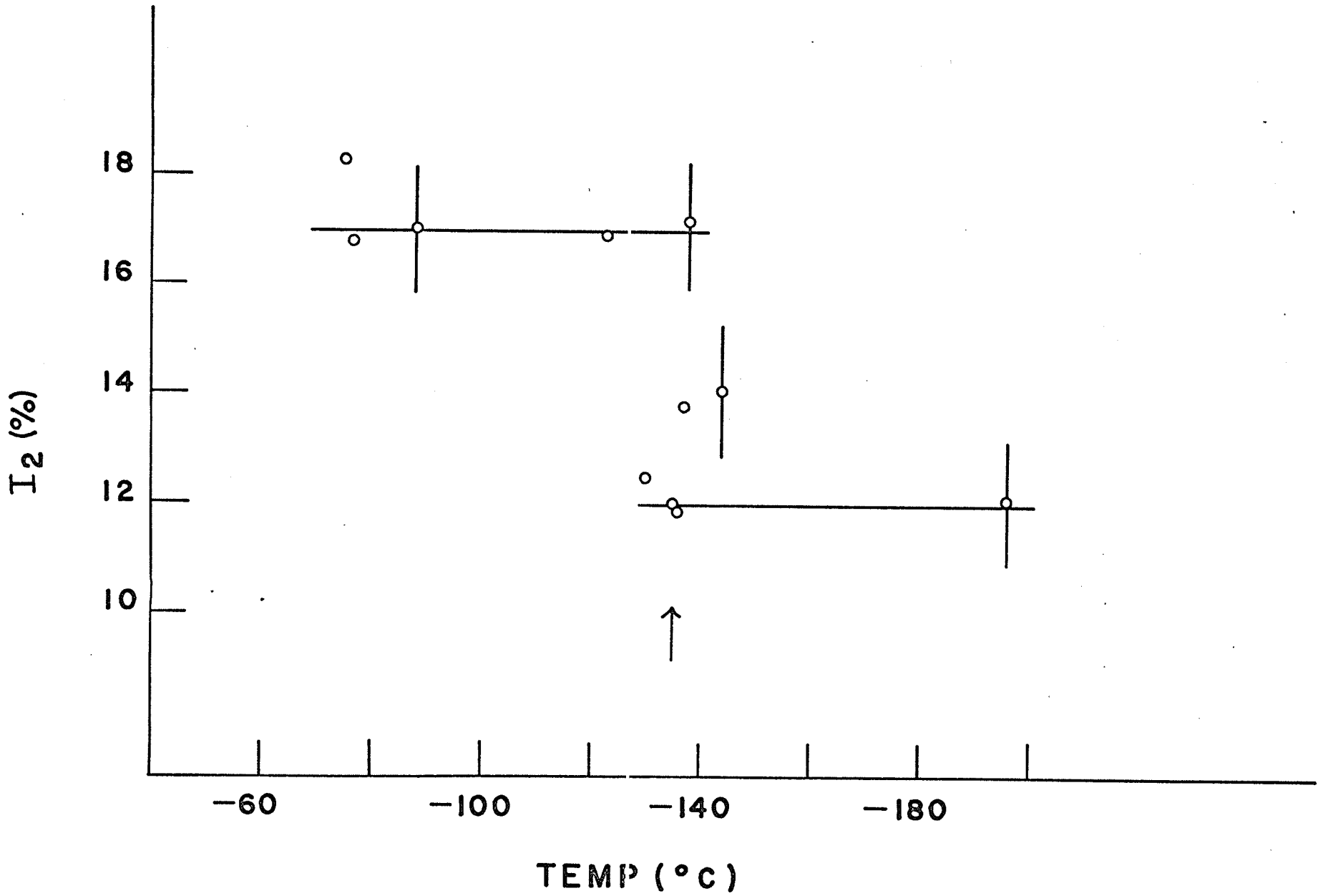
18
16
14
12
10
I_2 (%)
−60
−100
−140
−180
TEMP (°C)

Figure 4-35

Temperature Dependence of I_1 for Butane

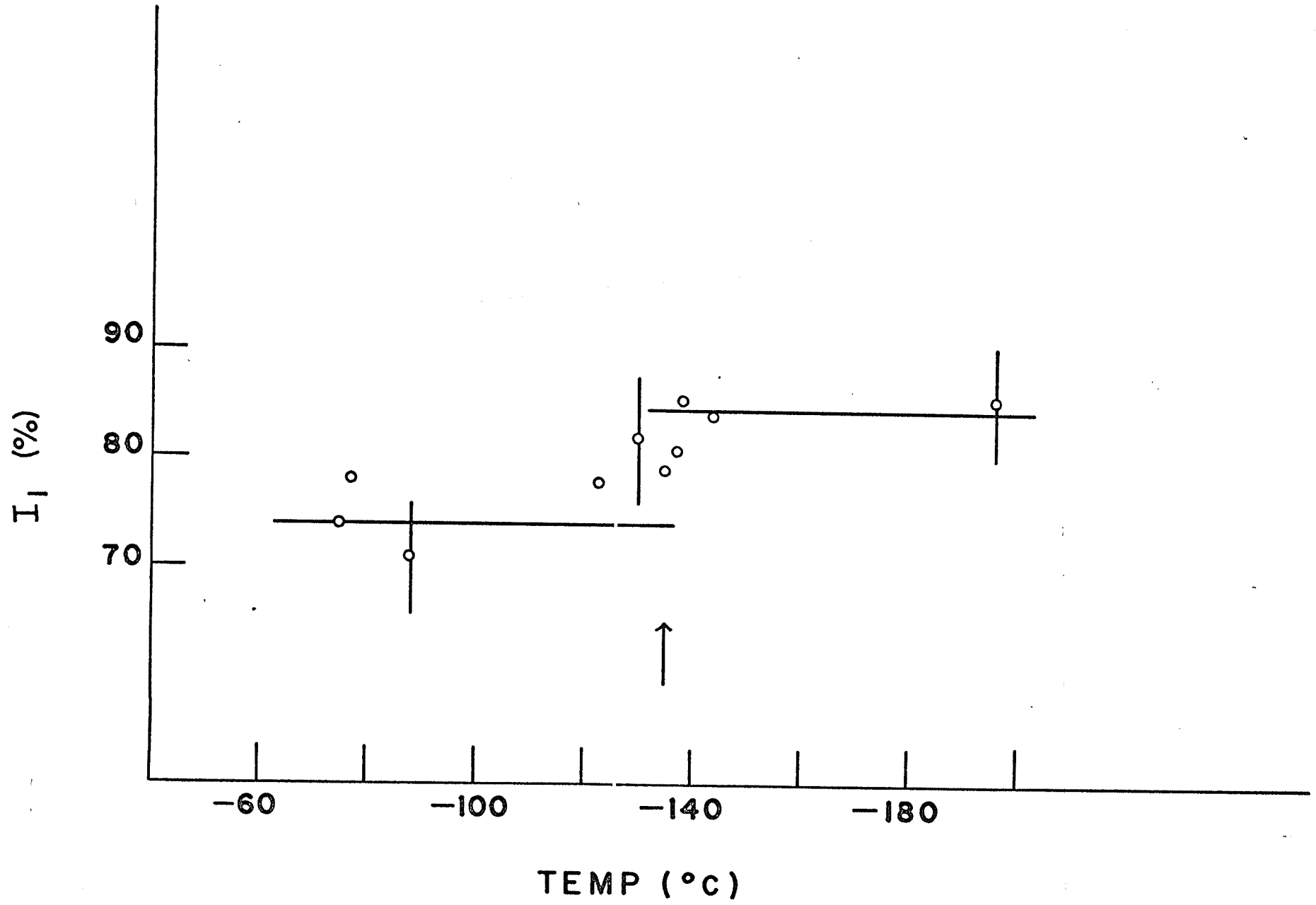
90
80
70
I_1 (%)
−60
−100
−140
−180
TEMP (°C)

CHAPTER V

DISCUSSION OF RESULTS

5.1 Introduction

During the last few years a number of investigations have been carried out to determine positron lifetimes and intensities in various materials under different conditions (C. Cottini et al. 1959, H. Clarke and B. G. Hogg 1962, G. Fabri, E. Germagnoli and G. Randone 1962, E. Kluth, H. Clarke and B. G. Hogg 1964, W. Brandt and I. Spirn 1966, A. Cooper, G. Laidlaw, and B. G. Hogg 1967, P. R. Gray, C. F. Cook and G. P. Sturm Jr. 1968. R. G. Lagu et al. 1969). These investigations were all designed to elucidate the various decay processes by which positrons annihilate in materials. Although at present no completely satisfactory theory is available which explains all the various experimental results, a number of semi-empirical models have been formulated to explain positron decay processes. This present work was carried out in order to test some of the present models and also to see what information could be gained through the use of positrons as a probe in studying some particular materials.

5.2 Lifetime Studies

After a positron enters a condensed medium it can eventually annihilate with an electron from the media to form gamma rays in two distinct ways. The first way is to annihilate

directly with an electron from the medium while the second way consists of the formation of a bound positronium atom before annihilation. For positronium atoms thus formed the decay rate in many cases is found to be a function of the physical and chemical state of the medium. In an attempt to explain the varying lifetimes in substances due to the changing of such parameters as pressure and temperature various modifications of what has come to be known as "The Free Volume Model" have been proposed.

The Free Volume Model in its simplest form attributes the variation in lifetime due to pressure or temperature as being due to the change in density of the material. Thus as the density is increased there is a corresponding reduction in the free volume available in the material for the positronium atom to occupy. Wallace in 1955 originally proposed a model in which positronium atoms resided in rectangular wells formed by repulsions from the surrounding atoms. Thus as the density was increased or the free volume of the substance was decreased the radius of the potential well was decreased. This caused the overlap of the positronium wave function with the electron clouds of the surrounding molecule to increase, resulting in a higher rate of pick-off annihilation.

Following Wallace's original idea Brandt, Berko and Walker in 1960 developed a simplified theoretical model in an attempt to explain the variation in positronium lifetime with

density. They started with the spin-averaged 2 γ annihilation rate for a positron in singlet positronium first worked out by Dirac in 1930.

5-1 $$\lambda_2 = \pi r_o^2 c \left| \Psi_- (\underline{r}_+) \right|^2$$

where $r_o = 2.8 \times 10^{-13}$ cm

c = velocity of light,

and the squared term represents the density of the electron at the position of the positron.

Thus in a lattice L of electron density distribution $\left| \Psi_L (\underline{r}) \right|^2$ composed of neutral atoms, the electron pickup rate or the pick-off annihilation rate of triplet positronium λp becomes:

5-2 $$\lambda p = \pi r_o^2 c \int_L \Psi_L^* (\underline{r}) \Psi_{+b}^* (\underline{r}) \Psi_{+b} (\underline{r}) \Psi_L (\underline{r}) \, d\underline{r}^3$$

where Ψ_{+b} is the wave function of the positron in the field of the electron to which it is bound as triplet positronium and the field of the lattice.

Equation 5-2 is then solved as a function of the properties of the lattice L under the following assumptions:

a) The mutual positronium and lattice polarization is neglected.

b) The lattice constituents are approximated by square potentials of height U_o, electron density ρ_o and radius r_o or excluded volume v_o, each centred in a cell v_1 of radius r_1. For $r_o \leq r \leq r_1$ $U_1 = 0$ and $\rho_1 = 0$; $v_1 - v_o$ is the free volume of the cell and $v^* = \frac{v_1}{v_o}$ the reduced cell volume.

c) The positronium atoms are thermalized and can be treated in the zero-velocity approximation ($K_{Ps} = o$).

Then by setting

5-3 $$\Psi_{+b}(\underline{r}_{+}) = \alpha(\underline{r}_{+o})\Psi_{Ps}(\underline{r}_{o})$$

where α is a polarization function and the subscript o refers to the centre of mass of the positronium Eq. 5-2 becomes:

5-4 $$\lambda_P = \pi r_o^2 c \rho_o \int_{V_o} \Psi_{Ps}^* \Psi_{Ps} \, d\,\underline{r}^3$$

Equation 5-4 is then evaluated in the Wigner-Seitz approximation giving an answer:

5-5 $$\lambda_P = \frac{\pi r_o^2 c \rho_o}{1+F(U_o, r_o, r_1)} = \frac{\pi r_o^2 c \rho_o}{1+F(P_o r_o^2, v^*)}$$

where $F(P_o r_o^2, v^*)$ can be evaluated for various lattice geometries (planar, hard sphere, long chain) as a function of the reduced cell volume v^* and a scattering parameter:

$$P_o r_o^2 = \frac{4m/\hbar^2}{U_o r_o^2}$$

The equations given to evaluate $F(P_o r_o^2, v^*)$ for the hard-sphere case are respectively:

5-6 $$E_o \coth E_o - 1 + \frac{(n_1 n_o+1)\sin(n_o-n_1)-(n_o-n_1)\cos(n_o-n_1)}{n_1 \cos(n_o-n_1)+\sin(n_o-n_1)} = 0$$

where: $$n_o = (P_o r_o^2 - E_o^2)^{\frac{1}{2}}$$

$$n_1 = n_o v^{*1/3}$$

5-7 $$F = \frac{E_o \cosh(2E_o)-1}{2n_o \sinh(2E_o)-2E_o} \times \frac{(1-n_1^2)\sin 2(n_o-n_1)+2n_1 \cos 2(n_o-n_1)-n_o(1+n_1^2)-n_1(1-n_1^2)}{n_1 \sin 2(n_o-n_1)+1-(1-n_1^2)\cos^2(n_o-n_1)}$$

Solving these equations by computer one then can find F as a function of the parameters $P_o r_o^2$ and v^*. Figures 5-1 and 5-2 show this dependence for various values of the parameter $P_o r_o^2$.

If the 3γ annihilation rate, which will be small compared to the pick-off rate, is neglected the triplet positronium lifetime due to pick-off is then given by:

5-8 $$\tau_2 = \frac{1 + F(P_o r_o^2, v^*)}{\pi r_o^2 c \rho_o}$$

Letting $\tau_o = \frac{1}{\pi r_o^2 c \rho_o}$ Equation 5-8 becomes:

5-9 $$\tau_2 = \tau_o(1 + F(P_o r_o^2, v^*))$$

Now if certain assumptions are made about τ_o and v_o Equation 5-9 can be compared with experimental results. In their work Brandt et al. (1960) assumed τ_o was equal to the mean life of freely annihilating positrons for which they chose the value $\tau_o = .35 \times 10^{-9}$ sec. In this work we have therefore followed their procedure choosing however for the lifetime τ_o the experimentally measured τ_1's since these should be equal to the lifetime of the free positrons in the various media.

In setting up the theory v_o is defined as the excluded volume due to the lattice potentials, while v_1 is simply the reciprocal density. In order to evaluate v_o Brandt et al. derive from the equation of state of a substance the condition that:

Figure 5-1

Dependence of F on v^* for a Hard Sphere Lattice

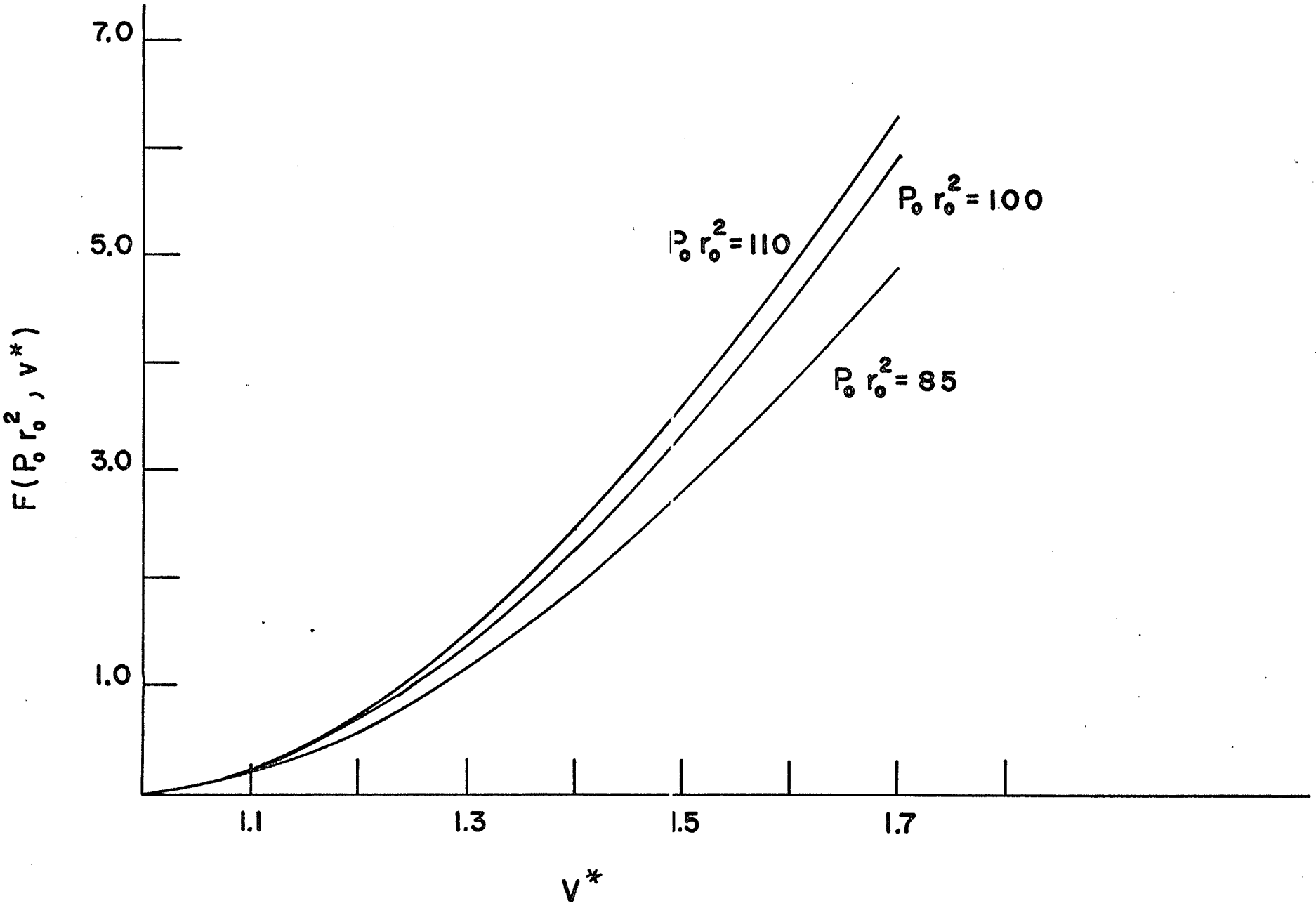
7.0
5.0
3.0
1.0
$F(P_o r_o^2, v^*)$
$P_o r_o^2 = 110$
$P_o r_o^2 = 100$
$P_o r_o^2 = 85$
1.1
1.3
1.5
1.7
v^*

Figure 5-2

Dependence of F on v^* for a Hard Sphere Lattice

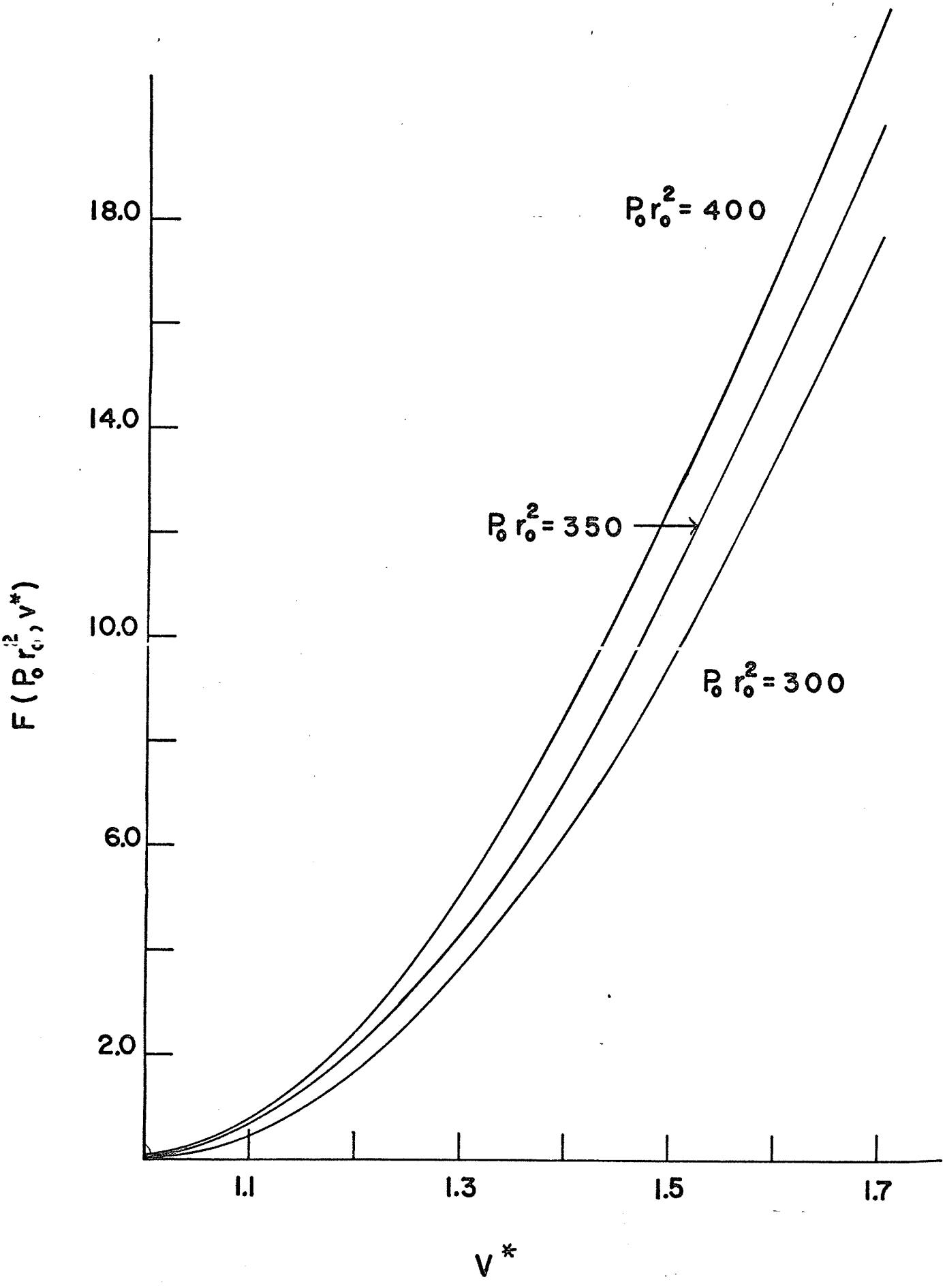
18.0
14.0
10.0
6.0
2.0
F (P0 r0^2, V*)
P0 r0^2 = 400
P0 r0^2 = 350
P0 r0^2 = 300
1.1
1.3
1.5
1.7
V*

$$\frac{v_1}{v_o} = \frac{3\sqrt{2}}{\pi} \quad \text{for spherical geometry}$$

$$\frac{v_1}{v_o} = \frac{2\sqrt{3}}{\pi} \quad \text{for cylindrical geometry}$$

for tightest packing at 0 degrees Kelvin. Thus by extrapolating v_1, the reciprocal density, to absolute zero one can find v_o.

Since v^* is defined as $\frac{v_1}{v_o}$ it can then be found for any given temperature through the use of temperature-density tables.

From our experimental results we can compare theory with experiment for Ammonia and Methane. Unfortunately density data is not available for Cyclohexane and Butane in the solid state so no calculations were carried out for these substances.

In the case of Ammonia temperature-density data was available from -185°C up to and beyond the highest temperatures measured (G. Jander, H. Spandau and C. Addison 1966). From this information the reciprocal density at 0°K was extrapolated as 1.18 cm^3/g. The v^* were then calculated for the region of interest and from Fig. 4-7 τ_o was found to be .35 x 10^{-9} sec. Since Ammonia belongs to the class of substances exhibiting hard-sphere geometry the curves of Fig. 5-1 were then used to find the parameter $P_o r_o^2$ which most closely fit the data. For Ammonia this was $P_o r_o^2 = 100$. The F's for the respective v^*'s

were then inserted in Equation 5-9 and the pick-off lifetimes τ_2 calculated for the various temperatures. Figure 5-3 shows the theoretical and experimental τ_2's over the range of temperatures studied.

In the work on Methane the temperature-density data was not as complete as for Ammonia (V. J. Johnson 1960) in that only one value for the density in the solid state was available. From the density data the reciprocal density at $0^{o}K$ was extrapolated to be 1.92 cm^3/g. The value of τ_o used in the calculations was .38 x 10^{-9} seconds as found from Fig. 4-25. Methane like Ammonia would have hard-sphere geometry so the curves of Fig. 5-2 were used to select the best value for the parameter $P_o r_o^2$. For Methane this value was 300. Using Equation 5-9 the pick-off lifetimes were then calculated for the various temperatures and Fig. 5-4 shows the experimental and theoretical lifetimes over the range of the experimental data.

As can be seen in Figures 5-3 and 5-4, for the chosen values of $P_o r_o^2$ the lifetimes in the liquid region fit well while the lifetimes in the solid region are slightly high for Ammonia and slightly low for Methane. Considering the simplified nature of the theory the agreement between theory and experiment would seem to be sufficient to justify the basic postulates of the theory as to the nature of the pick-off process.

Figure 5-3

Theoretical Fit of τ_2's for Ammonia as a Function of Temperature

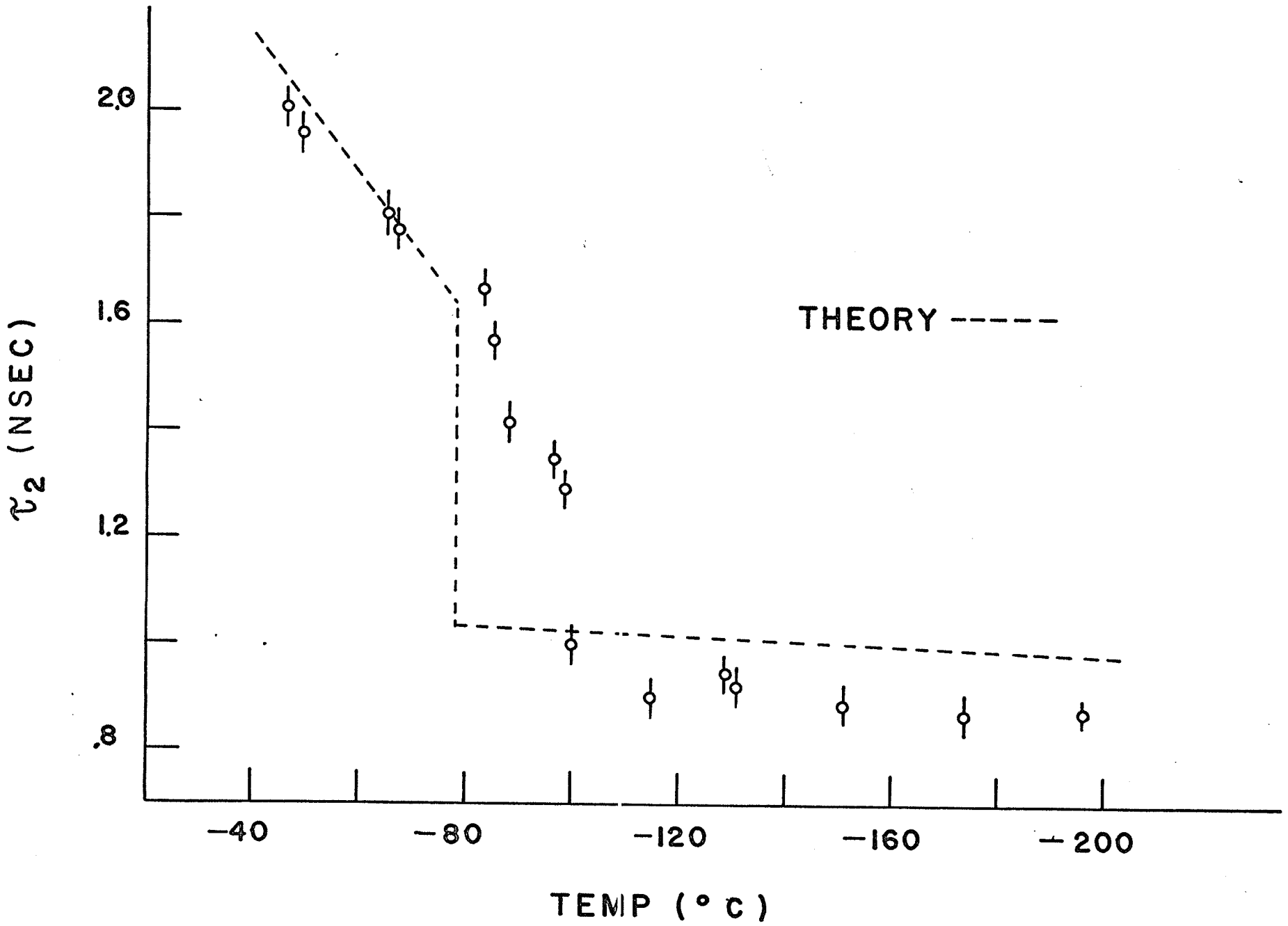
2.0
1.6
1.2
.8
τ_2 (NSEC)
THEORY -----
-40
-80
-120
-160
-200
TEMP (° C)

Figure 5-4

Theoretical Fit of τ_2's for Methane as a Function of Temperature

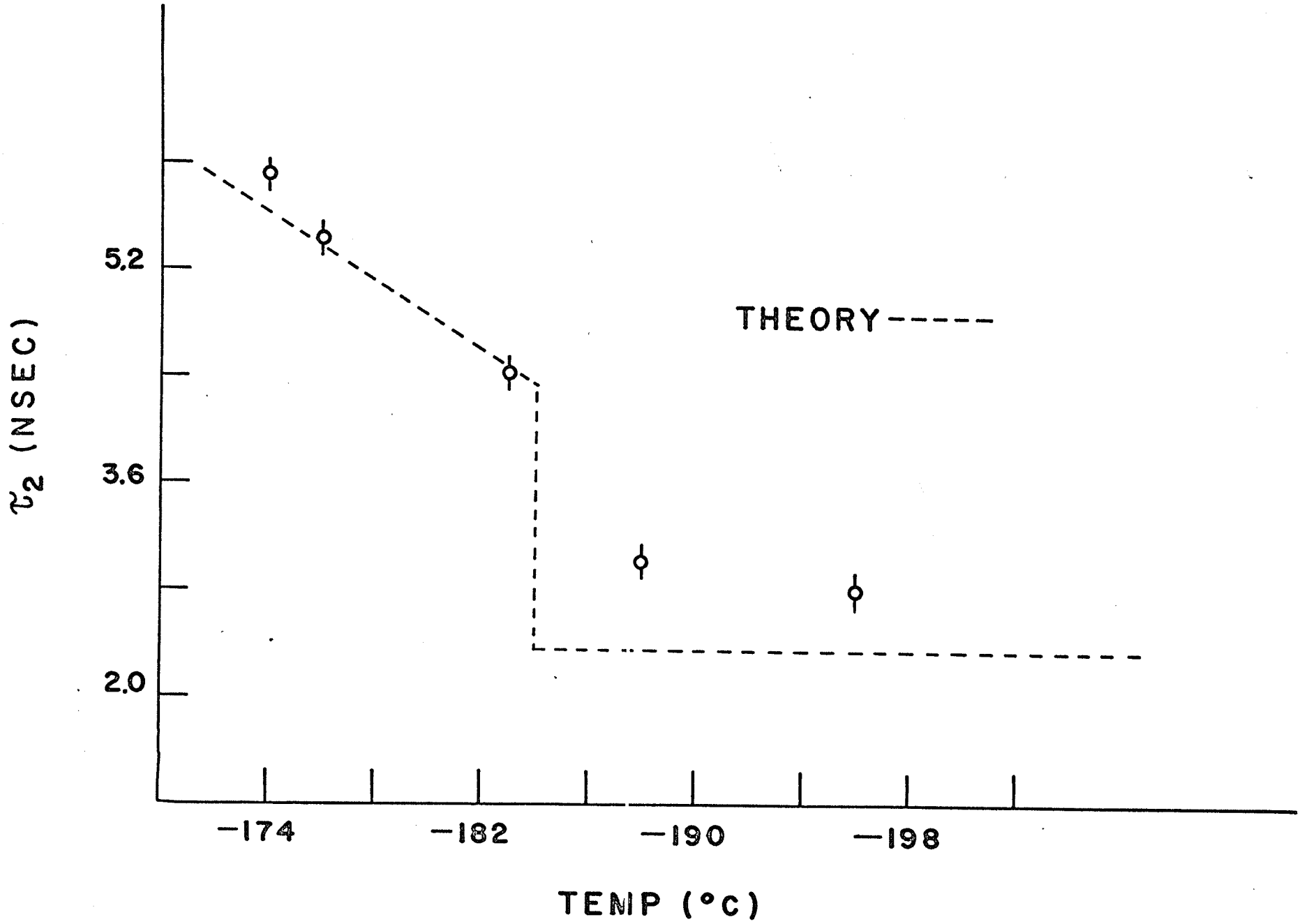
5.2
3.6
2.0
τ_2 (NSEC)
THEORY
-174
-182
-190
-198
TEMP (°C)

In a subsequent paper Brandt and Spirn (1966) modified the "free volume theory" to take into account thermal effects. With their modifications maxima were found to occur in the τ_2 versus temperature curve just before melting, for substances with high melting points. In the present work the τ_2 curves for Cyclohexane, Methane and Butane all show sharp transitions at the melting point with no evidence for maxima occurring before melting. In the case of Ammonia the transition is not sharp however since the lifetimes just before melting are higher than expected rather than lower, this cannot be due to a thermal effect. Thus we can conclude that in the temperature range of the present experiments the effect of thermal motion on the pick-off lifetime does not seem to be significant.

A final point to be considered is the effect of dissolved oxygen on the various lifetimes. As has been pointed out previously (J. Lee and G. J. Celitans 1965, A. M. Cooper, G. Laidlaw and B. G. Hogg 1967) dissolved oxygen has a large quenching effect on the triplet lifetime τ_2. This effect is noted for Cyclohexane in Figure 4-16. What is also interesting to note in Fig. 4-16 is that the quenching effect of the dissolved oxygen carries on into the solid phase of the material but disappears after the solid-solid phase transition. A possible explanation for this would be that in the high temperature solid phase the dissolved oxygen retained some mobility through the lattice and thus was able

to quench the positronium, while in the low temperature solid phase the dissolved oxygen was trapped in the lattice and therefore was not able to quench the positronium formed. As can be seen in Fig. 4-17 the dissolved oxygen had no effect on the short lifetime τ_1.

5.3 Positronium Formation

After a positron enters a medium one of the processes open to it before annihilation is the formation of a bound positron-electron pair or positronium. The factors which effect the formation of positronium in a given substance have been studied by a number of workers (A. T. Stewart 1955, H. S. Landes, S. Berko, and A. J. Zuchelli 1956, C. R. Hatcher, W. E. Millet and L. Brown 1958, R. L. de Zafra and W. T. Joyner 1958, C. R. Hatcher 1961, D. P. Kerr and B. G. Hogg 1962, W. A. Falk and G. Jones 1964, R. K. Wilson, P. O. Johnson and R. Stump 1963, C. Y. Leung and D. A. L. Paul 1967) and from these and other investigations various models concerning the probability of positronium formation have been advanced.

A useful model which describes the formation of positronium in substances is based on the concept of the "Ore Gap" first postulated by A. Ore (1949). In the Ore model the high energy positrons (having a β decay energy distribution with an end point of .54 MeV from Na^{22}) which enter a media are rapidly slowed to energies approximating the first ionization potential, V_i, of the media by non-elastic ionizing

collisions. During this time the annihilation probability will be less than a few percent (J. Green and J. Lee 1964). Also for energies above the first ionization potential positronium formation will be negligible compared with ionization since electron removal to the continuum will be much more probable than the formation of a discrete bound state. After the energy of the incident positron falls below the ionization potential of the media processes other than ionization are necessary in order for the positron to lose energy. In the case where the positron's energy exceeds the energy of the first excited state, E_1, excitation collisions are expected to be the dominant process for energy loss. After the positron's energy drops below E_1 positronium formation is considered to be the dominant process until such time that the positron loses sufficient energy such that positronium formation is no longer energetically possible. Below this point positrons will lose energy by elastic collisions until they annihilate freely with the electrons of the media.

Using this model certain predictions concerning the probability of formation of positronium can be made. Since the binding energy of a positronium atom is 6.8 eV and since V_i is generally greater than 6.8 eV only positrons with an energy greater than $(V_i-6.8)$ eV will be capable of forming positronium. Thus positronium formation is only probable in the energy region $E_1 > V > (V_i-6.8)$ the so-called "Ore Gap".

If one then makes the assumption that no positronium formation or annihilation takes place above V_i and that all energies are equally probable below V_i, and if one further assumes all excitation collisions between E_1 and V_i degrade the positron's energy below the Ore Gap while all positrons with energies within the Ore Gap form positronium, then an estimate can be made of the percentage of positrons forming positronium. This will be:

$$P = \frac{E_1 - (V_i - 6.8)}{V_i}$$

Then since statistically three-quarters of the positrons form positronium in the triplet state and one-quarter in the singlet state, I_2 the intensity of the long lived triplet state will be given by:

$$I_2 = \frac{3}{4}\left(\frac{E_1 - (V_i - 6.8)}{V_i}\right)$$

Using this simple theory reasonable agreement was found in the case of a number of gases (M. Deutsch 1953, T. A. Pond 1952, B. Gittelmen and M. Deutsch 1956). Also in 1961 Hatcher showed that the Intensity of the long lived component in Halogen derivatives could be explained on the basis of the Ore model by assuming the upper bound of the Ore Gap to be equal to the dissociation potential of the Carbon-Halogen bond. Thus in principle the Ore model would seem to be reasonably well founded.

In systems other than gases and some liquids however, the unmodified Ore theory predicts positronium formation probabilities which are at variance with the results of experiment. Thus various modifications of the Ore theory have been attempted to explain the various experimental results. These modifications fall into two main categories: those which attempt to explain the action of various substances which inhibit the formation of positronium (V. I. Goldanski 1968) and those which attempt to explain the formation probability as effected by physical changes to the system. In attempting to explain our experimental results we are interested in models of the second kind.

Table 5-1 shows Intensities as calculated by the Ore theory compared to our experimental results. As can be seen the agreement is poor. Also one is faced with the problem that the Ore theory does not differentiate among the various physical states of a given system while experimentally large changes may be found in going from one state to another.

Table 5-1

Substance	V_i* (eV)	E_1* (eV)	Calculated I_2 (%)	Experimental I_2 (%)	
				Liquid	Solid
Ammonia	10.34	4.51	7.0	25 ± 2	25 ± 2
Cyclohexane	10.0	4.08	6.6	31 ± 2	21 ± 2, 18 ± 2
Methane	12.99	4.38	0	32 ± 2	32 ± 2
Butane	9.0	3.47	11.0	17 ± 2	11 ± 2

* Vedeneyev et al. 1966

Recently two models have been proposed to explain positronium formation in liquid and solid systems and the changes which occur in passing through a phase change (W. Brandt and I. Spirn 1966, R. G. Lagu et al. 1969). In the model proposed by Brandt and Spirn they assume the percentage of positrons forming positronium in a given substance is a constant controlled by the nature of the media. In their work they identify three components in the decay curve. The longest lived component is attributed to triplet positronium decaying in regions of low density of the material and the shortest component (approximately .25 nsec) to the decay of singlet positronium plus the decay of triplet positronium in regions of high density. The third component (approximately .50 nsec) they attribute to the decay of free positrons. In their work they found the fraction of positrons decaying freely remained constant with temperature. Also they found that although the relative intensities of the longest and shortest components varied with temperature their sum remained constant. They then postulated that positronium formed in domains with a free volume less than some critical free volume, V_c, would annihilate in the fast component while positronium formed in domains with a free volume greater than V_c would annihilate in the longer component. They further assumed that the fraction of positrons forming triplet positronium in the low density domains would be given by:

$$I_2 = (\text{Total Positronium Formed}) \frac{3}{4} P_{CR}$$

where P_{CR} is the probability of formation in a domain with free volume greater than V_c.

They give P_{CR} as:

$$P_{CR} = \exp(-V_c/V_f)$$

where V_f is the average reduced free volume per molecule. Since V_f can be calculated from temperature-density tables they were then able to fit their experimental results by the choice of an appropriate V_c.

In this work we have two sets of experimental results available to us with which we are able to check the validity of this theory. The first of these is the experimentally measured I_2's as a function of temperature measured from the time spectra during the course of this work. The second is angular correlation datum from work performed in our laboratory for which the momentum distributions for a number of the substances studied have been worked out. In the momentum distributions two components, a high momentum component and a low momentum component are usually found. Figures 5-5 and 5-6 illustrate this for the case of Ammonia and Methane. Previous authors (A. T. Stewart 1955, R. L. de Zafra and W. T. Joyner 1958, R. A. Ferrell 1956, D. P. Kerr, S. Y. Chuang and B. G. Hogg 1965) have attributed the low momentum component to the decay of singlet positronium. If this is the case then since statistically three-quarters of the

Figure 5-5

Momentum Distribution for Ammonia from Angular Correlation Work

(A) - Singlet Positronium

(B) - Triplet Positronium and Free Annihilations

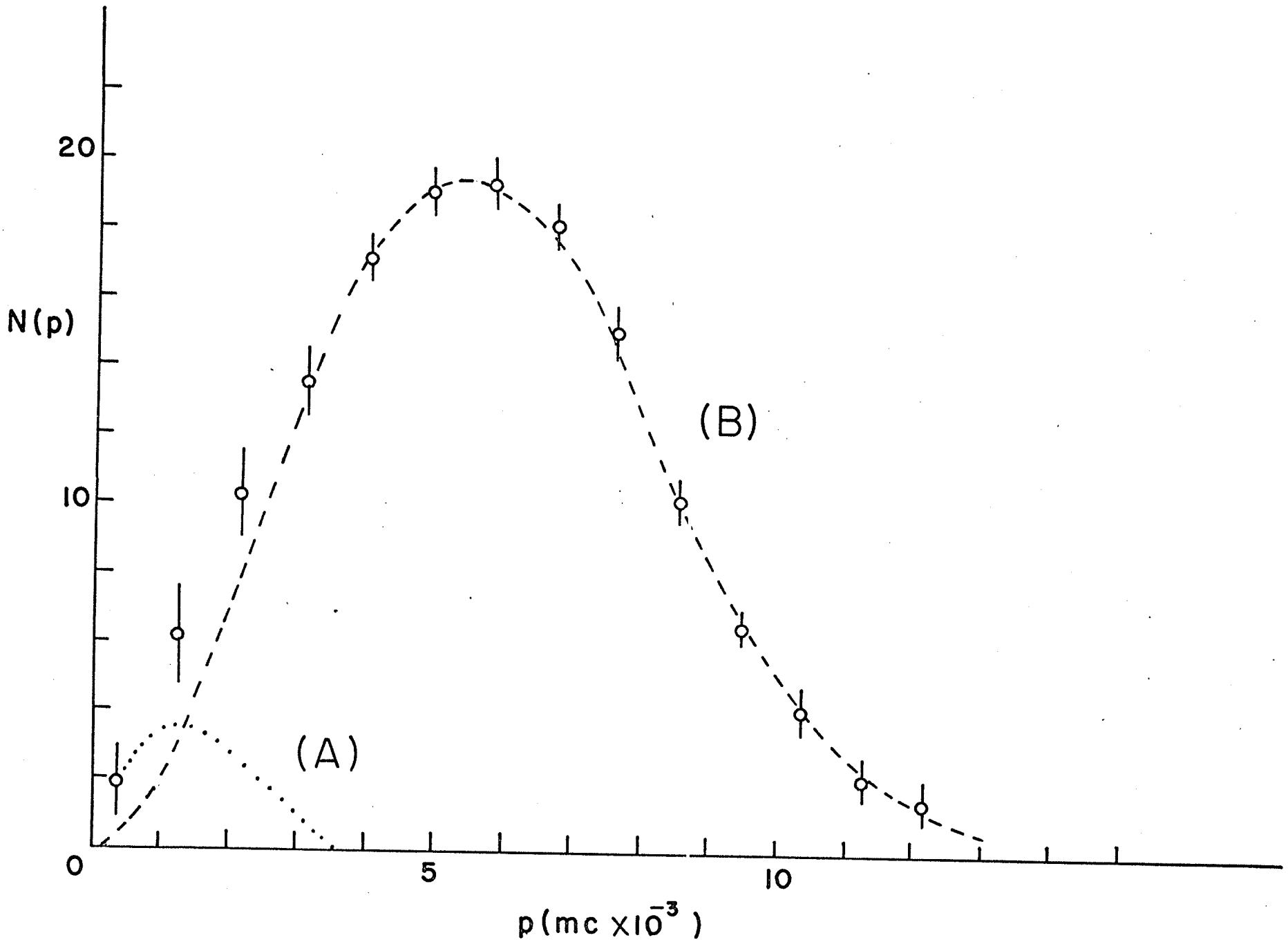
N(p)
20
10
0
5
10
p(mc x10⁻³)
(A)
(B)

Figure 5-6

Momentum Distribution for Methane from Angular Correlation Work

(A) - Singlet Positronium

(B) - Triplet Positronium and Free Annihilations

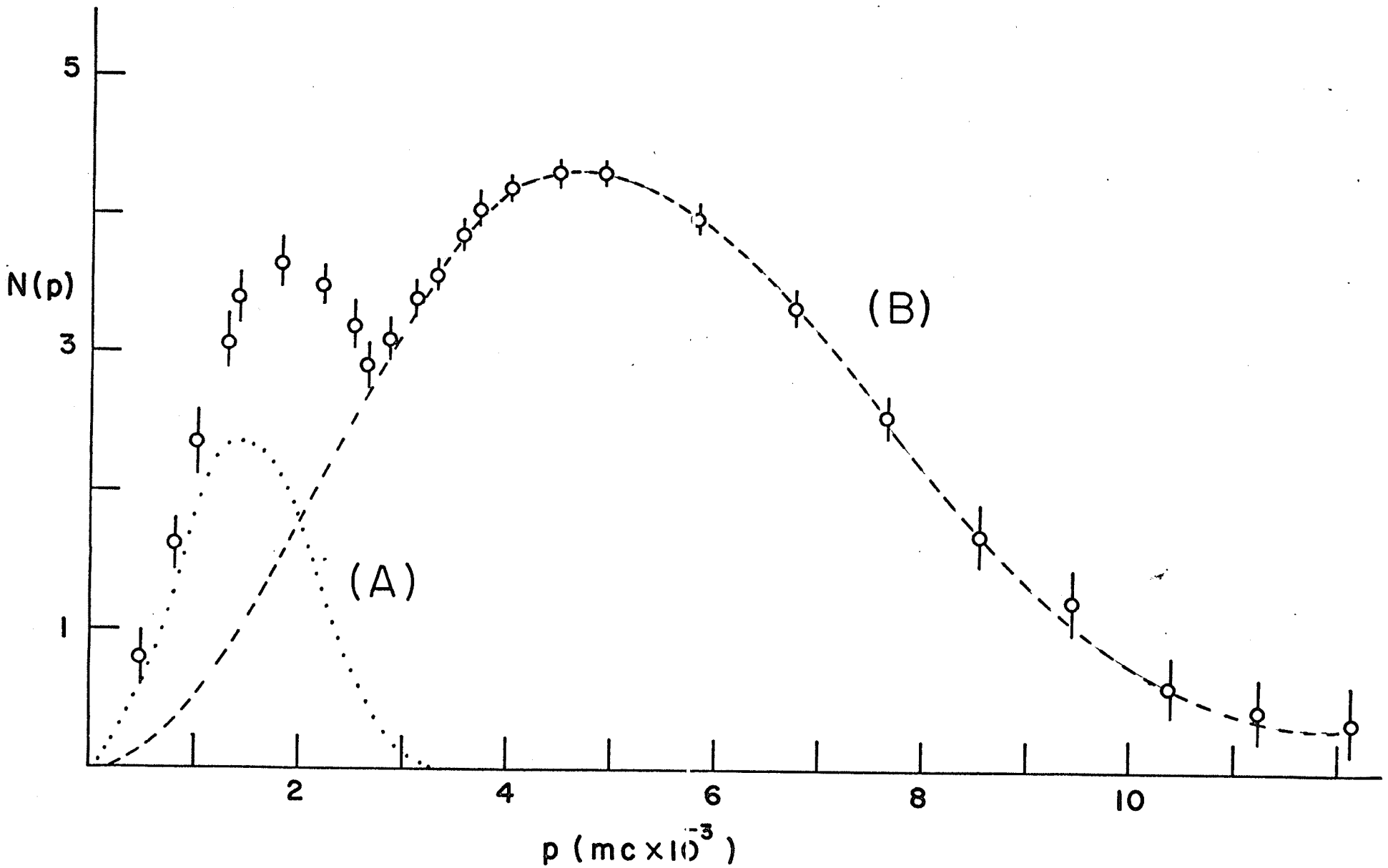
5
3
1
N(p)
(A)
(B)
2
4
6
8
10
p (mc x 10^-3)

positrons forming positronium will form in the triplet state and one-quarter in the singlet state, I_L the percentage of counts arriving in the low momentum component should equal one-third of I_2 the percentage of triplet positronium atoms formed. Table 5-2 gives the experimentally found I_2's and I_L's for three of the substances studied. As can be seen in all cases except for solid methane $I_2/3$ agrees within experimental error with I_L. In the case of solid methane the angular correlation data was taken with a strong Cu^{64} source ($\sim$2 Curies) and it is felt radiation damage in the sample may account for the anomalous result. Further studies are in preparation to clarify this point.

Table 5-2

Substance	Phase	I_L (%)	$I_2/3$ (%)
Ammonia	Liquid	7 $\pm$ 1	8 $\pm$ 1
Ammonia	Solid	7 $\pm$ 1	8 $\pm$ 1
Methane	Liquid	11 $\pm$ 1	11 $\pm$ 1
Methane	Solid	0	11 $\pm$ 1
Butane	Liquid	6 $\pm$ 1	6 $\pm$ 1
Butane	Solid	4 $\pm$ 1	4 $\pm$ 1

If we now consider the theory of Brandt and Spirn on the basis of these results a major discrepancy arises. In their work in each of the substances studied approximately one-half or more of the positronium formed was formed in regions

of high density and so decayed via the fast component. Thus this positronium does not appear in the long lifetime component of the spectra. However if one believes that the low momentum component found by angular correlation studies is due to the decay of singlet positronium then all the singlet positronium formed irregardless of whether it is formed in regions of high or low density should appear in the low momentum component. In our work, however, the percentage of positrons decaying in the low momentum component is found to agree with the amount of singlet positronium predicted on the basis of the long lived intensities as found by the time studies. Thus if the accepted picture of I_L being due to the decay of singlet positronium is correct the theory of positronium being formed in regions of high density from which it decays as a fast component would not seem tenable.

In the model proposed by Lagu et al. (1969), they attempt to correlate triplet positronium lifetimes and formation probabilities. To do this they make certain assumptions concerning the formation of positronium in solids and liquids. These assumptions are that in a substance positronium can only form in vacancies which are larger than the classical diameter of a positronium atom (1.06 angstroms) and that the fraction of positrons forming positronium in a substance is controlled by the number of vacancies with diameters above this critical size. They further assume that in a solid the number of vacancies

will remain reasonably constant, with a decrease in density of the material simply enlarging the existing vacancies without creating many new ones, while on passing through the liquid-solid phase transition more vacancies will be created as well as enlargement of existing vacancies. Thus if we apply this model to our results we see in the case of Cyclohexane that on passing through the solid-solid phase transition very little change in Intensity takes place, while on passing through the solid-liquid transition a large increase in the percentage of positrons forming positronium is found. Also in the case of Butane an increase in Intensity is found on melting. Thus in both these cases this model empirically explains the results. In the case of Ammonia and Methane however no change in Intensity, I_2, is noted on melting which is in disagreement with this model.

An explanation of these results is possible if one considers the relative size of the Ammonia and Methane molecules as compared to that of Cyclohexane. By taking the interatomic distances and the covalent radius of hydrogen (L. Pauling 1948) one can estimate the diameters of the various molecules as: Ammonia 1.2 angstroms, Methane 1.3 angstroms, Cyclohexane 3.8 angstroms. Thus Cyclohexane is more than three times larger than the other two molecules. If one then considers the intermolecular spacing as obtained from crystallographic data (C.R.C. Handbook 1962, W. J. Dunning 1961)

the various distances are found to be 5.15 angstroms for Ammonia, 5.89 angstroms for Methane and 6.1 angstroms for Cyclohexane in the cubic state. Thus the free volume for positronium formation in Cyclohexane is considerably smaller than in the case of the other two molecules. If one then postulates that a certain critical sized free volume, greater than the classical diameter of positronium, is necessary for positronium formation it seems possible that in the case of Ammonia and Methane there exists in the natural lattice sufficient free volume between molecules for positronium formation, while in the case of Cyclohexane this may not be so. In this case the number of defects in the solid causing free volumes over the critical size would control the amount of positronium formed and these would be expected to increase at melting. In the case of Methane and Ammonia however since the necessary free volume exists between molecules in the solid phase one would not expect to see an increase in intensity in going from the solid to the liquid phase.

This idea would seem to be born out by the results on Butane and by the previous work on Napthalene (H. Landes et al. 1956) since these are both large molecules which exhibit changes in I_2 at the phase transition.

A final point in the discussion of formation probabilities is the effect dissolved oxygen has on the intensity of triplet positronium. As can be seen in Fig. 4-18

no effect was noted for the case of Cyclohexane. This is in agreement with earlier work (D. P. Kerr et al. 1965).

5.4 Positron Lifetime Studies in Plastic Crystals

Recently positron annihilation studies have branched into two main areas. The first area contains those studies undertaken to elucidate the nature of the positron decay process under various conditions. Typical work of this type has been considered in the previous sections of this chapter. The second area is that in which the positron has been used as a probe in studying various properties of materials. Typical of this work has been the study of Fermi surfaces by angular correlation work (K. Fujiwara and O. Sueoka 1966, D. L. Williams et al. 1968) and the attempt to correlate the degree of crystallinity in materials with the various positron decay parameters (S. J. Tao and J. H. Green 1965, A. M. Cooper 1965, I. K. MacKenzie, B. T. A. McKee 1966).

Since numerous studies of "Plastic Crystals" have been performed in the past in an attempt to understand the molecular properties of these substances (Conference on Plastic Crystals 1961) it was felt that investigation by the method of positron annihilation should prove instructive in assessing the value of positrons as probes for studying materials of this type.

The aspect of those materials referred to as "Plastic Crystals" which most interested us was the fact that they all exhibit solid-solid phase changes. These phase changes refer

to the fact that the material undergoes a change in its crystallographic structure at some transition point.

The first Plastic Crystal studied was Cyclohexane since extensive work has been carried out on this material. Precision measurements of the molar heat capacities, C_{p_1} of Cyclohexane have established the existence of the solid-solid transition to be at -87.06°C (J. G. Aston, G. J. Szar and H. L. Fink 1943, R. A. Ruehrivein and H. M. Huffman 1943). X-Ray experiments have determined that the high temperature solid phase is cubic, while the low temperature phase has been described variously as having a low class of symmetry, a monoclinic structure and a triclinic structure (O. Hassel and H. Kringstadt 1930, O. Hassel and A. M. Sommerfelt 1938, K. Lonsdale and H. Smith 1939, R. Krishma Murti 1958, M. Renaud). Experiments with ultrasound indicate that both the longitudinal and transverse velocities suffer a discontinuity at the transition point (C. E. Scheie and J. R. Green 1964) and infra-red absorption above and below the transition temperature confirms the phase change (A. LeRoy 1965). Nuclear magnetic resonance experiments have shown that the line width and spin-lattice relaxation time change discontinuously at -86°C (E. R. Andrew and R. G. Eades 1953).

In our work lifetime studies were carried out on Cyclohexane as a function of temperature in the region -196°C to +50°C. As can be seen in Fig. 4-16 to 4-19 the long lifetime

τ_2 showed an abrupt change at the phase transition, while the other decay parameters remained constant or showed only small changes. Based on this result it would thus seem that positrons should be useful in detecting crystallographic differences in materials as well as the amount of crystallinity in a substance. Unfortunately since temperature-density data for Cyclohexane in the solid phase is not available it was not possible to calculate whether the change in τ_2 at the transition point is simply due to a density change as predicted by the Free Volume theory or whether some other mechanism is operating. Further work on other materials will be necessary to clarify this point, however at this time it would appear that the positron lifetime technique provides another method for detecting solid-solid phase changes in materials.

Methane which is also a Plastic Crystal exhibits a solid-solid phase change at 20°K and so with the present equipment we were not able to cool the sample sufficiently to investigate this particular transition.

REFERENCES

C. D. Anderson, Phys. Rev. 41, 405 (1932)

E. R. Andrew and R. G. Eades, Proc. Royal Soc. A216, 398 (1953)

J. G. Aston, G. J. Szar and H. Fink, J. American Chem. Soc. 65, 1135 (1943)

R. E. Bell and H. E. Petch, Phys. Rev. 76, 1409 (1949)

R. E. Bell, R. L. Graham and H. E. Petch, Can. J. Phys. 30, 35 (1952)

R. E. Bell and R. Graham, Phys. Rev. 90, 644 (1953)

R. E. Bell and M. Jorgensen, Can. J. Phys. 38, 652 (1960)

R. E. Bell, Coincidence Techniques and the Measurement of Short Mean Lives, II α, β, γ -Ray Spectroscopy, Editor Kai Siegbahn, North Holland Publishing Company (1966)

S. Berko and A. J. Zuchelli, Phys. Rev. 102, 724 (1956)

M. Bertolaccini and L. Zappa, Nuovo Cim. 52B, 487 (1967)

W. Brandt, S. Berko and W. W. Walker, Phys. Rev. 120, 1289 (1960)

W. Brandt and I. Spirn, Phys. Rev. 142, 231 (1966)

S. Y. Chuang, Ph.D. Thesis, University of Manitoba (1968)

H. C. Clarke and B. G. Hogg, J. Chem. Phys. 37, 1898 (1962)

Conference on Plastic Crystals, J. Phys. Chem. Solids 18, 1 (1961)

A. M. Cooper, Master's Thesis, University of Manitoba (1965)

A. M. Cooper, G. J. Laidlaw and B. G. Hogg, J. Chem. Phys. 46, 2441 (1967)

C. Cottini, G. Fabri, E. Gatti and E. Germagnoli, Nuovo Cim. 14, 454 (1959)

P. A. M. Dirac, Proc. Cambridge Phil. Soc. 26, 361 (1930)

M. Deutsch, Phys. Rev. 82, 455 (1951)

M. Deutsch, Phys. Rev. 83, 866 (1951)

M. Deutsch, Prog. Nucl. Phys. 3, 131 (1953)

R. L. de Zafra, W. T. Joyner, Phys. Rev. 112, 19 (1958)

W. J. Dunning, J. Phys. Chem. Solids 18, 21 (1961)

G. Fabri and E. Germagnoli, Nuovo Cim. 23, 572 (1962)

G. Fabri, E. Germagnoli and G. Randone, Phys. Letters 3, 6 (1962)

G. Fabri, G. Poletti and G. Randone, Phys. Rev. 135A, 328 (1964)

G. Fabri, G. Poletti and G. Randone, Phys. Rev. 151, 356 (1966)

W. A. Falk and G. Jones, Can. J. Phys. 42, 1751 (1964)

R. A. Ferrell, Rev. Mod. Phys. 28, 308 (1956)

J. S. Fraser and J. C. D. Milton, Chalk River Progress Report PR-P-20 (1953); Nucl. Instr. and Meth. 2, 275 (1958)

K. Fujiwara and O. Sueoka, J. Phys. Soc. Japan 21, 1947 (1966)

B. Gittleman and M. Deutsch, Ann. Prog. Report, Lab. Nuclear Science, M.I.T. (1956)

D. A. Gedcke and W. J. McDonald, Internal Report, Nuclear Research Centre, University of Alberta, (1967)

V. I. Goldanskii, Atomic Energy Review, Vol. 6, No. 1 (1968)

R. L. Graham, J. S. Geiger, R. E. Bell and R. Barton, Nucl. Inst. and Meth. 15, 40 (1962)

P. R. Gray, C. F. Cook and G. P. Sturm Jr., J. Chem. Phys. 48, 1145 (1968)

J. Green and J. Lee, Positronium Chemistry, Academic Press 27 (1964)

R. E. Green and R. E. Bell, Can. J. Phys. 35, 398 (1957)

O. Hassel and H. Kringstadt, Tids. Kemi Bergvesen X, 128 (1930)

O. Hassel and A. M. Sommerfelt, Z. Physik Chemie 40, 391 (1938)

C. R. Hatcher, W. E. Millet and L. Brown, Phys. Rev. III, 12 (1958)

C. R. Hatcher, J. Chem. Phys. 35, 2266 (1961)

G. Iaci, I. F. Quercia and E. Turrisi, Nuovo Cim. 24, 746 (1962)

G. Jander, H. Spandau and C. C. Addison, Chemistry in Nonaqueous Ionizing Solvents, Vol. 1, Chemistry in Anhydrous Liquid Ammonia, Interscience Publishers (1966)

V. J. Johnson, A Compendium of the Properties of Materials at Low Temperature (Phase 1), U. S. Air Force, Wright Patterson Air Force Base, Ohio, Distributed by Clearinghouse for Federal Scientific and Technical Information

D. P. Kerr and B. G. Hogg, J. Chem. Phys. 36, 2109 (1962)

D. P. Kerr and B. G. Hogg, Rev. Sci. Instr. 33, 391 (1962)

D. P. Kerr, A. M. Cooper and B. G. Hogg, Can. J. Phys. 43, 963 (1965)

D. P. Kerr, S. Y. Chuang and B. G. Hogg, Molec. Phys. 10, 13 (1965)

E. L. E. Kluth, H. Clarke and B. G. Hogg, J. Chem. Phys. 40, 3180 (1964)

R. G. Lagu, V. G. Kulkarni, B. V. Thosar and G. Chandra, Proc. Indian Acad. Sci. LXIX, 48 (1969)

H. S. Landes, S. Berko and A. J. Zuchelli, Phys. Rev. 103, 828 (1956)

J. Lee and G. J. Celitans, J. Chem. Phys. 42, 437 (1965)

A. Leroy, C. R. Acad. Sc. Paris 260, 6079 (1965)

C. Y. Leung and D. A. L. Paul, Positron Annihilation, edited by A. T. Stewart and L. O. Roellig, Academic Press 409 (1967)

K. Lonsdale and H. Smith, Phil. Mag. 28, 615 (1939)

I. K. MacKenzie and B. T. A. McKee, Can. J. Phys. 44, 435 (1966)

A. P. Mills and S. Berko, Phys. Rev. Letters 18, 420 (1967)

S. Mohorovicic, Astron. Nachr. 253, 94 (1934)

R. Krishma Murti, Indian J. Phys. 32, 460 (1958)

A. Ore, Univ. Bergen Arb. Naturvit. rekke, 9 (1949)

A. Ore and J. L. Powell, Phys. Rev. 75, 1696 (1949)

L. A. Page and M. Heinberg, Phys. Rev. 102, 1545 (1956)

D. A. L. Paul, Can. J. Phys. 36, 640 (1958)

L. Pauling, Nature of the Chemical Bond, Cornell University Press (1948)

T. A. Pond, Phys. Rev. 85, 489 (1952)

M. Renaud, Private Communication to A. Leroy (see A. Leroy)

A. E. Ruark, Phys. Rev. 68, 278 (1945)

R. A. Ruehrivein and H. M. Huffman, J. Am. Chem. Soc. 65, 1620 (1943)

C. E. Scheie and J. R. Green, U. S. A.E.C. Document SC-DC-64-2060X (1964)

A. Schwarzchild, Nucl. Instr. and Meth. 21, 1 (1963)

A. T. Stewart, Phys. Rev. 99, 594 (1955)

S. J. Tao and J. H. Green, Proc. Phys. Soc. 85, 463 (1965)

V. I. Vedeneyev, L. V. Gurvich, V. N. Kondratyev, V. A. Medvedev and Y. L. Frankevich, Bond Energies, Ionization Potentials and Electron Affinities, Edward Arnold Publishers (1966)

W. R. Wall, Ph.D. Thesis, University of Manitoba (1968)

P. R. Wallace, Phys. Rev. 100, 738 (1955)

D. L. Williams, E. H. Becker, P. Petrevich and Garth Jones, Phys. Rev. Letters 20, 448 (1968)

R. K. Wilson, P. O. Johnson and R. Stump, Phys. Rev. 129, 2091 (1963)

C. N. Yang, Phys. Rev. 77, 242 (1950)

Publications

On Oxygen Quenching of Positronium In Liquids, D. P. Kerr, A. M. Cooper and B. G. Hogg, Can. J. Phys. 43, 963 (1965)

Oxygen Quenching of Positron Lifetimes in Liquids, A. M. Cooper, G. Laidlaw and B. G. Hogg, J. Chem. Phys. 46, 2441 (1967)

Positron Annihilation in Condensed Ammonia, W. H. Holt, S. Y. Chuang, A. M. Cooper and B. G. Hogg, J. Chem Phys. 49, 5147 (1968)

Detection of the Polymorphic Transition at -86°C in Cyclohexane by Positron Annihilation, A. M. Cooper, G. deBlonde and B. G. Hogg, Phys. Letters 29A, 275 (1969)